

AIRCRAFT ATTITUDE MEASUREMENT USING
A VECTOR MAGNETOMETER

Research Report

R. Peitila & W. R. Dunn, Jr.

December 1, 1977

NASA Grant NGR 05-017-031

AIRCRAFT ATTITUDE
MEASUREMENT USING A
VECTOR MAGNETOMETER

Preface

The following report is based on work performed as a part of NASA Grant 05-017-031 by the University of Santa Clara, Department of Electrical Engineering and Computer Science.

Inquiries regarding this work can be directed to:

Dr. W. R. Dunn
c/o Department of Electrical Engineering & Computer Science
University of Santa Clara
Santa Clara, California 95053

TABLE OF CONTENTS

Acknowledgment	iii
Abstract	iv
I A VECTOR AUTOPILOT SYSTEM	
1-1 Introduction	1
1-2 Attitude Determination	2
1-3 Attitude Determination Employing Magnetic Field Components	6
1-4 A Possible System Configuration	8
1-5 Other Considerations	15
1-6 Conclusions	19
II AN ATTITUDE INDEPENDENT REMOTE MAGNETIC INDICATOR	
2-1 Introduction	20
2-2 An Algorithm to Compute Aircraft Heading	21
2-3 Mechanization of the Heading Algorithm	27
2-4 Conclusions	28
III DESIGN OF A MICROPROCESSOR BASED HEADING INSTRUMENT	
3-1 Introduction	30
3-2 Hardware Design Considerations	31
3-3 Software Design Considerations	37
3-4 Design of Subroutines	39
3-5 Conclusions	50
IV HEADING INSTRUMENT ERROR ANALYSIS	
4-1 Introduction	54
4-2 Sensor Errors	55
4-3 Analog Subsystem Error Analysis	74
4-4 Processing Errors	90
4-5 Measurement Error Summary	97
4-6 Sample Error Analysis	99
4-7 Conclusions	102

Table of Contents (Continued)

V	LABORATORY EVALUATION OF THE ATTITUDE INDEPENDENT REMOTE MAGNETIC INDICATOR AND HEADING INSTRUMENT	
5-1	Introduction	104
5-2	Test Apparatus	105
5-3	Heading Measurements With No Offset Correction	109
5-4	Heading Measurements to investigate Orthogon- ality Error	113
5-5	Conclusions	114
Appendix A:	Instruction Set of the Signetics 2650 microprocessor chip	127
Appendix B:	Assembly Language Program	130
Appendix C:	Table Generating Programs	156

CHAPTER I

A VECTOR AUTOPILOT SYSTEM

1-1 INTRODUCTION

An essential requirement of an aircraft attitude control system is that deviation of the body axes relative to a reference axes frame must be sensed. In addition, to overcome the ever-present possibility of errors or failure of the sensors, various configurations of redundant sensors are usually employed to assist in detection and correction of errors. To this end, there has been a continuing effort to improve existing sensors, to develop new sensor configurations, and to develop new sensor devices.

This chapter discusses the role of a vector magnetometer¹ as a new instrument for aircraft attitude determination. Although magnetometers have played a role in the attitude measurement of missiles and satellites [Ref. 1-1], there is an apparent lack of application in aircraft systems. By providing independent measures of attitude, the solid state vector magnetometer sensor system can not only assist in improving accuracy and reliability of existing systems but can also reduce component count with obvious benefits in weight and cost. Additionally, since a large number of aircraft heading reference systems depend on measurement of the Earth's magnetic field, it can be shown that by substituting a three-axis magnetometer for the remote sensing unit; both heading and attitude measurement functions can be derived using common elements, thereby further reducing the component count.

¹Aviation use to date has been essentially scalar magnetometry.

To investigate the feasibility of the above system, this chapter will proceed by developing a technique to determine attitude given magnetic field components. Sample calculations are then made using the Earth's magnetic field data acquired during actual flight conditions. Results of these calculations are compared graphically with measured attitude data acquired simultaneously with the magnetic data. The role and possible implementation of various reference angles are discussed along with other pertinent considerations. Finally, it is concluded that the Earth's magnetic field as measured by modern vector magnetometers can play a significant role in attitude control systems.

1-2 ATTITUDE DETERMINATION

Coordinate systems are usually defined by orthogonal right-handed sets of three unit vectors. An example of such a set is illustrated in Fig. 1-1 where the orientation of the body fixed frame used in this paper is delineated. Angular rotations are conventionally defined as rotations in the plane normal to a unit vector with the positive sense of rotation defined by the right-hand rule [Ref. 1-2].

To derive relationships of attitude variations as a function of magnetic vector component variation, we can proceed by considering matrix representations of an orthogonal transformation. If H_x , H_y , and H_z are the magnetic components measured at a desired airframe attitude and H_x' , H_y' , and H_z' are the components measured after any rotation of the body, vector $H' = [H_x' \ H_y' \ H_z']^T$ can be related to vector $H = [H_x \ H_y \ H_z]^T$ by an orthogonal linear transformation $H' = AH$. Here A must satisfy the orthogonality condition $AA^T = I$, where A^T is the transpose of A ; additionally, the determinant of A must be unity [Ref. 1-3, 1-4].

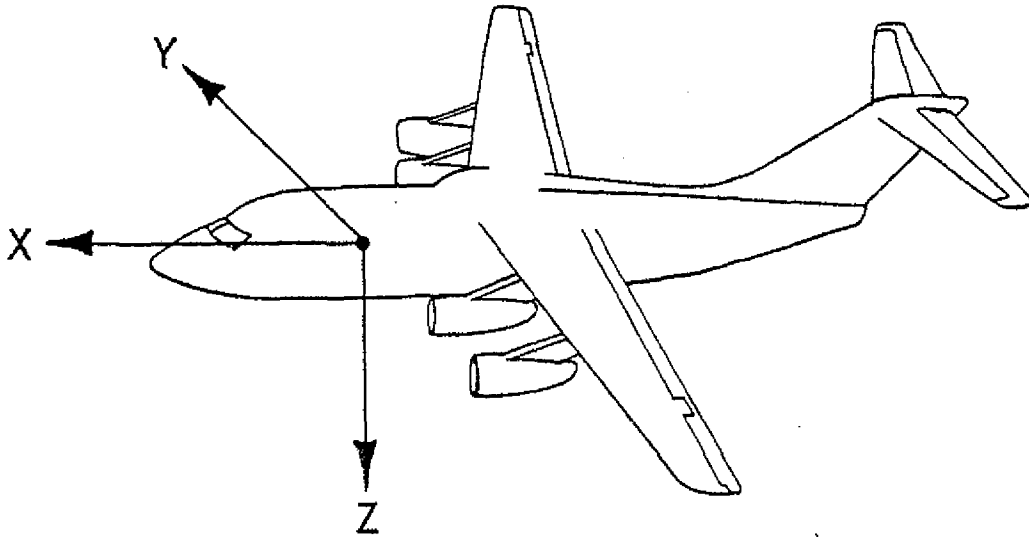


Fig. 1-1 AXIS ORIENTATION

Rotations about the z axis in Fig. 1-1 result in yaw deviations (ψ) and in new components (H'), as shown by

$$\begin{bmatrix} Hx' \\ Hy' \\ Hz' \end{bmatrix} = \begin{bmatrix} \cos \psi & \sin \psi & 0 \\ -\sin \psi & \cos \psi & 0 \\ 0 & 0 & 1 \end{bmatrix} \begin{bmatrix} Hx \\ Hy \\ Hz \end{bmatrix} \quad (1-1)$$

Similarly, independent rotations about the y axis and the x axis result in pitch (θ) and roll (ϕ) dependent variations in the measured H components, as shown by

$$\begin{bmatrix} Hx' \\ Hy' \\ Hz' \end{bmatrix} = \begin{bmatrix} \cos \theta & 0 & -\sin \theta \\ 0 & 1 & 0 \\ \sin \theta & 0 & \cos \theta \end{bmatrix} \begin{bmatrix} Hx \\ Hy \\ Hz \end{bmatrix} \quad (1-2)$$

$$\begin{bmatrix} Hx' \\ Hy' \\ Hz' \end{bmatrix} = \begin{bmatrix} 1 & 0 & 0 \\ 0 & \cos \phi & \sin \phi \\ 0 & -\sin \phi & \cos \phi \end{bmatrix} \begin{bmatrix} Hx \\ Hy \\ Hz \end{bmatrix} \quad (1-3)$$

The effect of a combined rotation can be expressed by using the product of the transformation matrices. In addition, if the rotations are small, the total rotation experienced by applying sequential rotations is independent of the order in which the rotations are performed [Ref. 1-3,1-4]

$$\begin{bmatrix} Hx' \\ Hy' \\ Hz' \end{bmatrix} = \begin{bmatrix} \cos \psi & \sin \psi & 0 \\ -\sin \psi & \cos \psi & 0 \\ 0 & 0 & 1 \end{bmatrix} \begin{bmatrix} \cos \theta & 0 & -\sin \theta \\ 0 & 1 & 0 \\ \sin \theta & 0 & \cos \theta \end{bmatrix}$$

$$\begin{bmatrix} 1 & 0 & 0 \\ 0 & \cos \phi & \sin \phi \\ 0 & -\sin \phi & \cos \phi \end{bmatrix} \begin{bmatrix} Hx \\ Hy \\ Hz \end{bmatrix} \quad (1-4a)$$

$$\begin{bmatrix} Hx' \\ Hy' \\ Hz' \end{bmatrix} = \begin{bmatrix} \cos \psi \cos \theta & \sin \psi \cos \phi + \sin \theta \cos \psi \sin \theta \\ -\sin \psi \cos \theta & \cos \psi \cos \phi - \sin \phi \sin \psi \sin \theta \\ \sin \theta & -\cos \theta \sin \phi \end{bmatrix}$$

$$\begin{bmatrix} \sin \phi \sin \psi - \sin \theta \cos \psi \cos \phi \\ \cos \psi \sin \phi + \sin \psi \sin \theta \cos \phi \\ \cos \phi \cos \theta \end{bmatrix} \begin{bmatrix} Hz \\ Hy \\ Hz \end{bmatrix} \quad (1-4b)$$

Assume that the angular variations θ , ψ , and ϕ are small enough so that the small angle approximations

$$\begin{aligned}\sin \theta &\approx \theta, \sin \psi \approx \psi, \sin \phi \approx \phi, \\ \cos \theta &\approx \cos \psi \approx \cos \phi \approx 1\end{aligned}$$

can be made. Then, if the products of small angles (in radians) can be assumed to be much smaller than the angles alone, the expression reduces to

$$\begin{bmatrix} Hx' \\ Hy' \\ Hz' \end{bmatrix} = \begin{bmatrix} 1 & \psi & -\theta \\ -\psi & 1 & \phi \\ \theta & -\phi & 1 \end{bmatrix} \begin{bmatrix} Hx \\ Hy \\ Hz \end{bmatrix} \quad (1-5)$$

Further modifications in the form of the matrices result in

$$\begin{bmatrix} Hx' \\ Hy' \\ Hz' \end{bmatrix} = \begin{bmatrix} -Hz & Hy & 0 \\ 0 & -Hx & Hz \\ Hx & 0 & -Hy \end{bmatrix} \begin{bmatrix} \theta \\ \psi \\ \phi \end{bmatrix} + \begin{bmatrix} Hx \\ Hy \\ Hz \end{bmatrix} \quad (1-6)$$

By subtracting, we arrive at an expression for the difference in H components as functions of angular deviation.

$$\begin{bmatrix} Hx' \\ Hy' \\ Hz' \end{bmatrix} - \begin{bmatrix} Hx \\ Hy \\ Hz \end{bmatrix} = \begin{bmatrix} \Delta Hx \\ \Delta Hy \\ \Delta Hz \end{bmatrix} = \begin{bmatrix} -Hz & Hy & 0 \\ 0 & -Hx & Hz \\ Hx & 0 & -Hy \end{bmatrix} \begin{bmatrix} \theta \\ \psi \\ \phi \end{bmatrix} \quad (1-7)$$

It is significant to note at this point that the transformation matrix is singular implying that solutions for θ , ψ , and ϕ are not independently available.

1-3 ATTITUDE DETERMINATION EMPLOYING MAGNETIC FIELD COMPONENTS

A given orthogonal set of three unit vectors can be displaced in Euclidean space by rotating the system through any angle δ about a directed rotation axis. It is also customary to represent this rotation vectorially as a directed line segment whose length is proportional to the rotation angle. This rotation is analogous to the rotation experienced by the body fixed frame of Fig. 1-1 as the aircraft experiences combined pitch, yaw, and roll variation. During flight the body fixed set rotates about this rotation axis assuming new (possibly erroneous) attitudes in space. The task of the attitude sensing system is to provide measures of compounded pitch, yaw, and roll that would result in the same attitude assuming that the rotations occurred sequentially about the x, y and z axes rather than the actual rotation axis.

It was shown in the previous section that a compounded rotation of an orthogonal set can be described by a product of respective transformation matrices. Additionally it was noted that for small angular rotations the order of multiplication is unimportant. Using the relationships of (1-7), expressions for the angular deviations in terms of measured magnetic vector components can be derived.

$$\Delta H_x = -H_z\theta + H_y\psi \quad (1-8a)$$

yields

$$\theta = (H_y\psi - \Delta H_x)/H_z \quad (1-8b)$$

$$\psi = (\Delta H_x + H_z\theta)/H_y \quad (1-8c)$$

Similarly,

$$\Delta H_y = -H_x \psi + H_z \phi \quad (1-9a)$$

yields

$$\psi = (H_z \phi - \Delta H_y) / H_x \quad (1-9b)$$

$$\theta = (\Delta H_y + H_x \psi) / H_z \quad (1-9c)$$

and

$$\Delta H_z = H_x \theta - H_y \phi \quad (1-10a)$$

yields

$$\theta = (\Delta H_z + H_y \phi) / H_x \quad (1-10b)$$

$$\phi = (H_x \theta - \Delta H_z) / H_y \quad (1-10c)$$

Assuming that H_x , H_y and H_z are nominal vector components as measured in a reference attitude and that H_x' , H_y' and H_z' are new field components at the new attitude, then $\Delta H_x = H_x' - H_x$, $\Delta H_y = H_y' - H_y$, $\Delta H_z = H_z' - H_z$ are expressions of the incremental changes in field components. Additionally, before using (1-8), (1-9) or (1-10) to solve for attitude variations (pitch, yaw, or roll), one additional angle from an auxiliary sensor² must be supplied. Using one additional angle of rotation (about any one axis) the remaining two rotations can then be calculated.

To illustrate this point, flight data acquired during the flight of a NASA flown Convair 900 instrumented with a three-axis magnetometer and a Litton inertial navigation system were used to calculate roll, pitch, and yaw.

²It was noted following (1-7) that a unique solution for attitude variation is not possible using magnetic field data alone.

Attitude variation about each of the three axes was calculated using measured magnetic field components supported by one angle from the inertial system. The results of these calculations are plotted in Figs. 1-2 through 1-4.

It is significant to note that the rotations shown occurred simultaneously (i.e., time base is the same for all three figures). The flight was at an altitude of approximately 5000 ft at an airspeed of approximately 250 nmi/h.

Although the data used to plot the attitudes shown in Figs. 1-2 through 1-4 were not acquired specifically for this purpose, the correlations in measured and calculated attitude clearly show that; within the limits of instrument accuracy, signals proportional to attitude variation can be derived using flight data.

1-4 A POSSIBLE SYSTEM CONFIGURATION

Since the intent of this chapter is to introduce the notion that magnetometer technology has advanced to the point where three-axis magnetometers can be incorporated in aircraft attitude sensing systems on a cost effective basis, the system discussion will be limited in scope to describing a possible combined heading and attitude measurement method.

Heading references fall into three classes; 1) those that depend on the Earth's magnetic field, 2) those that depend on the use of low-drift gyroscope to retain a preset azimuth, and 3) those (gyrocompasses) that depend on sensing the Earth's rotation [Ref.1-5]. By far the greatest number of aircraft heading systems depend on the Earth's magnetic field, although many of these include gyroscopes to improve the performance characteristics.

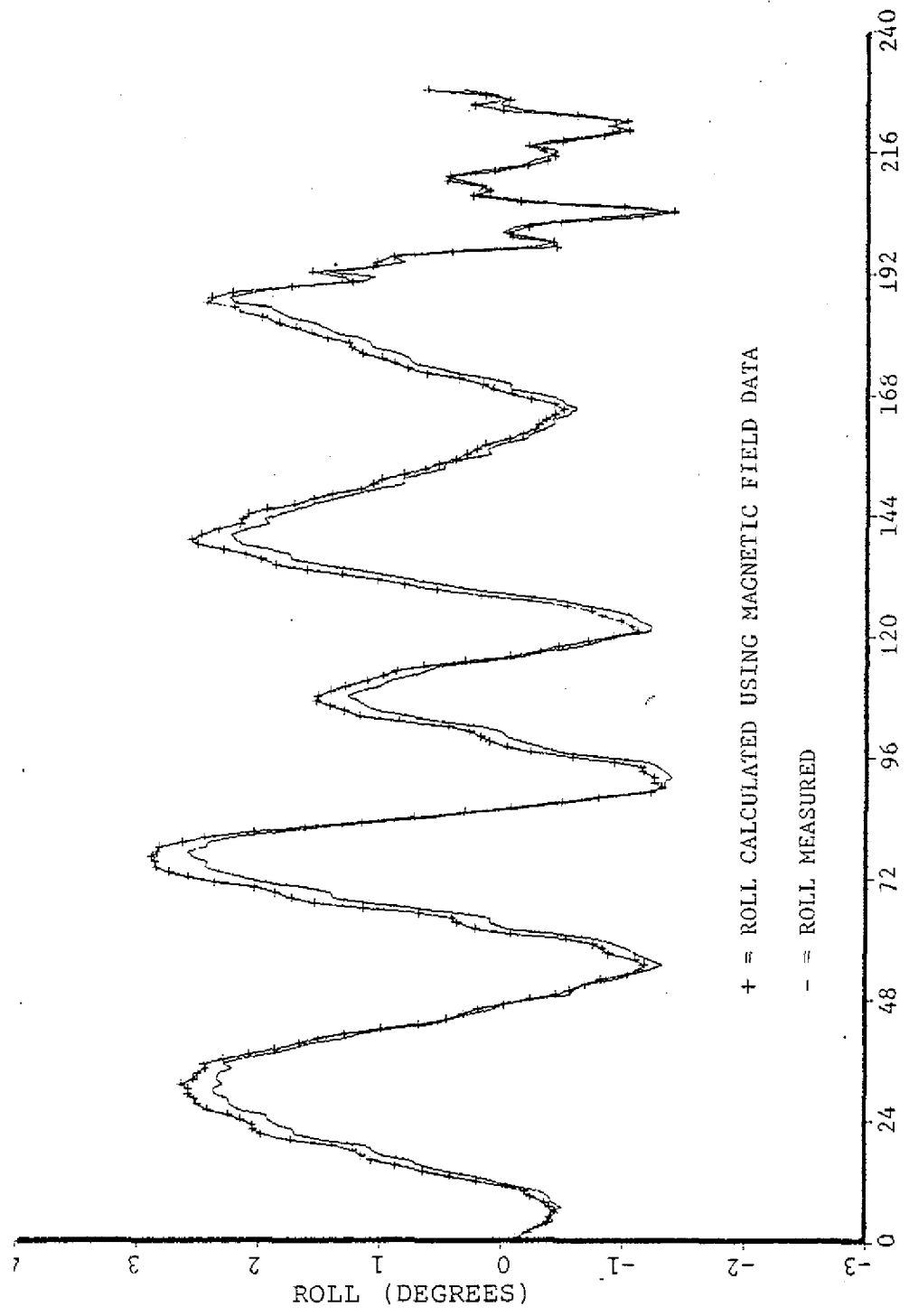


FIGURE 1-2 ROLL AXIS

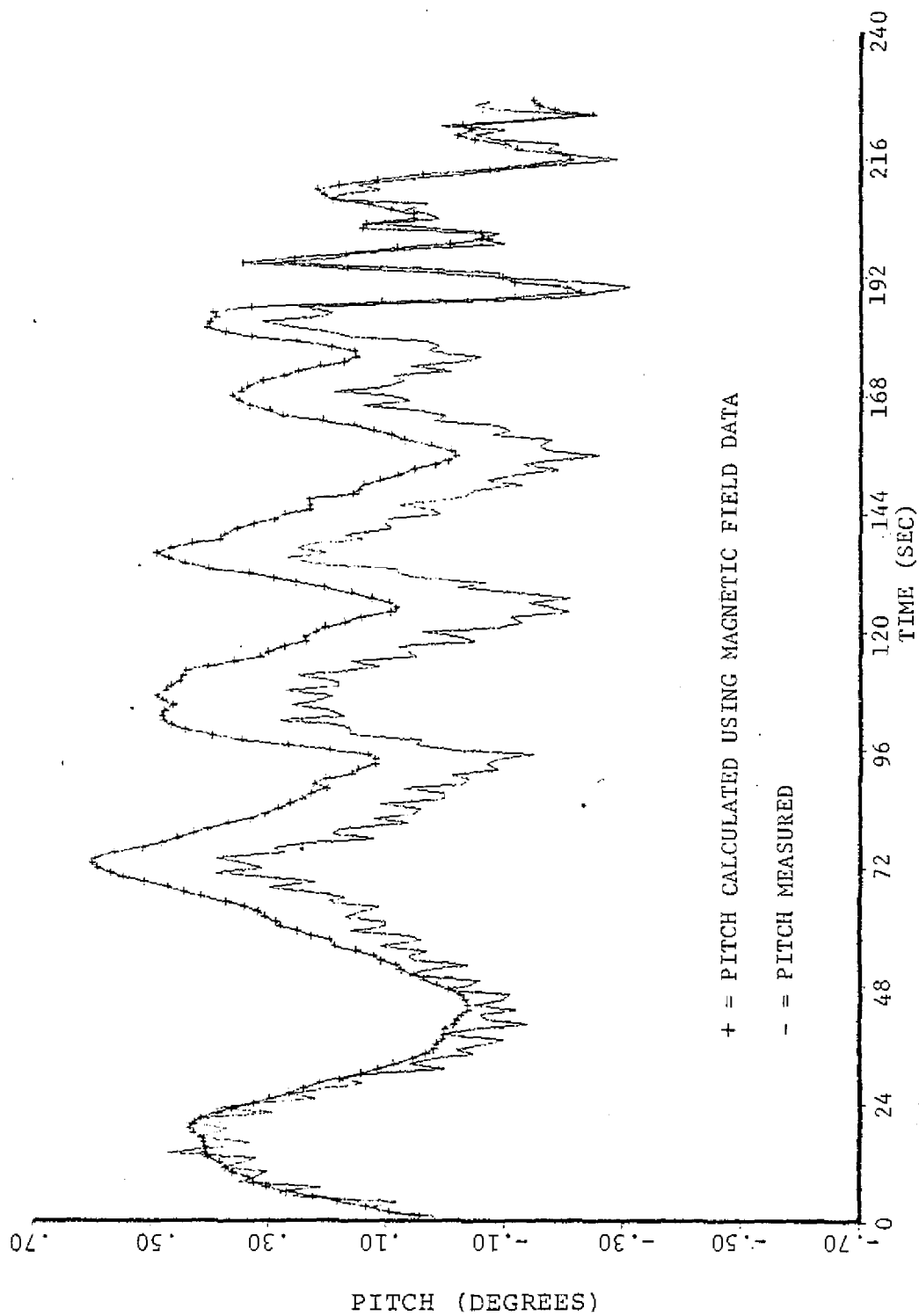


FIGURE 1-3 PITCH AXIS

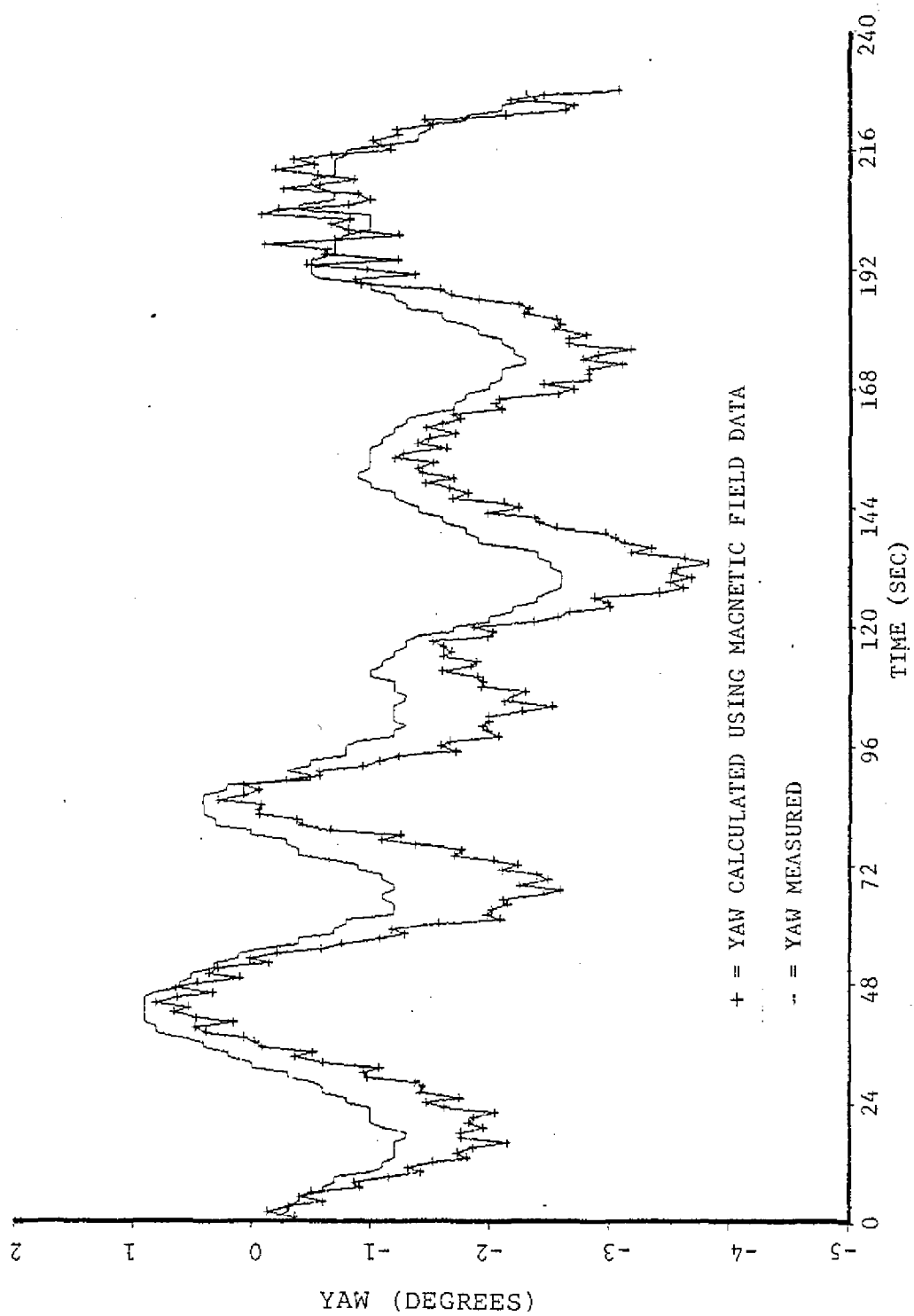


FIGURE 1-4 YAW AXIS

A popular system combination (with no gyro) is to combine a pendulous remote magnetic sensor and a synchro receiver in a null seeking circuit. The philosophy being to attempt to measure only the horizontal component of the Earth's magnetic field and to swing the receiver into alignment with it. Under acceleration, departures of the sensor unit from the horizontal result in angular heading errors ϵ [Ref. 1-5].

$$\epsilon = (aH/g) \tan \gamma \sin \theta$$

where aH is the horizontal acceleration, g is the acceleration due to gravity, θ is the angle between the acceleration vector and magnetic north, and γ is the magnetic field dip angle; \arctan (vertical field/horizontal field).

Accuracy of this system can be improved by incorporating a strapped-down solid state magnetic sensing unit (free of acceleration errors) that measures and displays the angle of the Earth's horizontal magnetic component relative to the aircraft. This system can be implemented as follows:

1) Determine the direction of the magnetic vector F relative to the sensors (and the airframe), by measuring the x , y and z components (Figs. 1-1 and 1-5). The direction cosines $\cos \alpha$, $\cos \beta$, $\cos \gamma$ are the cosines of the angles α , β , γ between the magnetic vector and the positive x , y and z axes. Additionally,

$$\cos \alpha = x/(x^2 + y^2 + z^2)^{\frac{1}{2}}$$

$$\cos \beta = y/(x^2 + y^2 + z^2)^{\frac{1}{2}}$$

$$\cos \gamma = z/(x^2 + y^2 + z^2)^{\frac{1}{2}}$$

- 2) Using either a vertical reference³ or knowledge of aircraft attitude, we can effectively rotate the body axes such that the x-y plane is horizontal (see Chapter II).
- 3) Simple application of direction cosines will yield the direction of magnetic north in the aircraft's x-y plane.

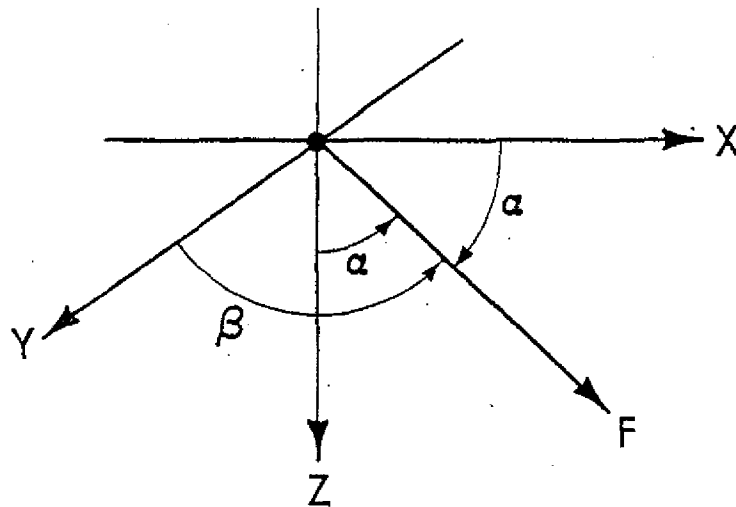


Fig. 1-5 FIELD VECTORS AND DIRECTION COSINES

Although the preceding discussion implies that heading can be determined by using a strapped-down magnetometer, there remains the problem of attitude determination. Another widely used system for obtaining a heading reference

³Not necessarily derived inertially [Ref. 1-11].

is to combine the relatively excellent short term stability of a directional gyroscope with the long term stability of magnetic field measurements. By slaving the directional gyroscope to the magnetic field [Ref. 1-5, sec. 10.4.7], gyroscopes with relatively large free drift error can be used to provide an excellent heading reference.

Replacement of the pendulous remote sensing unit of this type of system with a strapped-down vector magnetometer would result in both heading and attitude information on a continuous basis. This combination would operate as follows:

- 1) The system is initialized by determining a reference attitude (perhaps by using a primary inertial attitude system).
- 2) The angular position of the horizontal magnetic field component is computed as above and used to slave the directional gyroscope.
- 3) The directional gyroscope, with relatively good short term stability (devices with free drift of less than 0.5 deg/h have been designed), is used to determine yaw (ψ) errors.
- 4) For small angle deviations, (1-8), and (1-9), and (1-10) can be employed to recalculate aircraft attitude. The process loops back to step 2) closing the loop on a combined attitude and heading reference system.

The sampling frequency required to maintain an acceptable level of error is of course determined by the aircraft performance expected (angular rates) and by the gyro error (drift rate plus errors due to additional sources such as

gyroscope tilt from vertical). The overall system is such that heading can be determined as before with errors due to sensor departures from horizontal substituted for long term accumulation of attitude uncertainty (this can be corrected by looping to step 1) at a frequency dependent on error rates). Additionally one gains measurements of attitude with minimal computation and replacement of a mechanical remote sensing unit with a solid state strapped-down magnetometer sensor.

1-5 OTHER CONSIDERATIONS

The characteristics of the Earth's magnetic field and its variations have long been established [Ref. 1-6-1-10]. Since the field is to be used as a reference in the attitude measurement scheme, there is a need here to discuss its adverse characteristics. Although the field does experience variation, most of the variation is either in amplitude (ionospheric contributions) or has time constants that make the variation negligible (secular variation).

In traversing local anomalies, there will, however, be deflections in the ambient field due to the additive effect of local dipoles or monopoles. The effect of local terrain caused anomalies can be visualized by picturing the main field vector oriented in space with a second modulating vector rotating at its tip. Maximum angular error would occur when this modulating vector has maximum magnitude and is positioned at right angles to the main vector.

To illustrate the effect of local anomalies one can calculate the level of anomaly required to cause an error. Since the Earth's main field is typically in the order of 0.50 G it is readily apparent that a local anomaly of approximately 0.01 G at right angles to the local field is

required to cause an error of 1 deg. Furthermore, the local anomaly would have to be aligned with one of the aircraft body axes to result in one degree of attitude error in any one axis. Fortunately, anomalies with components of this magnitude positioned at right angles to the main field are extremely rare. In addition, the anomalies are localized over ore bodies or other geophysical irregularities, have magnitudes that diminish as the cube of altitude, and tend to average to zero over relatively short distances. In summary, the probability of encountering an anomaly that would cause as much as a 1 degree error is relatively small. The error, if introduced, will be short lived and, unlike drift error, will average to zero.

Fundamental to a magnetic field referenced system is the ability to measure orthogonal components of the field vector. Precision and accuracy of measurement of the components is of course specified by the desired control specifications.

Since the Earth's magnetic field varies in magnitude on a global basis between 0.3 G and 0.6 G (30,000 gamma to 60,000 gamma), it is apparent that full scale measurements of 0.6 G can be expected. Sensors mounted at right angles to the field will monitor no measureable field and thus define the lower limit of measurement to be zero. For the continental United States the declination varies between 60 and 80 deg, resulting in a range in horizontal component of 0.15 to 0.25 G with vertical component in the range of 0.4 to 0.55 G. Heading variations (yaw) result in changes of the horizontally sensed field components and would specify the maximum precision required. In addition, flight at $45 \text{ deg} \pm (n \times 90 \text{ deg})$ (where n is any whole number) with respect to magnetic north results in minimum sensitivity of the x and y

axes measurements. In this case sensor inputs would range between 0.106 and 0.177 G with minimum field at the north. Assuming the preceding ambient measurements, variations in component magnitude of approximately 0.0180 to 0.0305 G/deg for small angle variations can be expected.

A brief survey of commercial magnetometer manufacturers reveals that triaxial magnetometers that measure from zero to 0.6 G with linearities of 0.5 percent, noise less than ± 1 mG and sensitivities of at least 2.5 V per 600 mG are currently available. In addition, these devices have a bandwidth of direct current to at least 500 Hz and are rated to have less than 1 deg error in orthogonality.

From a precision standpoint, it is apparent that variations in yaw for this worst case situation can be sensed to better than 0.1 deg with currently available magnetometer technology. The sensor technology required to implement an attitude sensing system of reasonable specifications is available (more detailed analysis is presented in Chapter III).

Although the preceding calculations indicate that for small angular variations attitude can be calculated using measured magnetic data, there is a need to consider the effects of larger finite rotations. In this case the small angle assumptions would not be valid and an Euler transformation would have to be made. Measurement of three axes of field components could be used to develop the direction cosines required to determine the orientation of the axis of rotation, the angular rotation about it, and the three angular rotations of pitch, roll, and yaw.

For the special case where the axis of rotation aligns with the magnetic vector, there would of course be no

measured component changes.⁴ By measuring the attitude of a second vector (not in alignment with the magnetic vector), we could resolve the ambiguous situation cited above and provide additional redundancy.

The optimum auxiliary vector would be one that could be sensed without using inertial devices. The Earth's electric field can be considered. The main reason for considering this field as a means of providing an auxiliary angular reference is that the resultant system has the potential of being completely solid state. The electric field vector can be used to determine attitude variation in a manner analogous to the magnetic vector system. Inherent limitations of each single vector system can be obviated if the vectors are not coincident.

Although Hill [Ref. 1-11] reported success in controlling pitch and roll using the electrostatic field alone, comments by Markson [Ref. 1-12] indicate that the electrostatic field is not always a reliable vertical reference. Employment of the electrostatic field for this attitude measurement system is limited to augmenting the magnetic field measurements by eliminating ambiguity of motion around the magnetic vector. The requirement of vertical electrostatic field is thus removed and replaced by a requirement that the field direction is relatively stable.

By using two independently derived vectors we have sufficient data to obviate the ambiguity just cited and we have the potential of providing redundancy as well.

⁴An example of this would be yaw rotation while flying straight and level over the magnetic poles or roll rotation while flying towards a pole at the magnetic equator.

1-6 CONCLUSION

This chapter has identified a novel method of measuring aircraft attitude using relatively inexpensive, well developed instrumentation. It has recognized that magnetic field sensing systems have been used to some extent in attitude sensing and control of space vehicles; it has also suggested, however, that with appropriate support, magnetometers can find increased application in aircraft attitude measurement systems.

This claim is corroborated by actual flight test data. Magnetometers have evolved to a point where three axis measurements of the Earth's magnetic field can be made with sufficient precision and accuracy to enable measurement of small angle attitude variations.

This chapter has also discussed a possible system configuration combining heading determination and attitude measurement functions. By replacing the conventional remote sensing unit with a three-axis magnetometer, it has been suggested that both functions can be obtained with the hardware required previously for heading measurement alone.

As with any system, there are limitations imposed. The main limitation for a vector magnetometer system seems to be the inability to sense rotations around the magnetic vector itself. This problem is not unlike the ambiguity experienced by magnetic heading systems at high latitudes. By judiciously incorporating auxiliary instruments, not only can the ambiguities be removed but a degree of redundancy can be added while still maintaining a cost and weight advantage over comparable systems.

CHAPTER II

AN ATTITUDE INDEPENDENT REMOTE MAGNETIC INDICATOR

2-1 INTRODUCTION

Preliminary investigation [Ref.2-1] revealed that aircraft attitude can be calculated using measurements of earth's magnetic field vector and a single auxiliary rotation angle. An algorithm to compute the two remaining aircraft rotational angles was developed. Using flight data, it was demonstrated that an excellent correlation in computed versus actual aircraft attitude could be achieved. In addition to providing measurements of the magnetic field for redundant attitude computations (to improve accuracy and reliability of existing autopilot systems), it was noted that the vector magnetometer could substitute for the remote magnetic sensing unit. In this manner both heading and attitude measurements could be derived using common elements with obvious benefits in weight and cost.

This chapter discusses the mechanization of a microprocessor based computer system that uses a three axis magnetometer plus gyro data to compute heading. The magnetometer is a three axis solid state device that can be mounted in a strapped down configuration resulting in an attitude independent remote magnetic indicator. Gyro measurements of pitch and roll angle plus three axis magnetic measurements are used by the algorithm to compute aircraft heading. The system can function independently to compute heading or by simply increasing the stored program could implement the attitude computing algorithm of [Ref. 2-1] as well.

The chapter proceeds by developing an algorithm to compute aircraft heading using the strapped down magnetometer

and two gyro measured angles. Practical aspects of designing the system including both hardware and software are then presented. In addition, the limitations in instrument accuracy and operation as determined by sensor errors, signal processing errors, arithmetic precision and computation speed are discussed. Considerable computational capability inherent in the system enables minimization of systematic errors. It is demonstrated that inexpensive sensors can be employed with offset and orthogonality errors compensated by microprocessor programming. Finally, it is concluded that a microprocessor based computer with a solid state magnetometer can play a significant role in aircraft instrumentation.

2-2 AN ALGORITHM TO COMPUTE AIRCRAFT HEADING

Coordinate frames are usually defined by orthogonal right-hand sets of three unit vectors. An example of such a set is illustrated in Fig. 1-1 where the orientation of the body fixed frame used in this chapter is delineated. The reference coordinate frame referred to in this chapter is oriented with axes x and y in the horizontal plane and axis z vertical (z down is positive). Pitch attitude angle (θ) of an aircraft is defined [Ref. 2-2] as the angle between some preferred longitudinal axis and the horizontal reference. In this chapter, pitch angle is the angle between the x axis of the aircraft and the x - y plane of the reference axis set. Since angular rotations are conventionally defined as rotations in the plane normal to a unit vector with the positive sense of rotation defined by the right-hand rule [Ref. 1-2], we will define positive pitch angle (θ) as the "nose up" or positive rotation about the y axis when the y axis is horizontal. The roll and yaw angles (ϕ and ψ) will then simply be rotations about the x and y axes respectively.

By aligning the three magnetometer axes with the respective x, y and z axes of the aircraft, we can measure magnetic field components of the aircraft at any attitude. For the trivial case where pitch (θ) and roll (ϕ) are both zero degrees, Hx and Hy are the horizontal field components and we can compute yaw from the horizontal vectors as follows:

$$\psi_1 = \cos^{-1}(H_x / (H_x^2 + H_y^2)^{\frac{1}{2}}) \quad (2-1a)$$

or

$$\psi_1 = \sin^{-1}(H_y / (H_x^2 + H_y^2)^{\frac{1}{2}}) \quad (2-1b)$$

We select either (2-1a) or (2-1b) based on the relative magnitudes of Hx and Hy. By minimizing the numerator of the argument we guarantee that the inverse trigonometric operation results in an angle between zero and forty-five degrees with maximum sensitivity ensured. Heading is then computed using the signs of Hx and Hy to select the appropriate equation from Table 2-1.

<div style="text-align: center;"> <div style="display: inline-block; transform: rotate(-45deg);">Hx Hy</div> </div>	NEGATIVE	POSITIVE
Negative	$\psi = 180 - \psi_1$	$\psi = \psi_1$
Positive	$\psi = \psi_1 + 180$	$\psi = 360 - \psi_1$

Table 2-1. Formulae to Compute Heading

For most cases, the pitch and roll angles are not zero and inverse rotations are required to determine the actual horizontal field components Hx and Hy. Since any aircraft attitude can be represented as a sequence of rotations about each axis beginning at some reference attitude, we can

determine the reference Hx and Hy field components by performing an inverse roll followed by an inverse pitch computation¹.

The inverse roll computation can be developed by considering vector components of an arbitrary vector \bar{H} in Fig. 2-1. The first set (x_2, y_2, z_2) represents the vector components measured in a reference orientation. The second set has common origin and aligns with common x axis component. It is rotated (rolled) about the x axis resulting in new y and z values. We can describe vector \bar{H} in both coordinate frames as

$$\bar{H} = x_2 \cdot \hat{i}_2 + y_2 \cdot \hat{j}_2 + z_2 \cdot \hat{k}_2 \quad (2-2)$$

and

$$\bar{H} = x_3 \cdot \hat{i}_3 + y_3 \cdot \hat{j}_3 + z_3 \cdot \hat{k}_3 \quad (2-3)$$

Since the vector \bar{H} is unique, we note that equations (2-2) and (2-3) are equal. Furthermore if we form dot products we solve for the horizontal components x_2, y_2 , and z_2 in terms of the rotated values and the roll angle (ϕ).

From (2-2) we obtain

$$\bar{H} \cdot \hat{i}_2 = x_2(\hat{i}_2 \cdot \hat{i}_2) + y_2(\hat{j}_2 \cdot \hat{i}_2) + z_2(\hat{k}_2 \cdot \hat{i}_2) \quad (2-4a)$$

$$\bar{H} \cdot \hat{i}_2 = x_2 \quad (2-4b)$$

and from (2-3) we obtain

$$\bar{H} \cdot \hat{i}_2 = x_3(\hat{i}_3 \cdot \hat{i}_2) + y_3(\hat{j}_3 \cdot \hat{i}_2) + z_3(\hat{k}_3 \cdot \hat{i}_2) \quad (2-5a)$$

$$\bar{H} \cdot \hat{i}_2 = x_3 \quad (2-5b)$$

¹Since pitch is defined as the angle between the x axis and the horizontal plane we can assume that at any heading, aircraft attitude results due to a pitch followed by a roll.

then

$$x_2 = x_3 \quad (2-6)$$

Similarly,

$$\bar{H} \cdot \hat{j}_2 = y_2 = x_3(\hat{i}_3 \cdot \hat{j}_2) + y_3(\hat{j}_3 \cdot \hat{j}_2) + z_3(\hat{k}_3 \cdot \hat{j}_2) \quad (2-7a)$$

$$y_2 = y_3 \cos \phi - z_3 \sin \phi \quad (2-7b)$$

and

$$\bar{H} \cdot \hat{k}_2 = z_2 = x_3(\hat{i}_3 \cdot \hat{k}_2) + y_3(\hat{j}_3 \cdot \hat{k}_2) + z_3(\hat{k}_3 \cdot \hat{k}_2) \quad (2-8a)$$

$$z_2 = y_3 \sin \phi + z_3 \cos \phi \quad (2-8b)$$

These expressions can be summarized as

$$\begin{bmatrix} x_2 \\ y_2 \\ z_2 \end{bmatrix} = \begin{bmatrix} 1 & 0 & 0 \\ 0 & \cos \phi & -\sin \phi \\ 0 & \sin \phi & \cos \phi \end{bmatrix} \cdot \begin{bmatrix} x_3 \\ y_3 \\ z_3 \end{bmatrix} \quad (2-9)$$

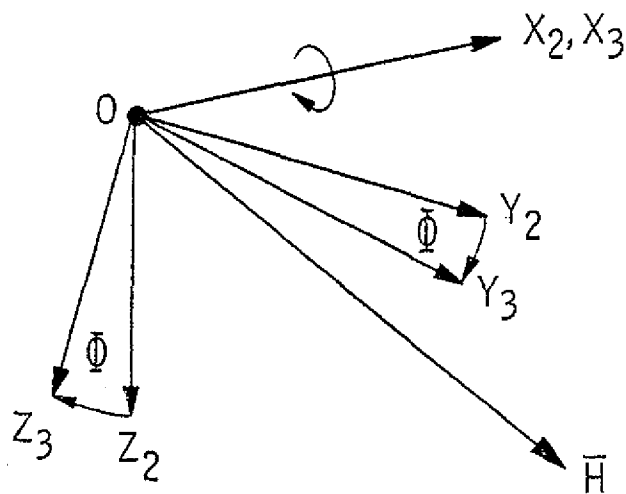


Fig. 2-1 AXES ROTATED IN ROLL

Similarly, considering an axis set rotated in pitch as shown in Fig. 2-2, we can express the reference set x_1, y_1, z_1 in terms of the rotated set x_2, y_2, z_2 as follows

$$\begin{bmatrix} x_1 \\ y_1 \\ z_1 \end{bmatrix} = \begin{bmatrix} \cos \theta & 0 & \sin \theta \\ 0 & 1 & 0 \\ -\sin \theta & 0 & \cos \theta \end{bmatrix} \cdot \begin{bmatrix} x_2 \\ y_2 \\ z_2 \end{bmatrix} \quad (2-10)$$

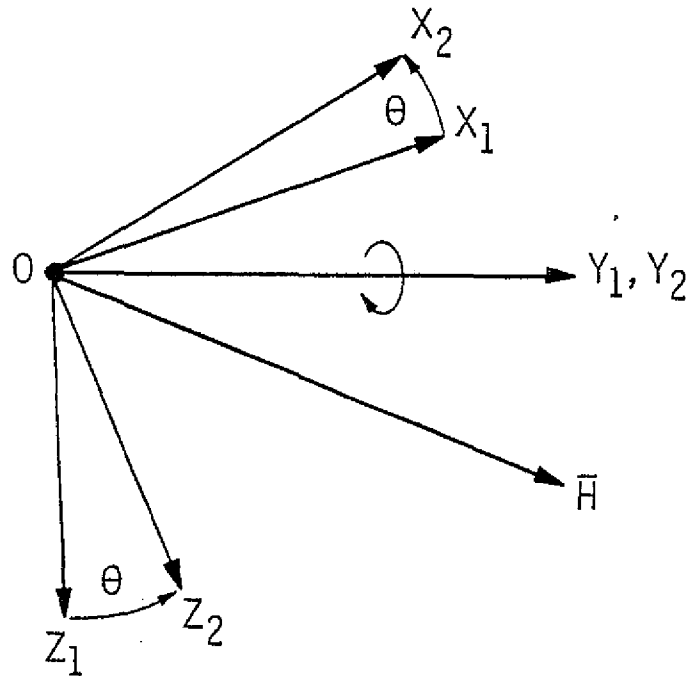


Fig. 2-2 AXES ROTATED IN PITCH

Finally, if we assume that the axis set subscripted with ³ represents components of Earth's magnetic vector measured at an arbitrary aircraft attitude, we can derive the magnetic components (H_{xh}, H_{yh}, H_{zh}) in the horizontal plane for a given heading

$$\begin{bmatrix} H_{xh} \\ H_{yh} \\ H_{zh} \end{bmatrix} = \begin{bmatrix} \cos \theta & 0 & \sin \theta \\ 0 & 1 & 0 \\ -\sin \theta & 0 & \cos \theta \end{bmatrix} \begin{bmatrix} 1 & 0 & 0 \\ 0 & \cos \phi & -\sin \phi \\ 0 & \sin \phi & \cos \phi \end{bmatrix} \cdot \begin{bmatrix} H_{x_3} \\ H_{y_3} \\ H_{z_3} \end{bmatrix} \quad (2-11a)$$

$$\begin{bmatrix} H_{xh} \\ H_{yh} \\ H_{zh} \end{bmatrix} = \begin{bmatrix} \cos \theta & (\sin \theta \sin \phi) & \sin \theta \cos \phi \\ 0 & \cos \phi & -\sin \phi \\ -\sin \theta & (\cos \theta \sin \phi) & \cos \phi \cos \theta \end{bmatrix} \cdot \begin{bmatrix} H_{x_3} \\ H_{y_3} \\ H_{z_3} \end{bmatrix} \quad (2-11b)$$

The algorithm to be implemented with the microprocessor would therefore require operations as outlined in Fig. 2-3. Details of programming method, modifications to the above equations to facilitate programming and computation speed versus accuracy tradeoffs are discussed in following sections.

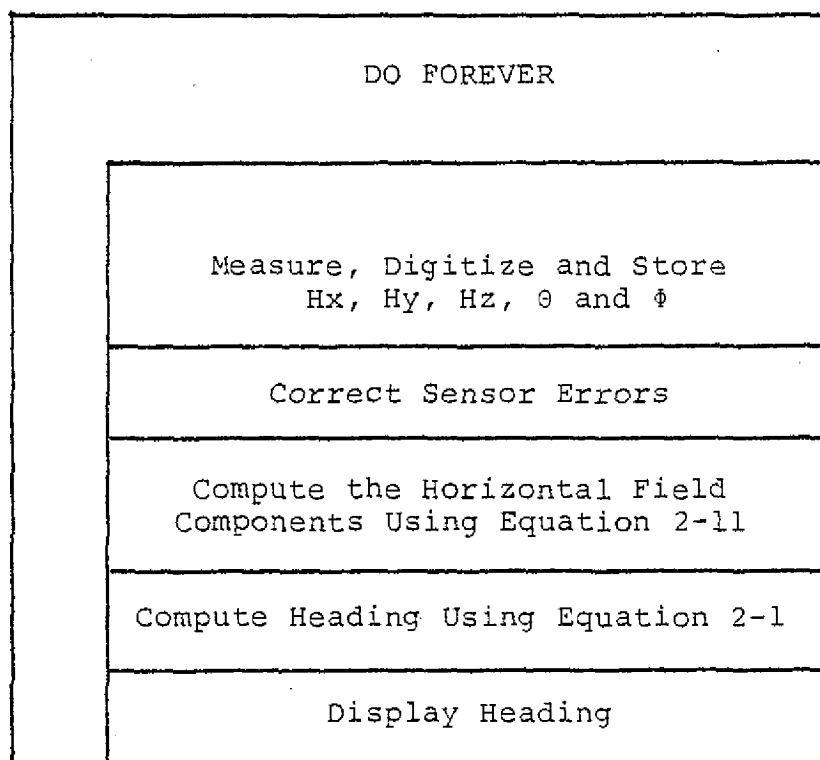


Fig. 2-3 LOGICAL OPERATIONS REQUIRED TO COMPUTE HEADING

2-3 MECHANIZATION OF THE HEADING ALGORITHM

A. General Considerations

To evaluate the performance of an integrated system experimentally, an instrument was designed to implement the algorithm developed above. Several approaches were considered to implement the heading instrument for experimentation:

1) A minicomputer implementation incorporating an HP-2100 minicomputer supported by peripheral interface and analog circuitry. Programming of the HP-2100 would have enabled the computer to control multiplexing and processing of sensor data as suggested by Parish and Lee [Ref. 2-3].

2) A hybrid system composed of a remote data acquisition system to collect data from sensors for subsequent processing by a computer (possibly an HP-2100).

3) A digital/analog electronic implementation incorporating the design of a special purpose computer to perform the required functions of a heading instrument.

The first two approaches were abandoned since it was desirable to perform the experiments at various locations remote from a computer facility and to have data available immediately without having to rely on off-line computations at a later date. The design task then evolved to the design of a special purpose computer system to implement the algorithm, provide a means for evaluating the performance of the proposed algorithm and to allow modifications to the system if required.

B. Design Criteria

Having decided on the general approach to implementing

the algorithm it became necessary to consider the performance criteria desired of the instrument.

1) Accuracy

As a design goal, an absolute accuracy of $\pm 1.0^\circ$ in heading uncertainty was selected for the laboratory implementation. This accuracy is compatible with commercially available heading systems.

2) Computation Speed

The bandwidth of the system is determined mainly by the computation speed of the computer². As a design goal, complete heading updates once per second was established.

3) Flexibility

A desirable feature of the laboratory evaluation instrument was considered to be flexibility. Revisions or additions to the algorithm as predicted by experimental data should be incorporated with minimal redesign of the instrument.

2-4 CONCLUSIONS

An instrument designed to implement the heading algorithm developed above uses a three axis magnetometer to measure magnetic field data in the vicinity of an aircraft. Since the magnetometer proposed is a solid state three axis fluxgate device and is permanently mounted in a strapped down configuration, the implementation results in an attitude independent

²The response times of the various sensors and analog circuitry are orders of magnitude greater than the desired one second sample interval.

remote magnetic indicator³.

Several factors will contribute to system inaccuracy. Although the major error sources can be evaluated mathematically (Chapter IV), there is a need to evaluate the implementation experimentally. Systematic errors that arise can be reduced by instrument computation. This capability (inherent with a computer based system) enables incorporation of less expensive sensors in the heading instrument with less concern with factors such as temperature regulation, sensor orthogonality and sensor offset⁴.

Since the algorithm can be implemented using a microprocessor as the major computer element, the resulting instrument will have inherent computation capability, be small in size and consume relatively little power. These factors make the instrument an ideal device for aircraft application where the need for redundant distributed processing capability is invaluable.

³Current remote magnetic indicators are pendulous and rely on gravity to enable measurements of the horizontal magnetic vector (not attitude independent).

⁴Assuming that the sensors have repeatable or measurable characteristics, algorithms can be developed to correct previously measured erroneous data.

CHAPTER III

DESIGN OF A MICROPROCESSOR BASED HEADING INSTRUMENT

3-1 INTRODUCTION

Progress in device and component technologies during the 1970's has led to an assortment of sophisticated integrated circuits (IC) devices [Ref. 3-1] which enable the design of instruments with a high degree of sophistication and accuracy. Of these devices, the microprocessor has to date been the most exploited component in industrial control and instrumentation applications [Ref. 3-2 through 3-7]. There have been many papers presented addressing the general application and feasibility of applying microcomputers to particular design tasks [Ref. 3-8 through 3-21].

Although much of the literature to date on microprocessors has addressed the design of commercial products (usually the final result of a carefully orchestrated effort beginning with a market survey), the design of a laboratory instrument for algorithm evaluation differs in design philosophy. In particular, the laboratory instrument is designed to evaluate a proposed algorithm under laboratory conditions. The traditional benchmark evaluations and attempts to match the microprocessor to the application is not only difficult but unnecessary. If the processor is much more powerful than necessary, the "overkill" is little noticed; but if an insufficiently endowed microprocessor is selected, the effects can be devastating. Not only will the program be difficult to write and voracious of memory, it would be difficult to change to a more powerful microprocessor part way through the project. With these considerations in mind, a general purpose, flexible microprocessor with powerful architecture and instruction set the Signetics 2650 microprocessor [Ref. 3-22] was selected.

3-2 HARDWARE DESIGN CONSIDERATIONS

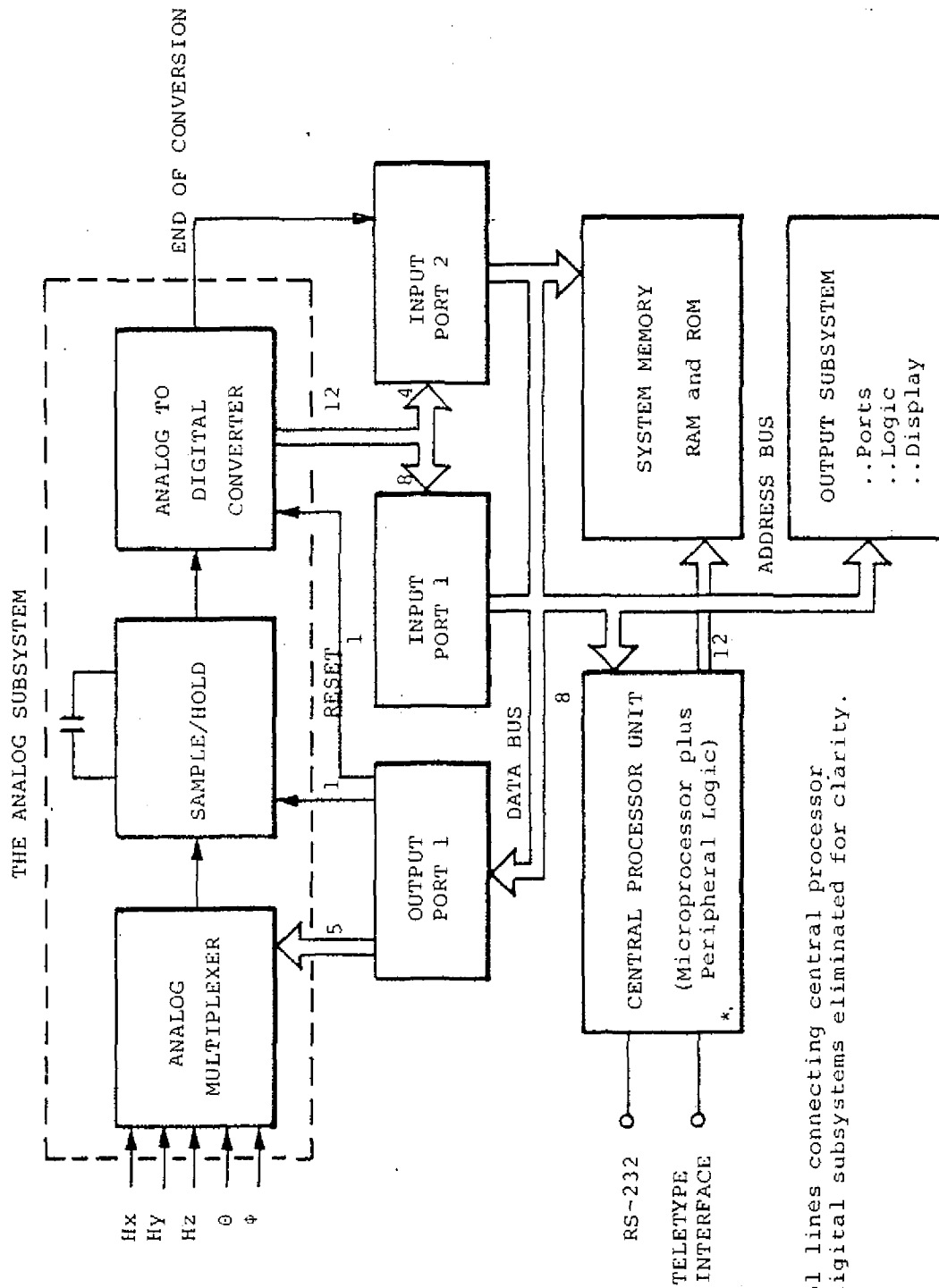
The design of a microprocessor based system begins by considering the total system level block diagram to be implemented (Fig. 3-1). Inputs from five sensors including x, y and z axis magnetic data plus pitch and roll angles (H_x , H_y , H_z , θ and ϕ) are to be multiplexed, sequentially sampled and converted to a digital representation prior to processing (executing the algorithm developed above). The main subsystem of Fig. 3-1, the central processing unit (CPU), operates under control of instructions stored in the system memory and interfaces with the input and output subsystems via data ports.

At this early stage in the design, it is significant to note that the block diagram of Fig. 3-1 differs slightly from that of a classical discrete hardware solution. The input subsystem (composed of analog multiplexer, sample and hold, and analog to digital converter) differs from a conventional data acquisition in that it is devoid of a control section. The microprocessor will control the data acquisition sampling and conversion in addition to performing the arithmetic function associated with the algorithm.

Having established a tentative block diagram of the instrument, the design continues by addressing relevant characteristics and limitations of each subsystem. These characteristics will then in turn be considered in configuring the final system and program to be executed.

1) The Analog Subsystem

Composed of the analog multiplexer, sample/hold and analog to digital converter, the analog subsystem of Fig. 3-1 affects both system accuracy and throughput rate. The



*Control lines connecting central processor to digital subsystems eliminated for clarity.

Fig. 3-1. SYSTEM BLOCK DIAGRAM

well-known Shannon theorem [Ref. 3-23, 3-24] on sampling theory defines one of the basic limits on throughput rate stating that the minimum frequency for sampling must be double the highest significant frequency of the signal, including the noise on the signal. This minimum frequency is necessary, the theorem states, if the sampled signal is to contain all of the information needed for undistorted reconstruction. At a lower sampling frequency ailiasing can occur¹. The minimum sampling rate for data to be used in this heading instrument (based on the design goal of Chapter II) then results in a system bandwidth of 30 hertz. The analog signals from each sensor are low pass filtered to reduce frequency content above 60 hertz. A survey of commercially available multiplexers, sample and hold modules and analog to digital convert modules (ADC) [Ref. 3-25 to 3-28] reveals that subsystems with throughput characteristics exceeding the requirements of a system sampled at one second intervals are readily available (pertinent specifications are discussed in more detail in Chapter IV). The limiting parameter determining total system speed performance will then be the execution time of the algorithm (a programming consideration). A further system consideration is the ability to adjust analog system offset and gain. These adjustments are made using variable resistors (trim pots) connected to appropriate leads on the sample and hold and analog to digital converter modules.

2) The Central Processing Unit (CPU)

The central processing unit (Fig. 3-2) is composed of the microprocessor (Signetics 2650) supported by peripheral logic elements (Fig. 3-2). Design of this subsystem involved medium

¹That is, the sampled data derived from a sine wave of frequency f sampled at a frequency less than $2f$ can be fitted with sine waves of a frequency other than f .

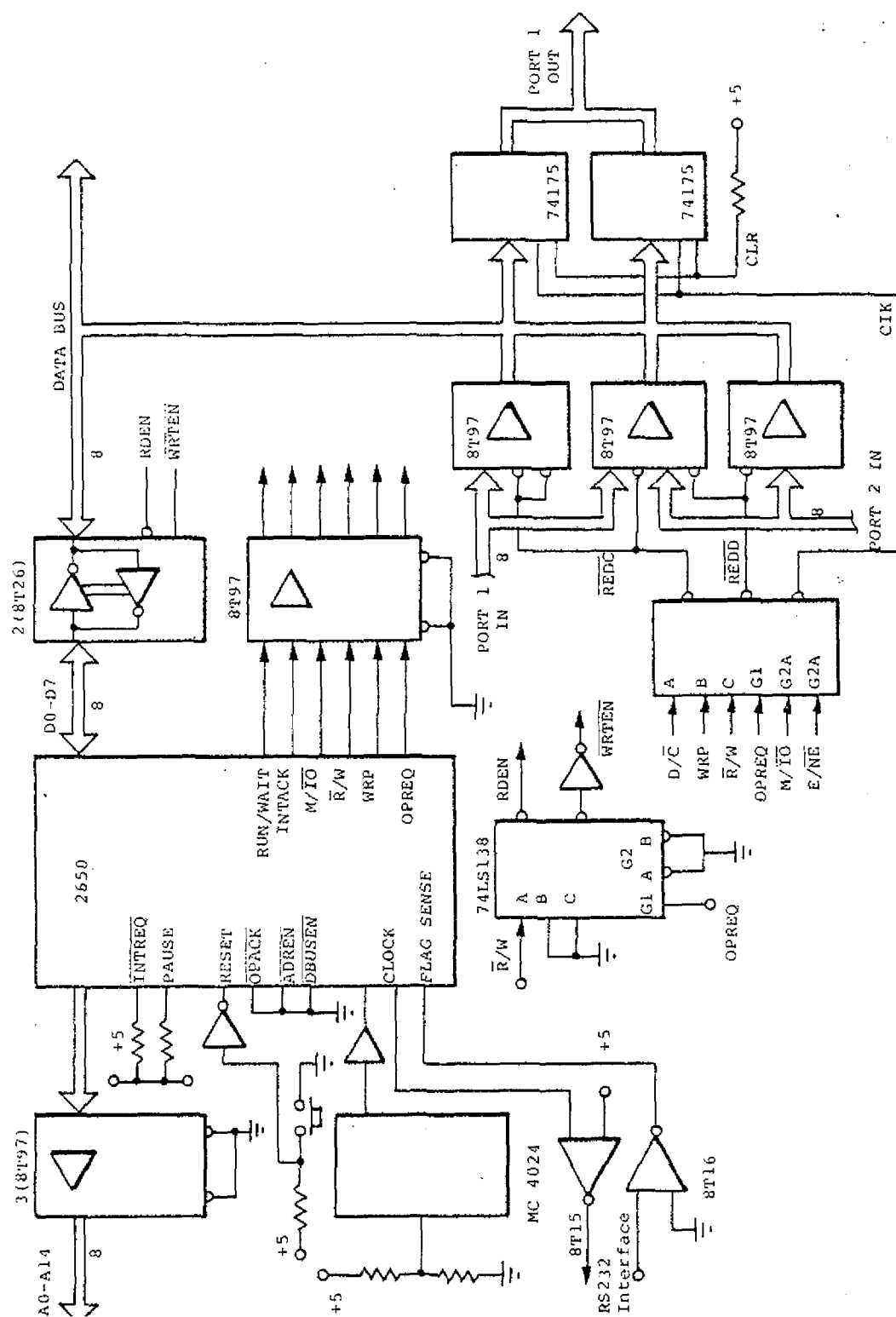


Fig. 3-2. THE CPU SUBSYSTEM

and small scale integrated circuits using well-known [Ref. 3-29 through 3-31] design techniques. To facilitate system development several features were included in the design of the CPU subsystem (features that would not necessarily be required in a production instrument). These include:

- a) System reset, single step and normal run mode operation controlled by switches and logic elements.
- b) An RS-232 teletype interface is included to enable manual intervention and development capability during program development. The program was developed by loading and executing instructions into the random access memory (RAM) under control of the PIPBUG² program.

3) The Memory Subsystem

The memory subsystem (Fig. 3-3) was organized onto cards each with two thousand byte capability. In this manner system memory could easily be expanded (or reduced) in increments of 2K bytes. The memory chips selected were organized as 256 four bit words and feature pin for pin compatibility with commercially available random access (RAM) and programmable read only memory (PROM) chips. Program segments could then be developed in RAM and finally "burned" into PROM chips for a permanent, nonvolatile operation. In this manner the system development begins with 1K bytes of memory devoted to the resident PIPBUG program (in ROM chips) with the remainder of memory allocated as RAM for both program and scratch pad usage.

²Signetics tradename for the 2650 resident loader and monitor program.

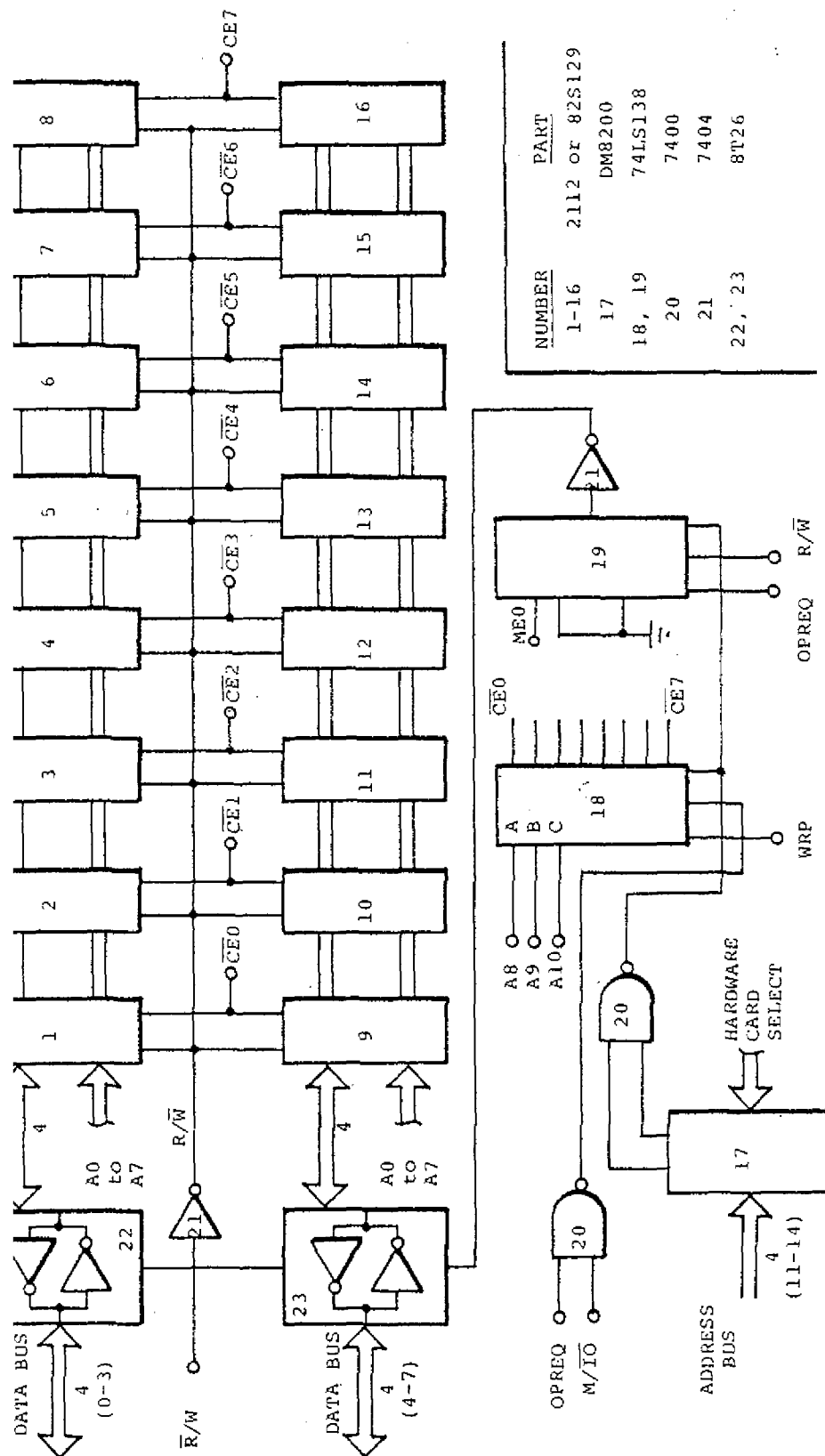


Fig. 3-3. MEMORY SUBSYSTEM (1 Card)

As the program is developed, additional memory is added in increments of 2K bytes per card or 256 bytes on the card. Modifications to the program can be easily made using the PIPBUG program and teletype.

4) The Output Subsystem

For laboratory development the output subsystem of Fig. 3-4 was designed to provide seven segment visual output of the aircraft heading with three significant digits displayed. To expediate the design cycle and to enhance system throughput rate, the outputs were designed as ports with latches and decoder driver functions provided by hardware. In other applications a hardware/software tradeoff could be made with the data decoding and driving implemented using table lookup and multiplexing controlled by the CPU.

3-3 SOFTWARE DESIGN CONSIDERATIONS

The general purpose processor selected to implement the CPU was designed to implement programmed logic and to perform conventional computer operations. This heading instrument takes advantage of both areas. Since the instrument is actually a special purpose computer under control of a stored program, the functional specialization resides in the program rather than the hardware logic. Modifications can be made relatively easily, satisfying the flexibility design goal of Chapter II.

Having decided on the tentative hardware structure described in Section 3-2 above, the program development leading to the final listing in Appendix B proceeded as follows:

- 1) Structured flow charts were developed depicting the total system operation as an ordered sequence of operations. Each

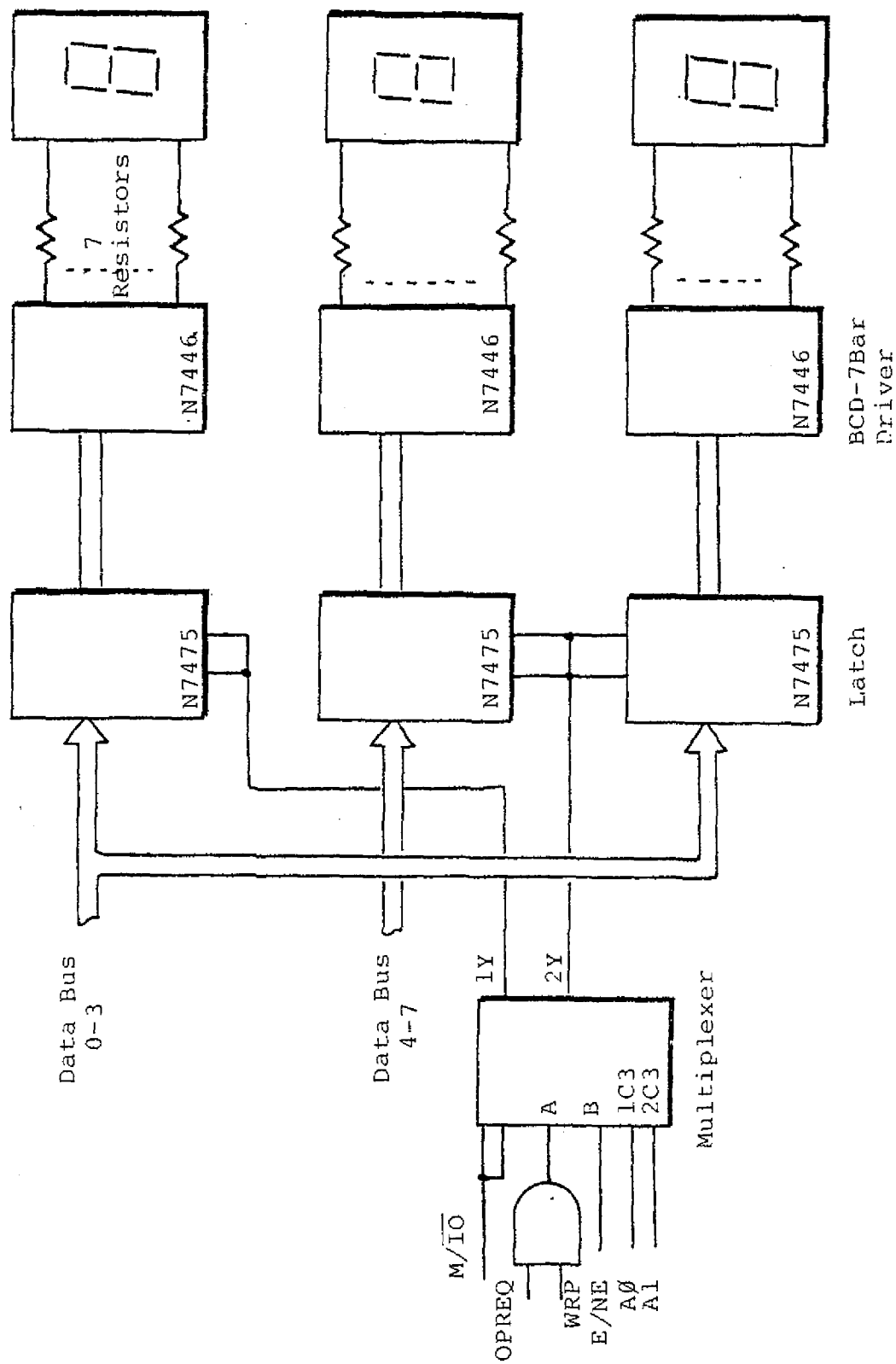


Fig. 3-4 THE OUTPUT SUBSYSTEM

operation is identified as a separate subroutine which in turn can have "nested" subroutines of its own (Fig. 3-5).

2) System accuracy requirements were next investigated (discussed in detail in Chapter IV) to ascertain the precision requirements³ of the various subroutines.

3) The respective subroutines outlined in 1) above were developed and implemented using a cross assembler program [Ref. 3-32]. Each subroutine was then loaded into the development hardware and "debugged" prior to total program integration. The above program development depicts a top down strategy of program development [Ref. 3-33] and leads to an expedient system development with subroutines being individually developed to yield a modular program construction.

3-4 DESIGN OF SUBROUTINES

The total program consists of an overall system program composed of nested subroutines. The discussion in this section is limited in scope to the design of the more complex subroutines required to implement the solid state remote magnetic heading algorithm.

1) Subroutine "SAMP" (Fig. 3-6a)

The first portion of this subroutine is dedicated to the control function of selecting an analog channel via the multiplexer, sampling and holding the data, resetting and reading data from the analog to digital converter (ADC). Prior to or during the programming of this section, data fields in

³This step is vital to determine whether the operations outlined in 1) above are to be carried out in a single or multiprecision manner.

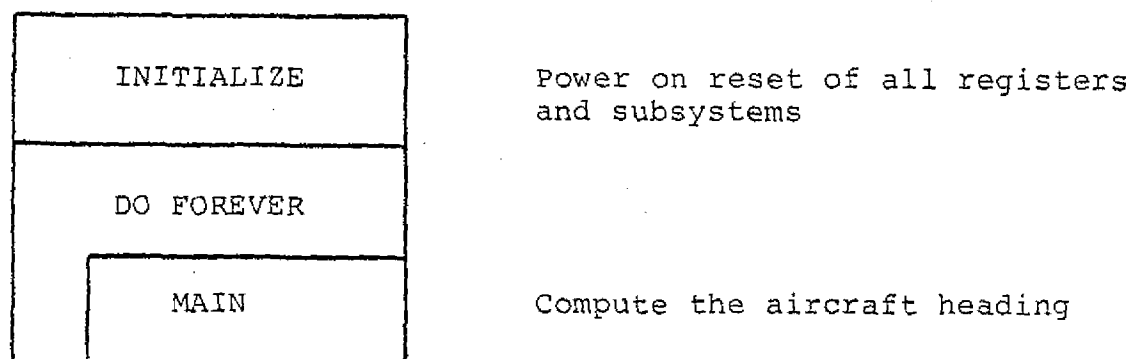


Fig. 3-5a. SYSTEM PROGRAM

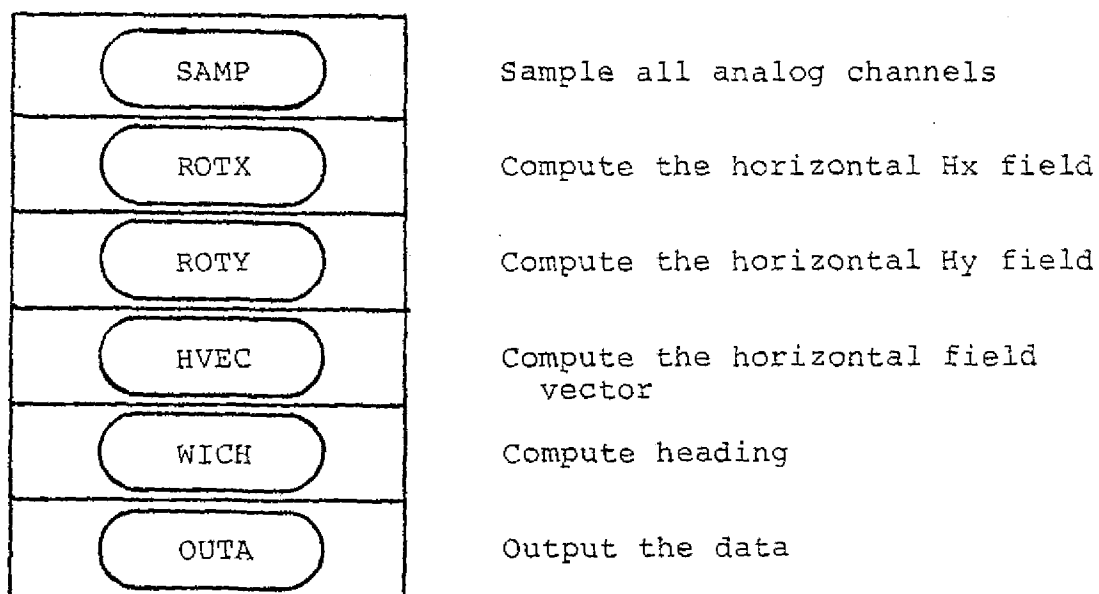


Fig. 3-5b. SUBROUTINE "MAIN"

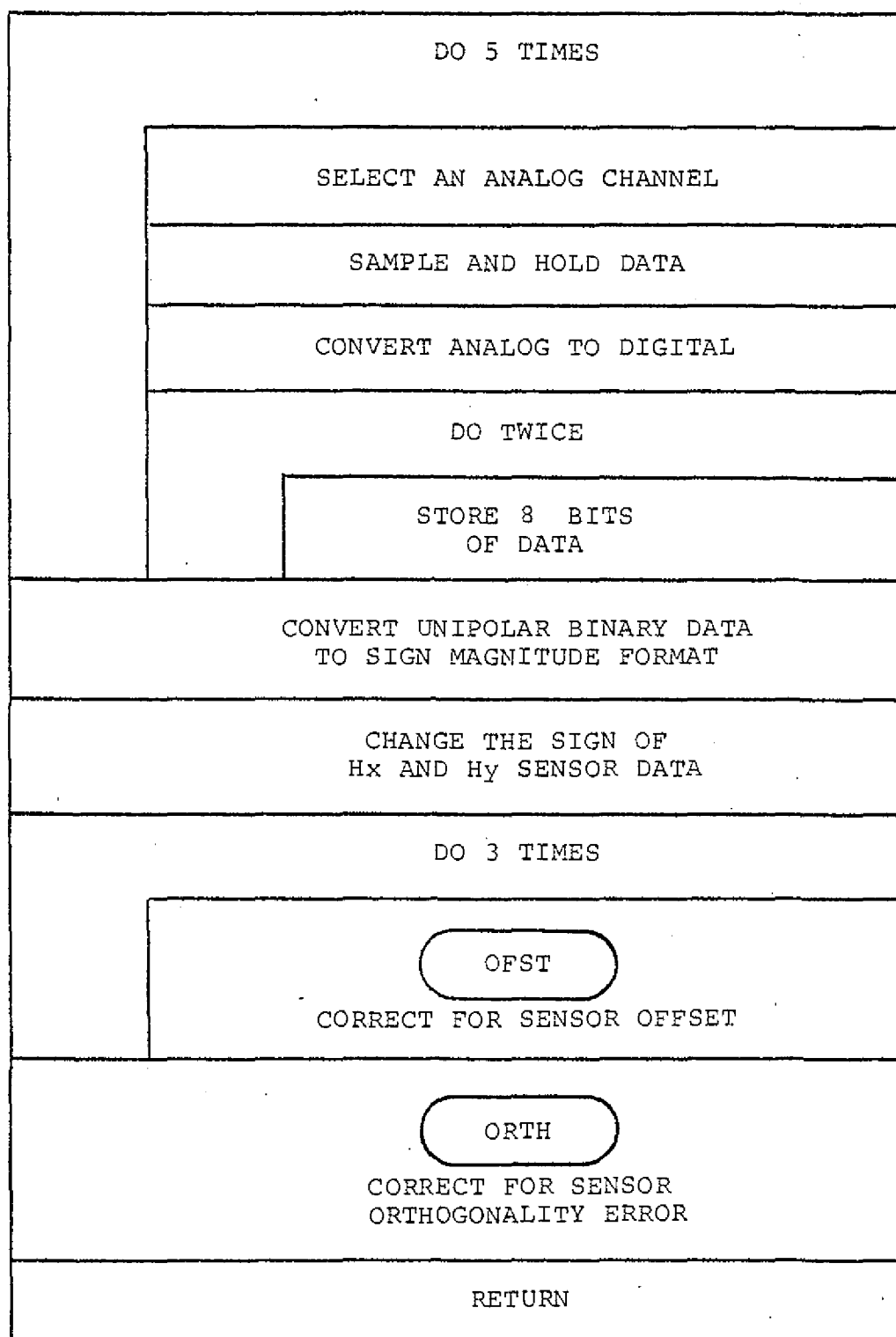


Fig. 3-6a. SUBROUTINE "SAMP"

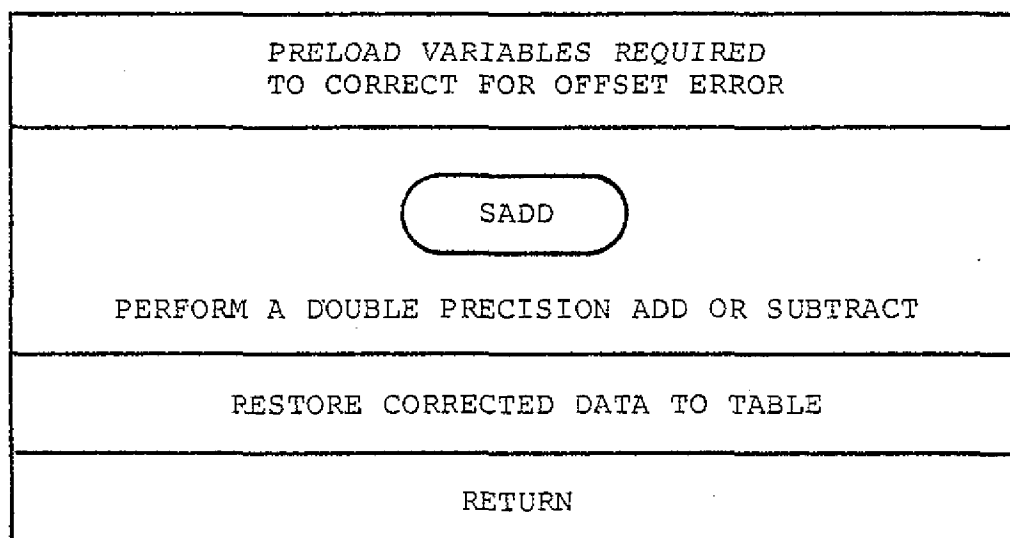


Fig. 3-6b. SUBROUTINE "OFST"

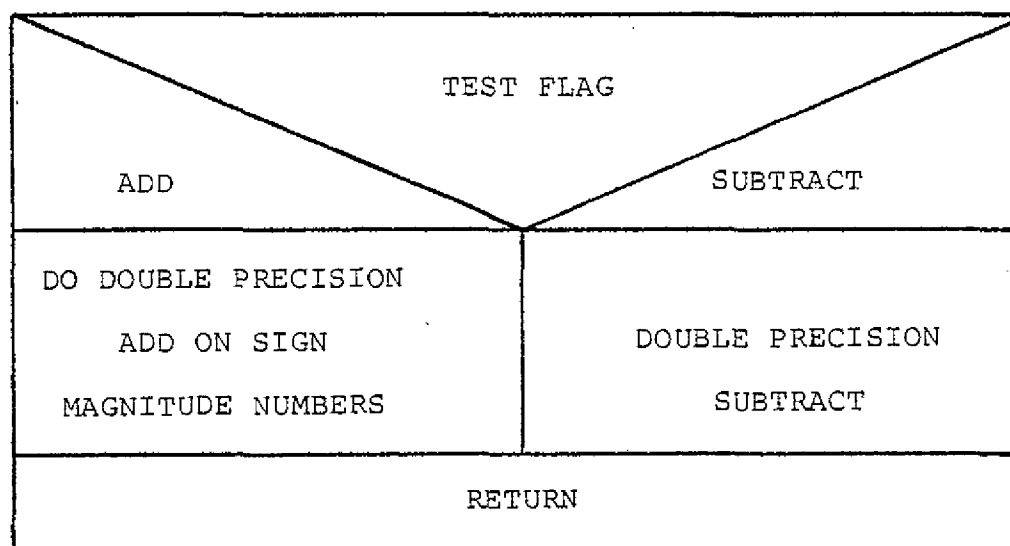


Fig. 3-6c. SUBROUTINE "SADD"

input ports 1 and 2 and output port 1 of Fig. 3-1 are allocated. Control information is then passed to the peripheral module by writing control words to output port 1. Analog to digital converter status and the 12 bit data field are sampled by reading input ports 1 and 2.

Sensor outputs were biased at +2.5 Volts with transfer characteristics as depicted in Fig. 3-7a [Ref. 3-34]. The ADC selected for this laboratory instrument had a binary output data format related to analog input as shown in Fig. 3.7b [Ref. 3-35]. The second function of the sampling subroutine "SAMP" was to convert data from a unipolar binary format to a sign magnitude format. Since the total transfer function from sensor input to ADC output (Fig. 3-7a and b) indicates an offset of 2.5 Volts or 1/2 the ADC output range, the sign magnitude format can be generated as shown in Fig. 3-8.

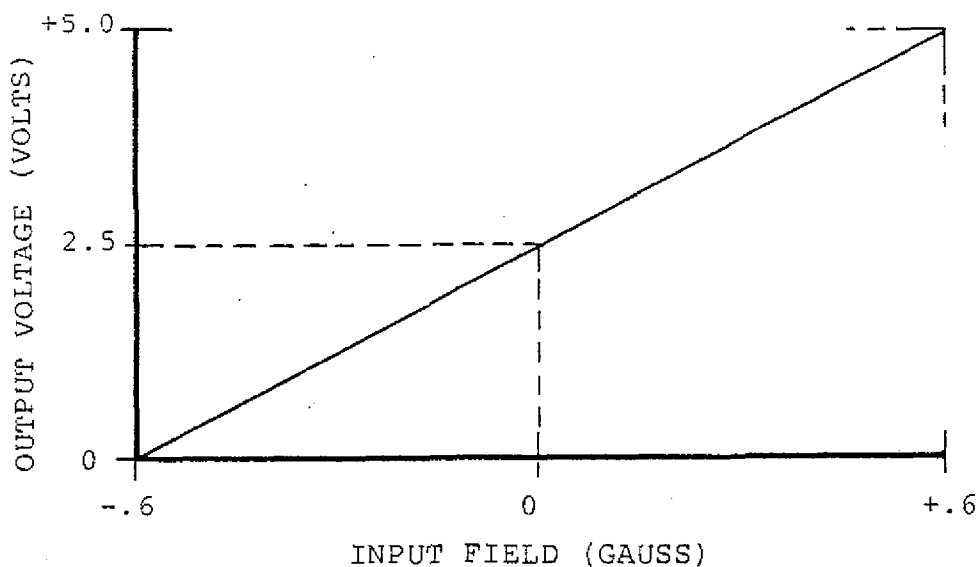


Fig. 3-7a. SENSOR TRANSFER CHARACTERISTIC

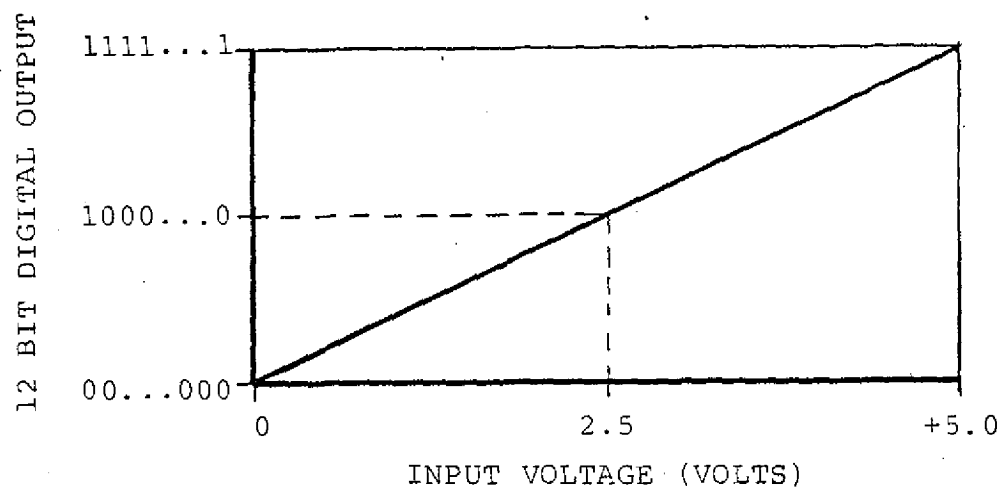


Fig. 3-7b. VDC TRANSFER CHARACTERISTICS

SIGN BIT	
1	0
$x = x_0 + \sum_{i=1}^{11} x_i \cdot 2^i$ <p>($x = x_0 + x^*$)</p> <p>Where:</p> <p>$x_0 = 0$</p> <p>$x^* =$ The 11 least significant bits of the binary number</p>	<p>$x = x_0 + 2$'s complement of the 11 least significant bits</p> <p>$x_0 = 1$ (indicating negative quantity)</p>

Fig. 3-8 CONVERSION OF DATA

The third function of the "SAMP" subroutine was to reverse the sign of the Hx and Hy data (to correct a test fixture problem) and to correct for sensor offsets. Although analog subsystem offsets are corrected by adjusting either the sample and hold module or the ADC, the independent sensors themselves have offsets⁴. Offset errors for the laboratory instrument were compensated by determining the offset correction term for each sensor (method described in detail in Chapter V) and then either adding or subtracting the term to the respective data during the sample subroutine. By characterizing the sensor errors⁵, actual datum could be improved further during this step.

The final function of the "SAMP" subroutine was to correct for sensor orthogonality error (subroutine "ORTH"). Although the sensors were physically aligned and specified to have orthogonality characteristic [Ref. 3-34] less than ± 1 degree relative to the base coordinates, this nonorthogonality contributes appreciably to total system error (see error analysis in Chapter IV). The physical misalignment of the sensors was determined experimentally (Chapter V) and determined to be mainly a misalignment of sensor x in the x-y plane as illustrated in Fig. 3-9.

The actual data measured with the x axis sensor is then related to the true Hx and Hy values as

$$Hx^1 = Hx \cos \epsilon - Hy \sin \epsilon .$$

⁴With zero stimulus applied the sensors have a finite nonzero output. This error in the fluxgate magnetometer is a function of temperature, voltage and magnetic remanence in the sensor magnetics [Ref. 3-36].

⁵Sensor characteristics relating the temperature and power supply coefficients of offset error and nonlinearity can be derived empirically.

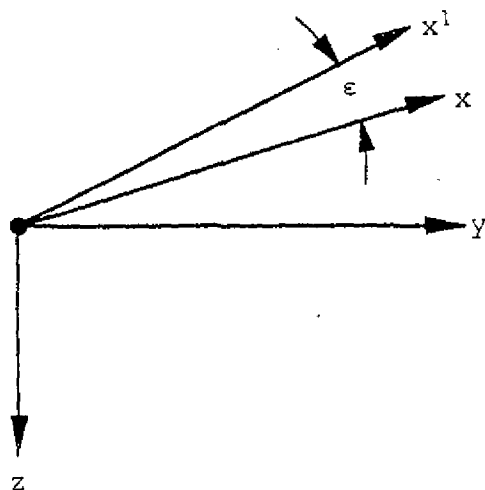


Fig. 3-9 X AXIS NONORTHOGONALITY

Using small angle approximations, we can solve for the desired true value of H_x

$$H_{x^1} \approx H_x - H_y \sin \epsilon \quad (3-1a)$$

$$H_x = H_{x^1} + H_y \sin \epsilon \quad (3-1b)$$

By measuring ϵ (Chapter V) and storing the angle as a constant, the x axis data was then restored using equation 3-1b above in subroutine "ORTH".

2) Subroutines ROTX and ROTY

These subroutines compute arithmetic values for H_{xh} and H_{yh} of equation 2-11b using sign magnitude quantities and table lookup to determine solutions for the transcendental functions. Subroutines "SADD" and "SMPY" are nested and used to perform double precision add and multiply as required.

3) Subroutine HVEC

Following computation of the horizontal X and Y axis magnetic vector, the subroutine "MAIN" calls subroutine "HVEC" to compute the square of the horizontal vector. Vectors Hx and Hy are squared by calling subroutine "SQU" then added, yielding $H(\text{HORIZONTAL})^2$.

4) Subroutine WICH

To compute heading, equation 2-1 (or a similar form) must be solved using the horizontal magnetic field vector and either the x or y axis horizontal field component. Although the square root operation implied in equation 2-1 could be implemented using a numerical technique [Ref. 3-37, 3-38], the computation time is decreased by using a table lookup method. Subroutine "WICH" (Fig. 3-10) compares the absolute magnitude of the two horizontal field vectors Hx and Hy to determine the relative heading of the aircraft⁶ with respect to the north-south and east-west axes (Fig. 3-11).

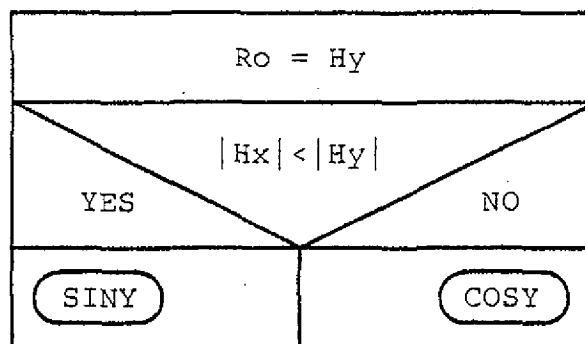


Fig. 3-10. SUBROUTINE "WICH"

⁶If $|Hx| < |Hy|$, then an equation similar in form to 2-1a must be used.

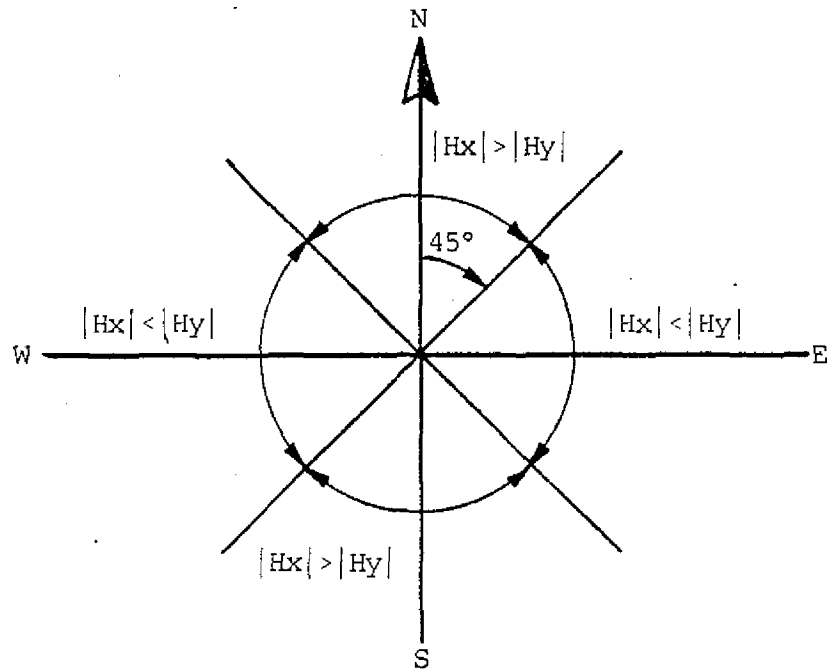


Fig. 3-11. MAGNITUDES OF H_x AND H_y RELATED AIRCRAFT HEADING

5) Subroutines COSY and SINY (Fig. 3-12, 3-13)

Depending on the relative absolute magnitudes of H_x and H_y , either "COSY" or "SINY" is called to compute aircraft heading. These subroutines invoke subroutine "DIVI" to form the quotient of the axis vector squared and the horizontal field vector squared (a double precision operation). Subroutine "ANGL" is then called to perform an associative table lookup operation using successive approximation and interpolation to complete the inverse cos squared operation. The double precision binary quantity is then converted to three digit binary coded decimal format (BCD) prior to computation of aircraft heading (subroutine "HDG").

The subroutine "SINY" of Fig. 3-12 includes a subtraction of the computed angle from 90 degrees following conversion to BCD format. This operation ensures that the angle passed to

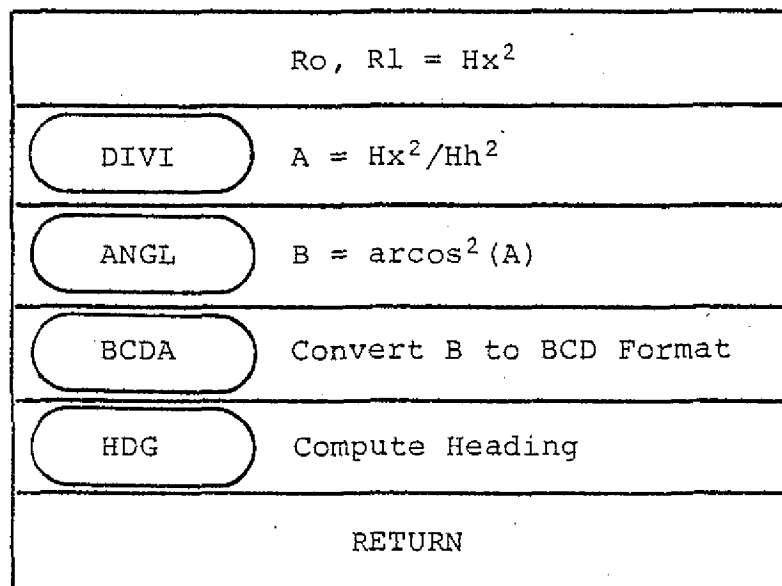


Fig. 3-12. SUBROUTINE "COSY"

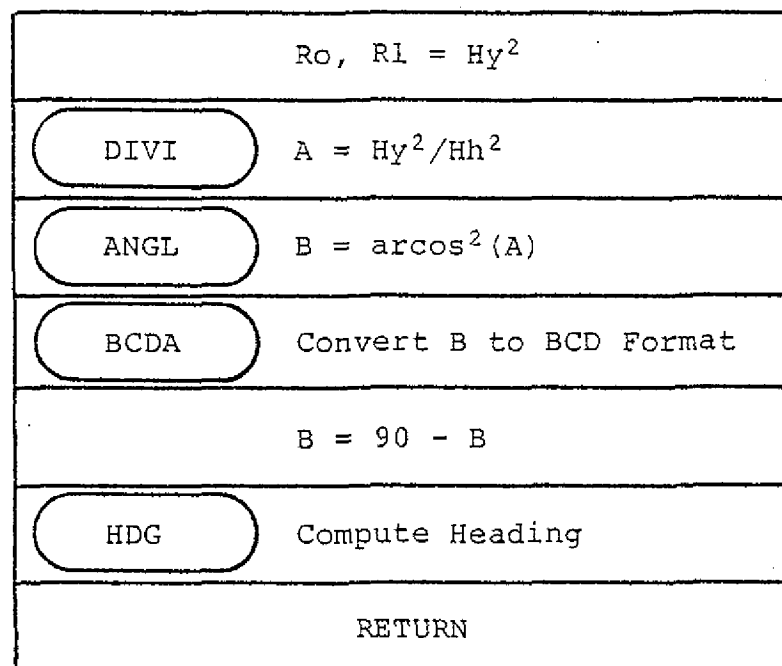


Fig. 3-13. SUBROUTINE "SINY"

the calling subroutine upon exiting either "SINY" or "COSY" is an aircraft heading angle relating sensor x to the north-south axis.

6) Subroutine HDG (Fig. 3-14)

The function of this subroutine is to compute aircraft heading having established the angle between the x axis sensor and the north-south geodetic axis. Determination of the actual heading is accomplished by comparing the signs of both the x and y axis horizontal vectors prior to computing heading (Fig. 3-15). It should be noted that all of the preceding computations leading to horizontal vector data were on sign magnitude quantities preserving the correct horizontal vector polarities⁷.

3-5 CONCLUSIONS

This chapter has outlined the practical aspects of designing an instrument to evaluate both the heading algorithms and solid state magnetic indicator proposed in previous chapters. The chapter outlined a design approach that can be used to implement a microprocessor based instrument. In particular, the need to consider the total system hardware requirements while simultaneously considering the programming requirements was identified. Design proceeded by outlining a system block diagram (Fig. 3-1) with major subsystems considered. The instrument required a special purpose computer with an analog subsystem to sample and digitize five sensor signals. Timing and control of the analog subsystem plus digital processing of data was controlled by a microprocessor based central processing unit (CPU). Memory for permanent storage of

⁷It is possible at certain attitudes to require sign reversals when computing horizontal vectors.

SIGN OF Hx ?			
POSITIVE		NEGATIVE	
SIGN OF Hy		SIGN OF Hy	
POSITIVE	NEGATIVE	POSITIVE	NEGATIVE
HDG = 360 - ANGLE	HDG = ANGLE	HDG = 180 + ANGLE	HDG = 180 - ANGLE
<div> <div>HDG</div> <div>=360 360</div> </div>			
HDG = 0			
RETURN			

Fig. 3-14. SUBROUTINE "HDG"

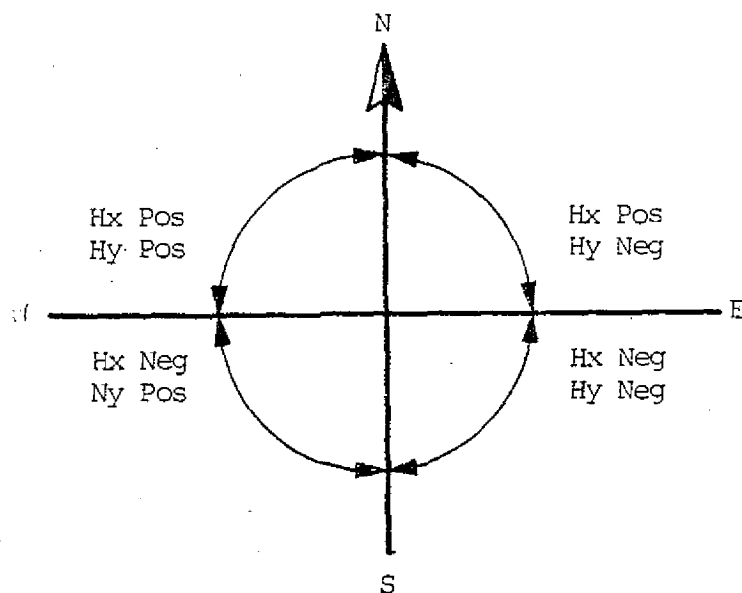


Fig. 3-15. POLARITIES OF HORIZONTAL VECTORS RELATED TO AIRCRAFT HEADING

instructions and temporary storage of data was implemented using memory chips organized on cards with 2048 byte capacity. The particular memory chips selected feature pin compatibility⁸ with both read only and volatile random access versions. System inputs consisted of sensor signals from a three axis solid state fluxgate magnetometer plus two analog signals simulating gyroscope outputs. System outputs consist of visual seven segment readout displaying computed heading. In addition, an RS-232 teletype interface was provided to facilitate system development and experimentation.

By identifying the total system in block diagram form at the very beginning, the role and requirements of each subsystem as well as the supporting software were identified. The design then evolved on a modular basis with each subsystem and its supporting program developed in parallel. In this manner pin assignments for input/output ports and critical timing requirements that involved both hardware and software consideration were handled efficiently. By outlining the program requirements in flow chart form (analogous to the block diagram of the hardware subsystem), subroutines were identified facilitating a modular program development. Where possible, subroutines were shared in a nested manner avoiding replication of programming and waste of memory.

Details of error analysis and calculation of overall system throughput rate were deferred to Chapter IV. It was pointed out however, that errors induced by imprecision of data plus truncation and roundoff during processing of the algorithm were to be considered early in the design phase. These data were required to select the sensors and the analog to digital

⁸Memory integrated circuit (IC) devices of both types can be used in the same mechanical sockets with actual chip type being used transparent to the remainder of the system.

converter as well as to design the supportive software for the analog subsystem. In addition, the data precision requirements were necessary prior to programming the algorithm⁹.

By incorporating a microprocessor as the main CPU element, considerable sophistication in both control and computing performance was achieved. The overall system was designed relatively quickly, provided a convenient laboratory instrument for evaluation of the proposed algorithms and featured inherent flexibility.

⁹Some of the subroutines required double precision manipulations to maintain overall system accuracy.

CHAPTER IV

HEADING INSTRUMENT ERROR ANALYSIS

4-1 INTRODUCTION

The heading instrument designed to evaluate the heading and solid state remote magnetic indicator algorithms is prone to error from many sources. These errors will accumulate and degrade the accuracy of aircraft heading or yaw angle computations. This chapter addresses the various error sources to determine their relative magnitudes and effects on the overall computation.

Prior to beginning the hardware design of the microprocessor based instrument many of these potential error sources were considered. Their effects were considered in establishing parameters such as word lengths, A/D converter precision, computation speeds, sampling rates, magnetometer sensor accuracies, system noise tolerance, etc. As the design of the microprocessor based system evolved, the error analysis refined. Ultimately, important limitations in instrument design and operation were identified by combined error analysis and empirical data. By carefully analyzing the source and extent of the limiting parameters (such as sensor offset and non-orthogonality), the magnitude of errors unique to this laboratory sensor array were identified. Specialized software was then added (with empirically derived constants) to correct for the otherwise limiting sensor irregularities improving the total system performance.

In this manner, it is apparent that error analysis is an integral part of instrument design. Not only are important parameters identified early in the design cycle (prior to system block diagram development), but shortcomings in conventional

sensors can be improved by judicial application of error correcting algorithms. In this case, data constants were determined after the final instrument became operational. The sensor peculiarities were analyzed empirically using the instrument itself.

The chapter begins by first identifying and carefully analyzing potential error sources in the sensors. This analysis is followed by a similar consideration of errors originating in the analog subsystem. Processing errors that originate due to the finite word length and precision of the microprocessor along with the effects of simplifications made to the algorithms are finally analyzed. The chapter then concludes with a summary of measurement errors, a sample error analysis, a comparison of predicted to measured error and a summary.

4-2 SENSOR ERRORS

The heading computation algorithm employing the remote magnetic indicator (Chapter II) is prone to error proportional to both fluxgate magnetometer sensor and gyroscope measurement errors. Errors inherent in the fluxgate magnetometer are summarized on the data sheet [Ref. 3-34]. Since the experimentation employed simulated gyroscope sensors with voltage levels accurately represented, the analysis of sensor errors will assume ideal gyroscope sensors to predict experimental data.

A) Sensor Offset Error

Magnetometer sensors exhibit error caused by both electronic and magnetic phenomena. Errors in the Develco sensors were outlined by Workentine [Ref. 4-1]. These offset errors are induced in the Develco sensors by both electronic offset voltages and currents in the respective sensor electronics and

by residual magnetic fields in the magnetic mass of the sensor assemblies. Although the physical and electronic design attempts to reduce offset error, a finite non-zero output can exist when a zero input is applied.

Offset error for each sensor in the Develco model 9200C three axis magnetometer assembly is specified [Ref. 3-34] as "Zero Field Bias +2.5 Volts $\pm 1.0\%$ ". This offset translates into a worst case maximum error voltage of

$$E_{\text{OFFSET}} = \pm(2.5\text{V} \times 0.01) = \pm 25\text{mV}$$

Since the offset error is sensor dependent, correction cannot be made at a single physical point (as for analog subsystem offsets described in Section 4-3). Corrections can however be made to the measured data by simply adding or subtracting a constant equal to the offset magnitude following each data measurement¹.

Offset values for each sensor used in the experiment were obtained by rotating the sensor into alignment with earth's magnetic field vector to measure both positive and negative maximum values. The difference in magnetic measurement (assuming negligible analog subsystem error) is related to system offset error composed of sensor electronic and sensor plus test fixture induced magnetic offset error. The actual offset error can be calculated using these two measurements

¹Offset corrections were made in the sample subroutine "SAMP" illustrated in Fig. 3-6a.

$$\begin{aligned}
 |E_{\max}| &= E_f + E_o \\
 |E_{\min}| &= E_f - E_o \\
 |E_{\max}| - |E_{\min}| &= (E_f + E_o) - (E_f - E_o) = 2 E_o \\
 E_o &= (1/2) (|E_{\max}| - |E_{\min}|)
 \end{aligned}$$

where

E_{\max} = The maximum positive voltage recorded when the sensor aligns with earth's field vector.

E_{\min} = The maximum negative voltage recorded when the sensor aligns 180° with earth's field vector.

E_f = The magnitude of earth's magnetic vector represented in volts.

E_o = The sensor offset voltage due to both electronic and magnetic phenomena

Data recorded during x, y and z axis offset measurements as described above are recorded in Table 4-1. Since the offset error is a function of sensor magnetic permeability, the actual offset value will vary with time depending on induced magnetic fields².

Final offset correction values were determined by rotating two sensors in the horizontal plane around the third vertical axis and measuring offsets in two sensors at a time. Recorded data for each sensor was previously corrected for orthogonality error by the sample subroutine "SAMP" (discussion

²For example, magnetized screwdrivers or other tools used near the sensor will alter the residual magnetic field.

SENSOR AXIS	DATA RECORDED (HEXADECIMAL)		OFFSET (HEXADECIMAL PLUS SIGN)
	Emax	Emin	
X	628	E78	+40
Y	640	E5D	-15
Z	637	E68	-25

Table 4-1 OFFSET DATA DERIVED BY MEASURING
EARTH'S FIELD

of this correction follows in Section 4-2B). Data recorded in this manner appears in Tables 4-2 and 4-3. Final correction terms for correcting sensor offset error were calculated using these data. Offset terms to be added or subtracted from respective data channels are tabulated in Table 4-4.

By correcting system offset errors in this manner, the effective error contribution can be reduced appreciably (see final data discussion Chapter V). For a flight instrument, sensor offset characteristics as a function of temperature variation and supply voltage can be derived empirically and appropriate offset corrections made by computing the value of the correction term variable. Magnetically induced offsets can be reduced by degaussing the sensor assembly periodically.

B) Axis Alignment Errors

The error specification of [Ref. 3-34] indicates that the maximum axis alignment error is ± 1 degree relative to base referenced coordinates. This error results in sensor directional uncertainty as illustrated in Fig. 4-1. Each sensor is located within a right circular cone with axis along the true sensor axis and vertex at the common sensor origin. Although this alignment uncertainty contributes no error in determining the total magnetic vector

$$\bar{H} = (\bar{H}_x^2 + \bar{H}_y^2 + \bar{H}_z^2)^{\frac{1}{2}},$$

there is considerable uncertainty in attempting to resolve the true magnetic field component along any axis of the reference coordinate system. This alignment uncertainty of magnetic sensors limits system performance of conventional field direction measuring apparatus [Ref. 4-1].

Protractor Heading Measurement (Degrees)	Data Measured		Protractor Heading Measurement (Degrees)	Data Measured		Error Due To Offset	
	Hx	Hy		Hx	Hy	X	Y
(Units)	(Units)		(Degrees)	(Units)		(Units)	
0	8	-759	180	83	720	75	-39
345	199	-743	165	-112	704	87	-39
330	383	-677	150	-292	638	91	-39
315	540	-569	135	-448	527	92	-42
300	666	-421	120	-573	381	93	-40
285	749	-249	105	-658	206	91	-43
270	783	- 62	90	-696	14	87	-48
255	770	132	75	-681	-179	89	-47
240	706	314	60	-616	-362	90	-48
225	597	473	45	-504	-521	93	-48
210	449	601	30	-359	-645	90	-44
195	273	687					
180	(DATA UNAVAILABLE DUE TO TEXT FIXTURE LIMITATION)						
165							
TOTAL OFFSETS						978	477
AVERAGE OFFSETS						88.9	43.4

Table 4-2 X AND Y AXIS ERROR MEASURED BY ROTATING
X, Y AROUND Z IN THE HORIZONTAL PLANE

Protractor Heading Measurement (Degrees)	H _z Data Measured (Units)	Protractor Heading Measurement (Degrees)	H _z Data Measured (Units)	Offset Error (Units)
0.5	0	180.5	-56	-56
315.5	-527	135.5	469	-58
270.5	-763	90.5	707	-56
225.5	-571	45.5	513	-58
TOTAL OFFSET				-228
AVERAGE OFFSET				-57

Table 4-3 Z AXIS OFFSET ERROR MEASURED BY ROTATING
THE Z AXIS AROUND THE VERTICAL X AXIS

Sensor Axis	Total Average Offset (Units)	Required Correction	Amount of Correction Decimal	Binary	Hex
X	88.9	Subtraction	45	00101101	02D0
Y	43.4	Addition	22	00010110	0160
Z	47.0	Addition	29	00011101	01D0

Table 4-4 OFFSET CORRECTION VALUES

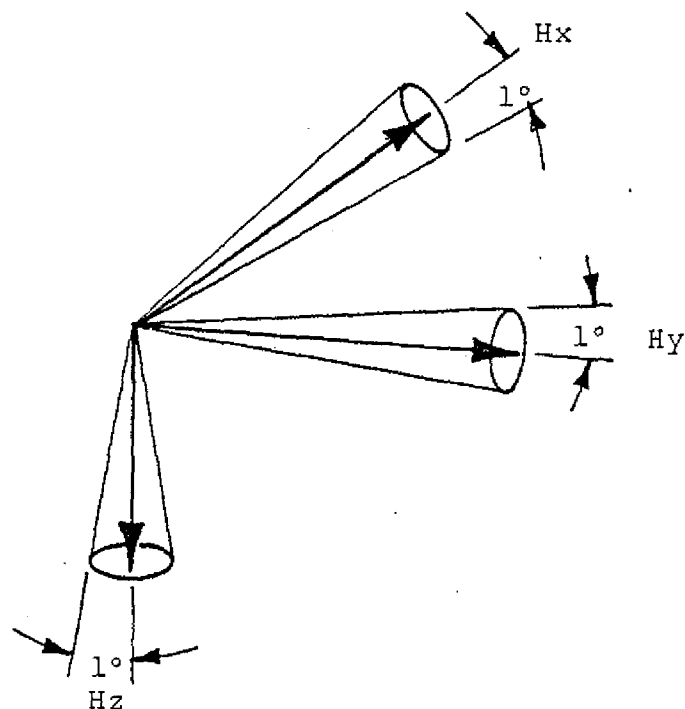


Fig. 4-1 SENSOR ALIGNMENT UNCERTAINTY

Although this error source can be reduced by physically aligning the sensors more accurately during assembly, cost of the sensors increases. Ultimately, directionality of the magnetic sensors becomes a function of the physical sensor itself and more accurate sensors are required as pointed out by Gise [Ref. 4-2]. A heading system that tolerates sensor misalignment is therefore a very desirable alternative to requiring precise alignment or more elaborate sensors.

During assembly of the Develco fluxgate magnetometer sensor array, sensor misalignment is determined by using earth's magnetic field and a precision mechanical rotation assembly. A sensor (assume the X axis) is aligned with earth's magnetic

vector by positioning the sensor to maximize electrical output³. One of the other sensors (assume the y axis) is aligned with the rotation axis of the precision calibration assembly (Fig. 4-2) and perpendicular to the first by rotating the sensor array around the second sensor axis (y axis in this case) and adjusting its relative position until a null output is achieved at all rotation angles. Mechanical orthogonality of the sensors is then limited only by the mechanical imprecision of the calibration device (orthogonality within ± 0.01 degrees can be easily achieved in the calibration tool) and by the directional characteristics of the physical sensors.

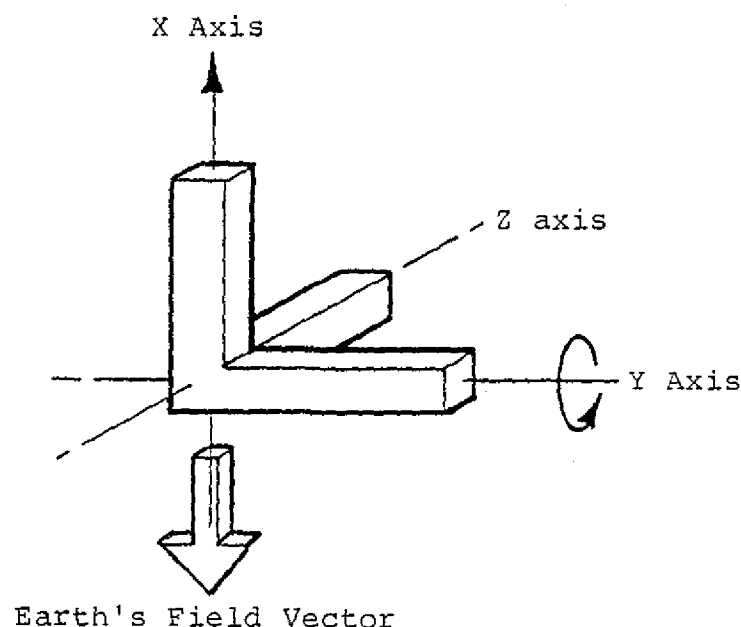


Fig. 4-2 MECHANICAL ORIENTATION OF THE MAGNETOMETER SENSORS DURING CALIBRATION

In addition to functioning as an alignment apparatus, the calibration device described above provides a convenient means

³By maximizing or nulling a measurement, the mechanical positioning is a function of only the field and the resolution of the voltage measuring device obviating errors due to physical position measurement.

to characterize sensor assemblies after final assembly adjustments are made. Any misalignment of the second sensor relative to the first results in a coning of the second sensor around the rotation axis⁴ with a sinusoidal output voltage that is a function of total earth's magnetic field and axis alignment error. The peak to peak voltage resulting from sensor coning is recorded during the final alignment test and made available to sensor purchasers. Coning voltages developed for the sensor assembly used with this experiment were obtained from Develco [Ref. 4-3] and are recorded in Table 4-5. Sensor misalignment for each axis can be derived using additional data provided by Develco along with additional empirical data derived by experimentation.

The total ambient magnetic field at the Develco laboratory is measured using the three sensors (applying equation 4-1) and is supplied as digital data. In our case, the total field measured was 1573 units or

$$\frac{1573 \text{ units}}{2048 \text{ units Full Scale (F.S.)}} \times 60,000 \text{ gamma F.S.} = 46,084 \text{ gamma } (\gamma)$$

$$\text{Sensitivity of the sensor} = \frac{2.5 \text{ Volts F.S.}}{60,000 \gamma \text{ F.S.}} = 42 \mu\text{Volts}/\gamma$$

Considering the X axis sensor, coning resulted in a signal of 38 mV peak to peak (or 19mV peak). Misalignment of the X axis sensor from the Y-Z plane can then be calculated as

⁴Assume that the first axis is initially adjusted for maximum output to align it with earth's field and the rotation axis is perpendicular to the field.

SENSOR ASSEMBLY NO. S/N 1043-013

Rotation Axis	Coning Voltage (Peak-Peak mV)	Orthogonality Error (Degrees)
X	38	0.57
Y	8	≈0
Z	51	0.76

Table 4-5 MAGNETOMETER ORTHOGONALITY MEASUREMENTS

Peak Signal = 19 mV or 456 gamma angular misalignment

$$\epsilon_x = \sin^{-1} \frac{456}{46,084}$$

$$\epsilon_x = 0.57 \text{ degrees}$$

Similarly, the Y and Z axis have misalignment errors of $\epsilon_y \approx 0$ and $\epsilon_z = 0.76$ degrees with respect to the X-Z and X-Y planes respectively (sensor orthogonality errors are tabulated in Table 4-5).

Having established that sensor orthogonality errors exist, the remaining task is to identify the direction that the sensor axis points relative to the other two sensor axes. Since the Y axis has relatively little orthogonality error, it will be assumed to be perpendicular to the X-Z plane. In addition, since the Hz data enters into the algorithm in a second order manner relative to the Hx and Hy measured data, correction and characterization of the Hx sensor was considered to be of primary concern. Orientation of the X axis sensor relative to the Y and Z axes was determined empirically.

Angular position of the X axis sensor can be described using the error angles ϵ_{xy} and ϵ_{xz} as delineated in Fig. 4-3. Characterization of sensor orthogonality error in terms of these two angles would enable algorithmic corrections of measured data.

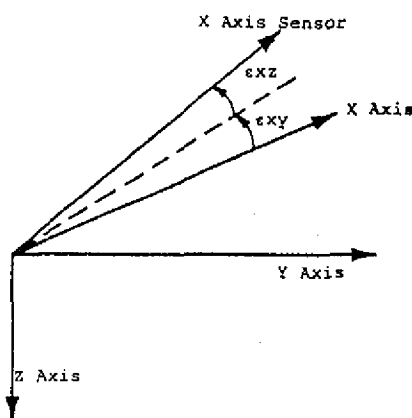


Fig. 4-3 X AXIS SENSOR ORIENTATION

1) Empirical Determination of ϵ_{xz}

The angle ϵ_{xz} (angle between the x axis sensor and the z axis of the geodetic coordinate system) was determined in several steps using the test apparatus described in Chapter V.

- i) The x and y sensors were oriented in the horizontal plane with the z axis sensor vertical downward.
- ii) The x and y sensors were rotated around the z axis with magnetic data measurements (corrected for sensor offset error as described in Section 4-2A) recorded in Table 4-6 for incremental rotation angles.
- iii) The total horizontal field at each angular position was calculated

$$H_{ht} = (H_x^2 + H_y^2)^{\frac{1}{2}}.$$

- iv) Average horizontal field H_{av} was computed by averaging the results of iii) above.
- v) The horizontal field deviation H_d was computed for each angular position; tabulated in Table 4-6 and plotted on Fig. 4-4.

$$H_d = (H_{av} - H_{ht})$$

The horizontal field deviation or error (as shown on Fig. 4-4) was now examined. An angular error ϵ_{xz} should cause the horizontal field error curve to peak at 90 and 180 degrees. Since this obviously was not the case, it was concluded that major error in x axis orthogonality was due to the component ϵ_{xy} .

Physical* Heading (Degrees)	Displayed** Heading (Degrees)	Measured Data (Units)		Total Computed Horizontal Field (Hht) (Units)	Hd (Hav-Hht) (Units)
		Hx	Hy		
355	90	12	-727	727	-3
335	70	258	-682	729	-1
315	50	477	-555	732	2
295	30	637	-362	733	3
275	10	720	-127	731	1
255	350	718	127	729	-1
235	330	628	363	725	-5
215	310	464	569	734	4
195	290	242	687	728	-2
175	270	-10	731	731	1
155	250	-258	686	733	3
135	230	-476	557	733	3
115	210	-635	362	731	1
95	190	-721	123	731	1
75	170	-718	-133	730	0
55	150	-628	-371	729	-1
35	130	-460	-565	729	-1

Total Hht = 12415

Average (Hav) = 730

*Measured using a protractor on the test apparatus.

**Computed and displayed digitally by the instrument.

Table 4-6 MEASUREMENT OF HORIZONTAL FIELD

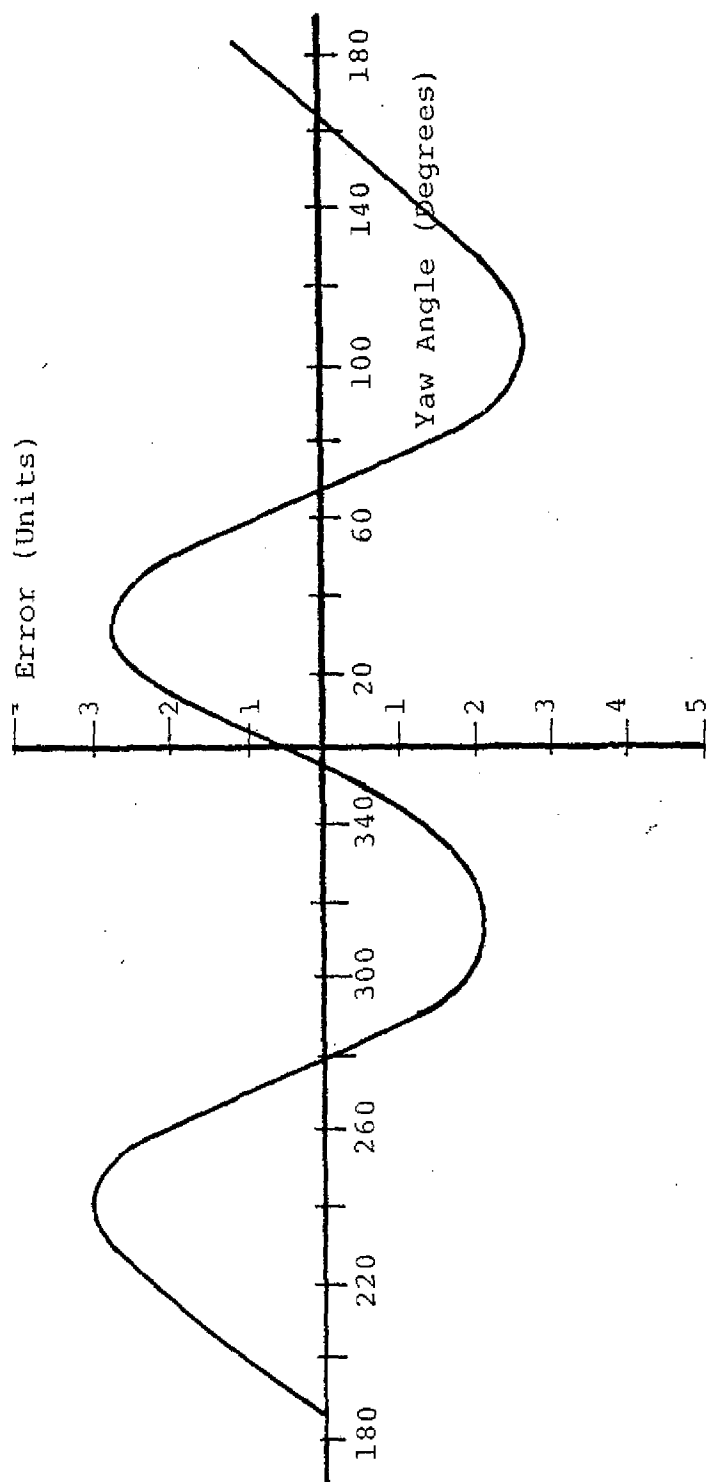


Fig. 4-4 DEVIATIONS OF THE HORIZONTAL FIELD MEASUREMENT FROM THE MEAN

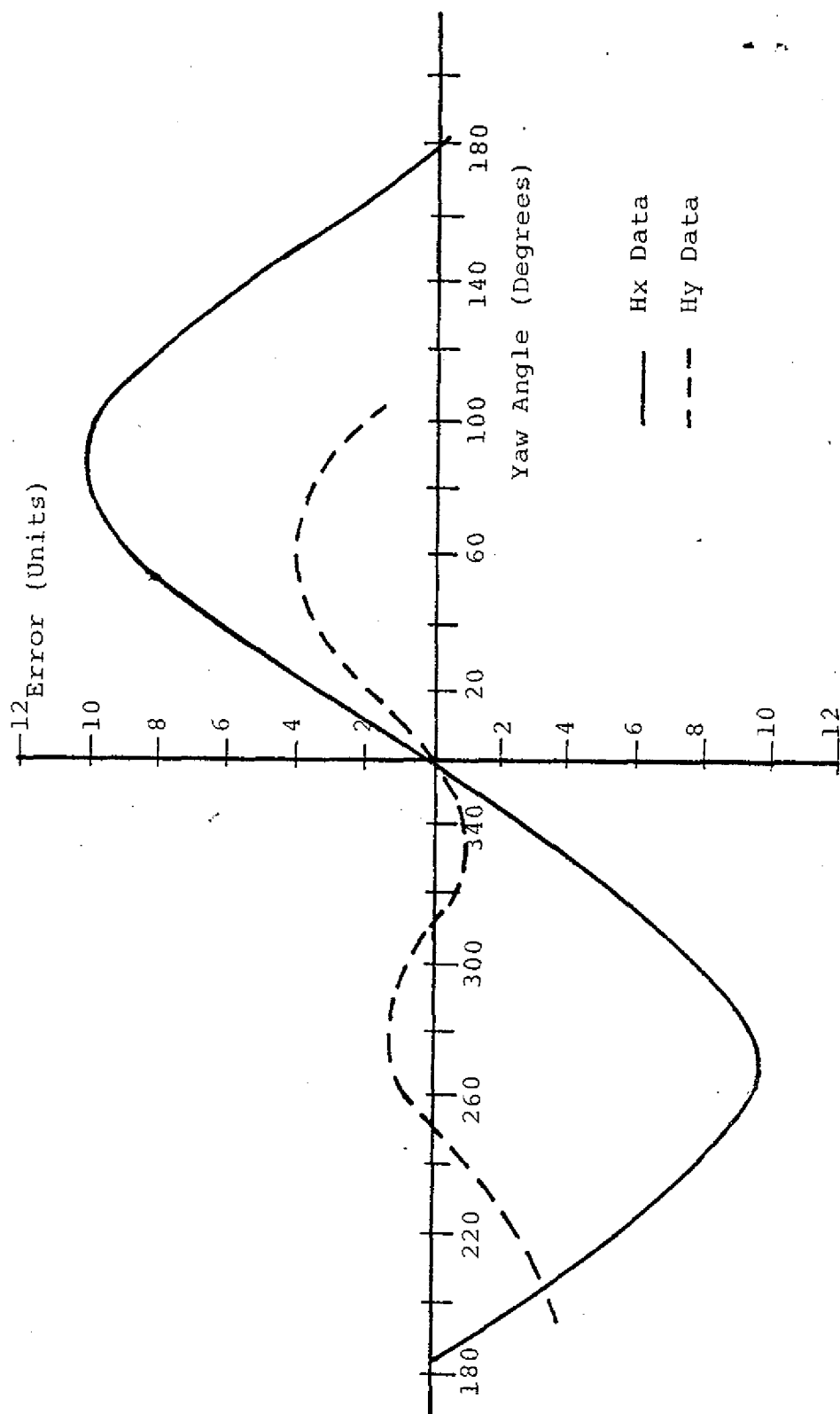


Fig. 4-5 DEVIATION OF Hx AND Hy DATA FROM THE COMPUTED FIELD COMPONENTS AS A FUNCTION OF YAW

2) Empirical Determination of ϵ_{xy}

The angle ϵ_{xy} representing x axis sensor misalignment relative to axis y was measured as follows:

Steps i) and ii) above were repeated with the exception that the calculated values for H_x and H_y (H_{xc} and H_{yc} respectively) were recorded with measured H_x and H_y data (H_{xm} and H_{ym} respectively) in Table 4-7. The calculated values were obtained by assuming that the angle ϵ_{xz} as determined above was negligible and that the y axis sensor was perpendicular to the x-z plane. With these assumptions, we note that at the heading of zero degrees (extrapolated between display of 10 and 350 degrees of Table 4-7 and Fig. 4-5), there is no error in yaw due to either H_x or H_y . By physically rotating the sensors in fixed intervals from yaw = 0 degrees and noting that the horizontal field $H_h = 730$ units, we can then compute expected H_x and H_y data at respective yaw orientations.

Physical orientation of the x axis sensor is easily determined by considering orientation at the maximum error excursions. These observations are illustrated in Fig. 4-6. We note that the only possible orientation of the x axis sensor satisfying the data in Fig. 4-5 is that of Fig. 4-6.

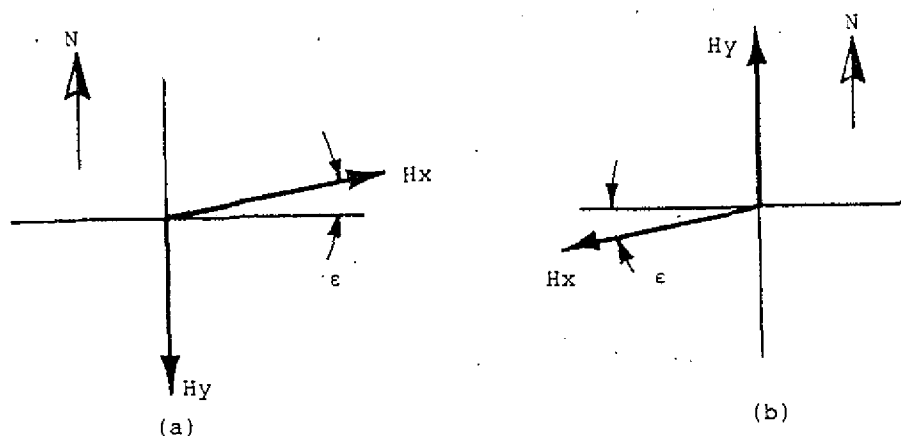


Fig. 4-6 (a) SENSORS ORIENTED AT YAW = +90 degrees
(b) SENSORS ORIENTED AT YAW = +270 degrees

Physical* Heading (Degrees)	Displayed** Heading (Degrees)	Measured Data (Units)		Computed Data (Units)		Deviation (Units) (Hxm-Hxc) (Hym-Hyc)	
		Hxm	Hym	Hxc	Hyc	(Hxm-Hxc)	(Hym-Hyc)
355	90	12	-727	0	-730	+12	+ 3
335	70	258	-682	250	-686	+ 8	+ 4
315	50	477	-555	469	-559	+ 8	+ 4
295	30	637	-362	632	-365	+ 5	+ 3
275	10	720	-127	719	-127	+ 1	0
255	350	718	127	719	+127	- 1	0
235	330	628	363	632	365	- 4	- 2
215	310	464	569	469	559	- 5	10
195	290	242	687	250	686	- 8	1
175	270	-10	731	0	730	-10	1
155	250	-258	686	-250	686	- 8	0
135	230	-476	557	-469	559	- 7	- 2
115	210	-635	362	-632	365	- 3	- 3
95	190	-721	123	-719	+127	- 2	- 4
75	170	-718	-133	-719	-127	1	- 6
55	150	-628	-371	-632	-365	4	- 6
35	130	-460	-565	-489	-559	9	- 6

* Measured using a protractor on the test apparatus.

** Computed and displayed digitally by the instrument.

Table 4-7 MEASURED AND COMPUTED HX AND HY DATA
IN THE HORIZONTAL PLANE

Magnitude of the angle ϵ_{xy} can be computed as follows using data from Fig. 4-5

Max. delta from Fig. 4-5 = 10 units
Average horizontal field = 730 units

$$\epsilon_{xy} \text{ max} = \sin^{-1} \frac{10}{730}$$

$$= 0.79 \text{ degrees}$$

We note that the angle of 0.79 degrees is approximately the same as determined by Develco during manufacture of the sensors (Table 4-5). The added error is due to test set inaccuracy.

C) Fluxgate Sensor Noise Induced Error

The analog output from the fluxgate sensors can exhibit an error due to signal uncertainty resulting from noise. Although the data sheet [Ref. 3-34] indicates that 5mV peak to peak of ripple can exist on the output, the frequency content centers in the 550 kHz range (driver frequency of the fluxgate magnetometer) and no appreciable ripple⁵ exists below 60 Hz (especially when the sensor output is filtered prior to data sampling). The noise specification of less than 1 gamma peak to peak in the 1 Hz bandwidth region is also negligible. In summary, no appreciable error due to noise on the magnetometer signal lines is evident.

D) Magnetometer Gain Error

The magnetometer is specified to have gain (sensitivity) of 2.5 Volts/600 milligauss, $\pm 1\%$ which translates into a maximum signal uncertainty of

⁵Verbally confirmed by Workentine of Develco [Ref. 4-1].

$$\pm(2.5V \times 0.01) = \pm 25 \text{ mV.}$$

This represents a sensor transfer function of 4.16 Volts/gauss or 0.24 gauss per volt. The uncertainty then can be expressed as

$$\begin{aligned} \pm(0.24 \text{ gauss} \times 0.01) &= \pm 2.4 \text{ milligauss} \\ &= \pm(2.4 \times 10^2) \text{ gamma} \end{aligned}$$

Since this error is not corrected in the laboratory instrument it will be considered in total in the final error analysis. It is worth noting however, that should the magnetometer gain uncertainty be characterized, gain corrections for each sensor could be made during computation by the computer. In addition the error term is proportional to actual signal level applied.

E) Magnetometer Linearity Error

D.C. linearity of the magnetometer is specified to be $\pm 0.5\%$ of signal level. This uncertainty at full scale can be expressed as $\pm(2.5 \text{ Volts} \times 0.005) = \pm 12.5 \text{ mV}$. Alternately, linearity error can cause a signal uncertainty of ± 1.2 milligauss or $\pm(1.2 \times 10^2)$ gamma. Linearity error is also not corrected during computation and is considered in the final error analysis. By simply characterizing and correcting the linearity characteristics of each sensor, considerable improvement in system accuracy could be achieved.

4-3 ANALOG SUBSYSTEM ERROR ANALYSIS

The analog subsystem of the instrument is outlined in block diagram form in Fig. 4-7. This subsystem accepts analog signals from magnetometer and gyroscope transducers, performs a time division multiplexing between the signals and digitizes

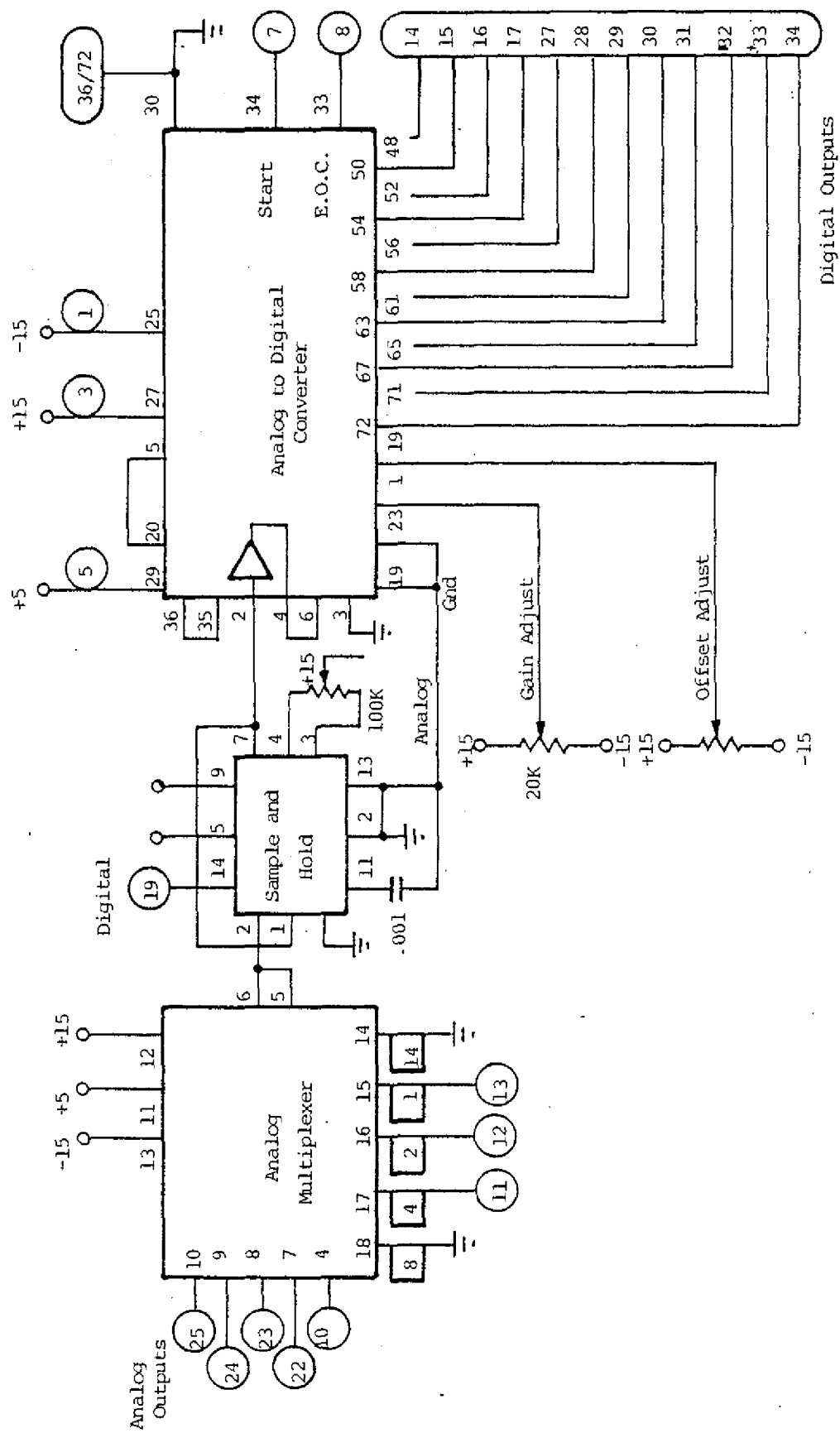


Fig. 4-7 THE ANALOG SUBSYSTEM

the respective signals prior to subsequent processing by the computer. During this data acquisition and conversion process, errors are introduced into each of the signals. This section addresses the potential error sources and computes the respective error contributions to be expected during operation of the instrument.

Although the multiplexer and sample and hold blocks of Fig. 4-7 could be eliminated (eliminating possible error sources) by digitizing each signal with a unique analog to digital converter, it can be shown that such a system would be expensive and difficult to implement. The analog to digital converter (A/D) quantizes an analog signal in a finite amount of time. Speed of conversion is predicted in a finite amount of time by both the resolution of the converter and the frequency of the signal to be converted. Time required to perform a conversion is generally called the "aperature time".

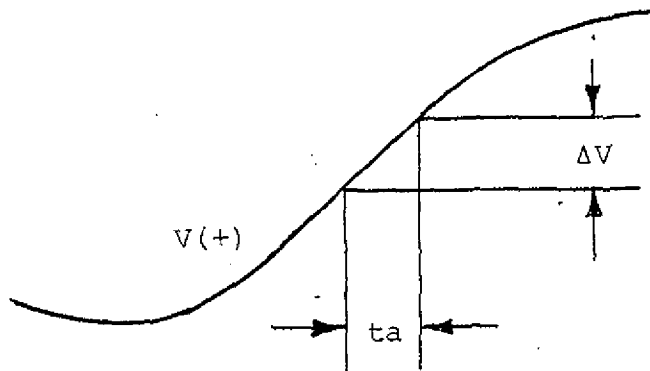


Fig. 4-8 APERATURE TIME AND AMPLITUDE UNCERTAINTY

As illustrated in Fig. 4-8, aperature time and amplitude uncertainty are related by the time rate of change of the analog signal. For the particular case of a sinusoidal signal to

be converted, the maximum rate of change occurs at the zero crossing of the waveform and the amplitude change is:

$$\Delta V = \frac{d}{dt} (V \sin wt)_{t=0} \times t_a \quad (4-1a)$$

$$\Delta V = V w t_a \quad (4-1b)$$

$$\text{giving } \frac{\Delta V}{V} = w t_a = 2 \pi f t_a. \quad (4-2)$$

From this result we can determine the aperture time required to digitize a 30 Hz signal to 12 bits resolution (a resolution of 1 part in 4096 or 0.0244%).

$$t_a = \frac{V}{\Delta V} \times \frac{1}{2 f} = \frac{.000244}{6.28 \times 30} = 1.3 \times 10^{-6}$$

This result indicates that to remain within 1 bit of resolution (0.0244%) we require an aperture time of 1.3 microseconds to process analog signals varying at a rate of 30 Hertz. It can be seen that the system would require fast A/D converters plus extremely fast computational capability to accommodate this configuration of sensors and analog subsystem. By using multiplexing and sample and hold circuitry we can however reduce the number of A/D converters required to one and alleviate the aperture and processing requirements imposed above.

The operation of sampling to be used by the instrument is illustrated in Fig. 4-9 which shows an analog signal and a train of sampling pulses. The pulses are provided by the central processing unit. A switch connects the analog signal for a very short period of time to the hold circuitry charging a capacitor and storing the sampled voltage until the next sample is required. This type of sampler is called sample and hold.

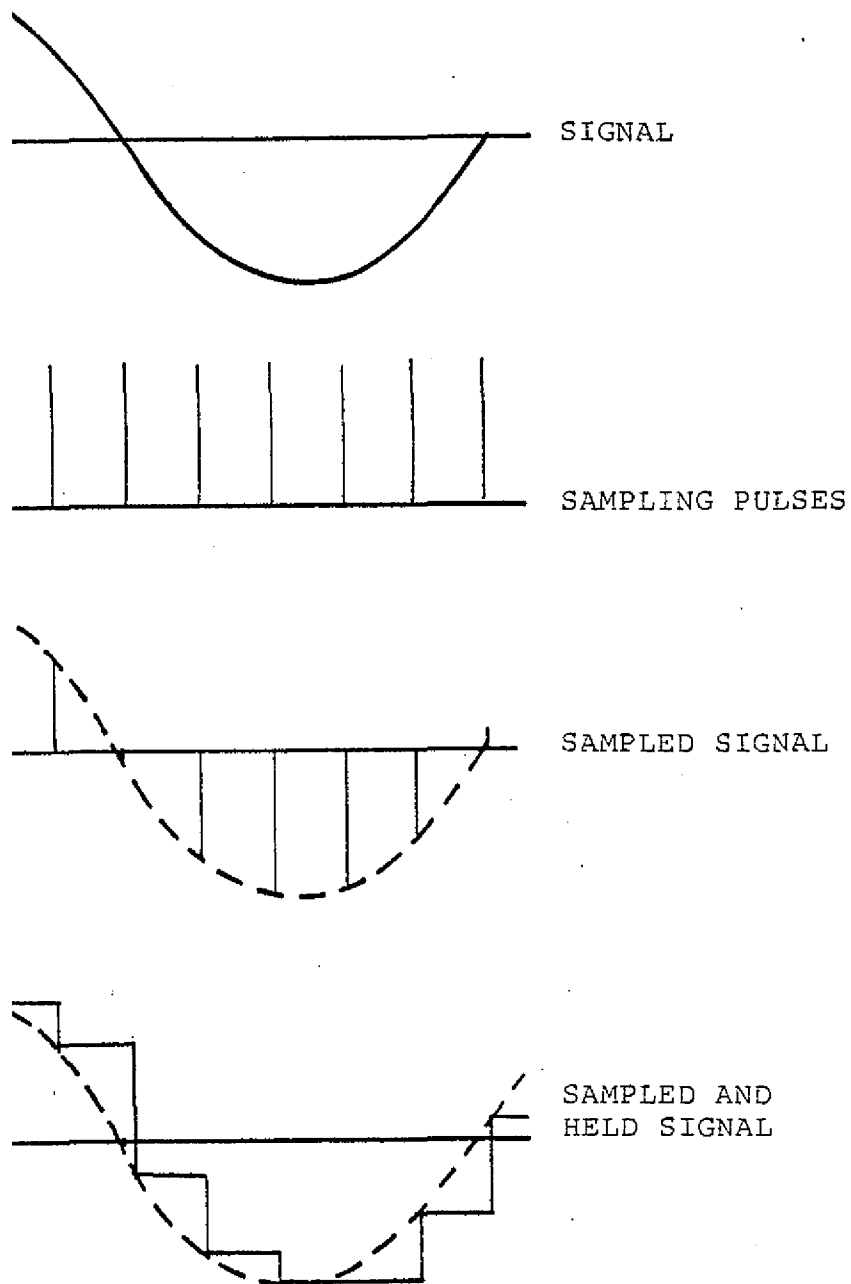


Fig. 4-9 SIGNAL SAMPLING PROCESS

A) Sampling Rate Errors

The process of uniformly sampling a function of continuous time can yield a significant source of error if the sampling period T is selected too large [Ref. 4-4, 4-5]. This error can be illustrated by considering an analog signal $x_a(t)$ that has the Fourier representation [Ref. 4-6]

$$x_a(t) = \frac{1}{2\pi} \int_{-\infty}^{\infty} X_a(j\Omega) e^{j\Omega t} d\Omega \quad (4-3a)$$

$$X_a(j\Omega) = \int_{-\infty}^{\infty} x_a(t) e^{-j\Omega t} dt \quad (4-3b)$$

The sequence $x(n)$ with values $x(n) = x_a(nT)$ is said to be derived from $x_a(t)$ by periodic sampling and T is the sampling period. The reciprocal of T is called the sampling frequency or sampling rate. In order to determine the sense in which $x(n)$ represents the original signal $x_a(t)$, it is convenient to relate $X_a(j\Omega)$, the continuous-time Fourier transform of $x_a(t)$, to $X(e^{j\Omega})$, the discrete-time Fourier transform of the sequence $x(n)$. From (4-3a) we note that

$$x(n) = x_a(nT) = \frac{1}{2\pi} \int_{-\infty}^{\infty} X_a(j\Omega) e^{j\Omega nT} d\Omega \quad (4-4)$$

From the discrete-time Fourier transform we also obtain the representation [Ref. 4-4]

$$x(n) = \frac{1}{2\pi} \int_{-\pi}^{\pi} X(e^{j\omega}) e^{j\omega n} d\omega \quad (4-5)$$

To relate the equations (4-4) and (4-5) we can express (4-4) as a sum of integrals over intervals of length $2\pi/T$, as in

$$x(n) = \frac{1}{2\pi} \sum_{r=-\infty}^{\infty} \int_{(2r-1)\pi/T}^{(2r+1)\pi/T} X_a(j\Omega) e^{j\Omega nT} d\Omega \quad (4-6)$$

Each term in the sum can be reduced to an integral over the range $-\pi/T$ to $+\pi/T$ by a change of variables to obtain

$$x(n) = \frac{1}{2\pi} \sum_{r=-\infty}^{\infty} \int_{-\pi/T}^{\pi/T} X_a \left[j \left(\Omega + \frac{2\pi r}{T} \right) \right] e^{j \left(\Omega + \frac{2\pi r}{T} \right) nT} d\Omega \quad (4-7a)$$

$$x(n) = \frac{1}{2\pi} \sum_{r=-\infty}^{\infty} \int_{-\pi/T}^{\pi/T} X_a \left(j\Omega + j\frac{2\pi r}{T} \right) e^{j\Omega nT} e^{j2\pi rn} d\Omega \quad (4-7b)$$

If we now change the order of integration and summation and note that $e^{j2\pi rn} = 1$ for all integer values of r and n , we obtain

$$x(n) = \frac{1}{2\pi} \int_{-\pi/T}^{\pi/T} \left[\sum_{r=-\infty}^{\infty} X_a \left(j\Omega + j\frac{2\pi r}{T} \right) \right] e^{j\Omega nT} d\Omega \quad (4-8)$$

Substituting $\Omega = \omega/T$ we get

$$x(n) = \frac{1}{2\pi} \int_{-\pi}^{\pi} \left[\frac{1}{T} \sum_{r=-\infty}^{\infty} X_a \left(\frac{j\omega}{T} + j\frac{2\pi r}{T} \right) \right] e^{j\omega n} d\omega \quad (4-9)$$

which is identical in form to equation (4-5). We can therefore make the identification (equating like terms of (4-5) and (4-9))

$$X(e^{j\omega}) = \frac{1}{T} \sum_{r=-\infty}^{\infty} X_a \left(\frac{j\omega}{T} + j\frac{2\pi r}{T} \right) \quad (4-10)$$

We can also express (4-10) in terms of the analog frequency variable Ω (where $\Omega = \omega/T$) as

$$X(e^{j\omega T}) = \frac{1}{T} \sum_{r=-\infty}^{\infty} X_a \left(j\Omega + j\frac{2\pi r}{T} \right) \quad (4-11)$$

The last two equations clearly reveal the relationship between the continuous-time Fourier transform and the Fourier transform of a sequence derived by sampling. For example, if $X_a(j\Omega)$ is as depicted in Fig. 4-10a then $X(e^{j\omega})$ will be as shown in Fig. 4-10b when the sampling period T is too long and as shown in Fig. 4-10c if T is short enough.

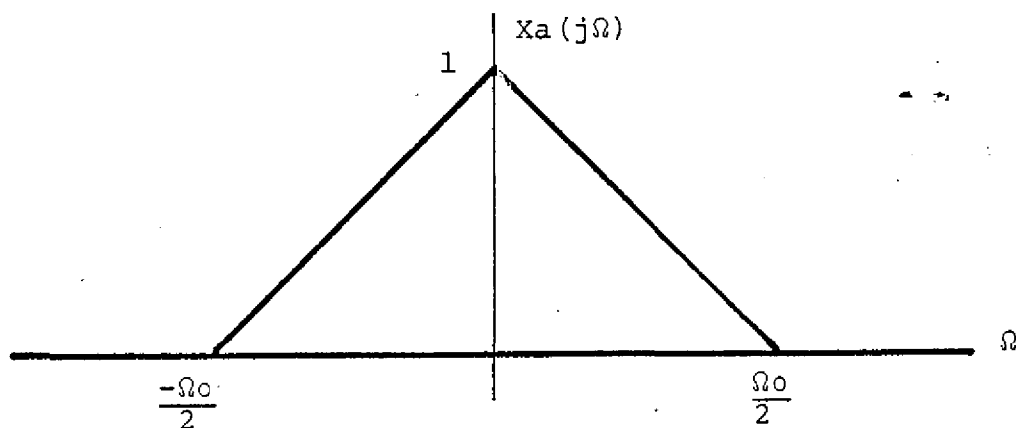
From Fig. 4-10c it is obvious that if $\frac{\Omega_0 T}{2} < \pi$, i.e., we sample at a rate at least twice the highest frequency of $X_a(j\Omega)$, then $X(e^{j\omega})$ is identical to $X_a(\omega/T)$ in the interval $-\pi \leq \omega \leq \pi$ and can be recovered from the samples $x_a(nT)$ by an appropriate interpolation formula.

For the remote magnetic indicator instrument designed in previous chapters, the analog signals are filtered with a low pass section reducing frequency content above 30 Hz. The sampling rate must therefore exceed 60 Hz ($T < 16.67$ m.s.) to enable accurate dynamic operation of the system.

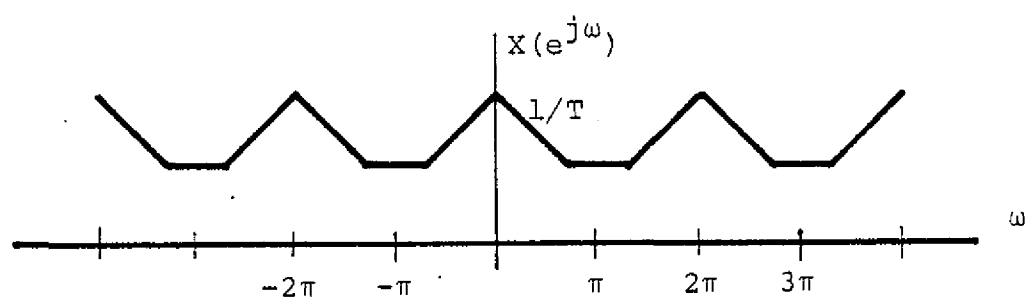
Laboratory measurements of sampling rates on the functional microprocessor based instrument revealed that the analog subsystem operated at a sampling rate of 62.5 Hz (16 m.s.) indicating that the algorithm execution rate supported a system bandwidth of 31.25 Hz. If frequency content of the analog signals is less than 31.25 Hz there is no error due to sampling.

B) Analog Multiplexer Induced Error

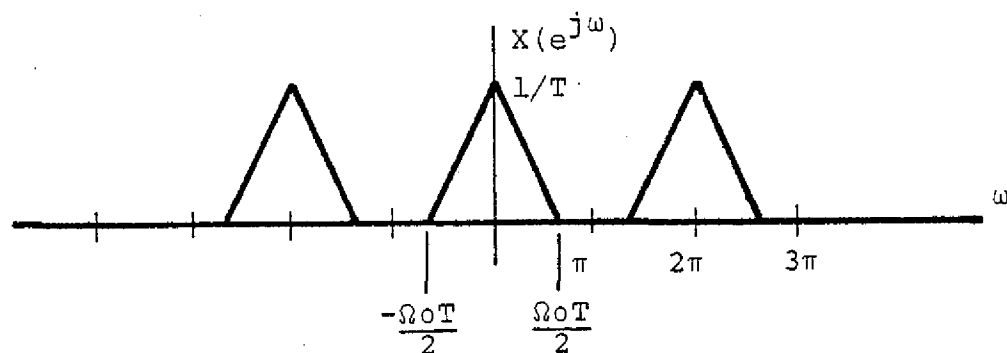
The analog multiplexer of Fig. 4-7 selectively connects one analog transducer output at a time to the input of the sample and hold subsystem. The Datal Systems, Inc., multiplexer [Ref. 4-7] selected for the remote magnetic indicator experiment features eight MOS-FET switches with associated driver circuits,



(a) Fourier transform as a continuous-time signal



(b) Fourier transform of the discrete-time signal obtained by periodic sampling (T is too large)



(c) Same as (b) except T is short enough

Fig. 4-10 FOURIER TRANSFORMS OF CONTINUOUS AND DISCRETE-TIME SIGNALS

FET pull-up to reduce propagation delays and all of the necessary decoding logic to enable random channel addressing with a four bit parallel binary input.

Several important parameters are used to characterize analog multiplexers and can contribute error.

1) Transfer Accuracy

Transfer accuracy is a function of the source impedance, switch resistance, load impedance (if the multiplexer is not buffered) and the signal frequency. It expresses the input to output error as a percentage of the input. In our case the system configuration predicates a maximum error due to transfer accuracy of ($\pm 0.01\%$) yielding an error term of

$$\pm 0.0001 \times 2.5 \text{ Volts} = \pm 25 \text{ mV}$$

2) Settling Time

This parameter defines the time elapsed from the application of a full scale step input to the time when the output has entered and remained within a specified error band around its final value. In our case the selected multiplexer has a maximum settling time of 1 microsecond to $\pm 0.01\%$ full scale (F.S.) Since the control system selecting channels is implemented using a microprocessor, the minimum time between analog subsystem commands will always be greater than 3.0 microsecond⁶. The multiplexer will therefore always have settled to the final value before the sample and hold circuit (following this subsystem) can be activated with no error due to the settling time parameter.

⁶One machine cycle time for the 2650 microprocessor with 1 MHz clock frequency.

3) Throughput Rate

The highest rate at which the multiplexer can switch from channel to channel at its specified accuracy is in this case 500 kHz. Since this rate is more than four orders of magnitude greater than the operational rate of the subsystem there is no error due to throughput rate limitations.

4) Input Leakage Current

The amount of signal coupled to the output as a percentage of input signal applied to all OFF channels together can be calculated by considering the maximum leakage current specified from OFF channels to the ON channel. In our case the maximum error signal can be calculated

$$\text{Error} = [4 (8 \text{ na} \times 2000 \text{ ohms source imped.})^2]^{\frac{1}{2}}$$

$$\text{Error} = 32 \text{ microvolts}$$

Note that in this case the voltage levels are statistically independent allowing an R.S.S. of error sources to calculate total error [Ref. 4-8, 4-9].

C) Sample and Hold Circuit Induced Errors

The sample and hold subsystem consists of a switch and capacitor arrangement as shown in Fig. 4-11. The Datel Systems, Inc., model SHM-IC-1 integrated circuit sample and hold device [Ref. 4-10] features a self-contained high gain differential input amplifier, a digitally controlled electronic switch and a high input impedance buffer amplifier. The external components used with the sample and hold circuit in the solid state remote magnetic indicator instrument consisted of the 0.001 μ f holding capacitor and a 100K offset trimpot. By connecting

the output back to the negative input of the input amplifier (Fig. 4-11), the sample and hold subsystem operated in a unity gain, noninverting mode. When the switch is closed, the unit is in the sampling or tracking mode (Digital Control = 0 Volts), and will follow a changing input signal.

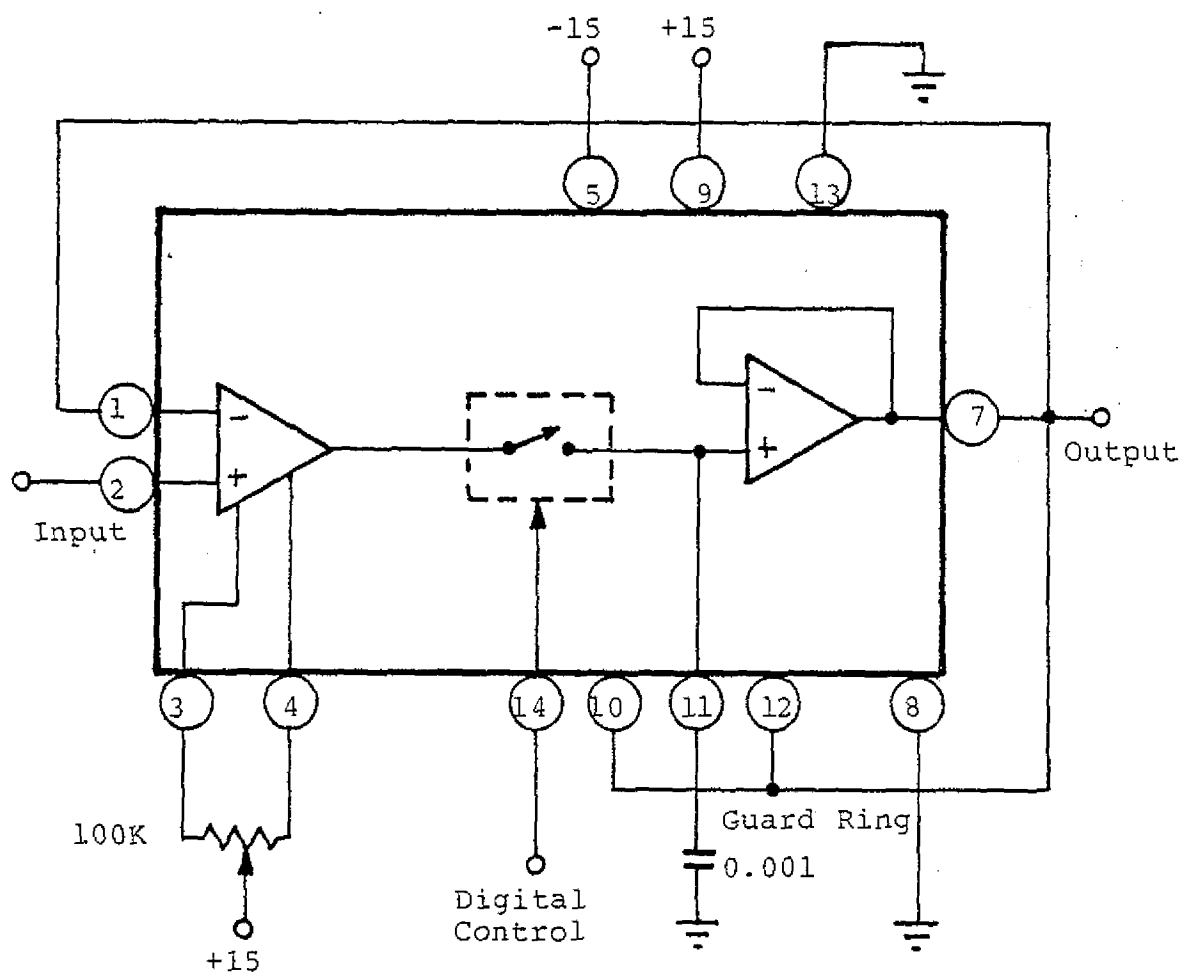


Figure 4-11 SAMPLE AND HOLD SUBSYSTEM

When the switch opens the unit is in the hold mode and retains a voltage on the capacitor for some period of time depending on capacitor and switch leakage. Sample and hold devices are characterized by a number of important parameters that must be considered in the design of a data acquisition subsystem.

1) Acquisition Time

The time lapse between the time that the sample command is given to the point where the output enters and remains within a specified error band around the input value is specified to be less than 4 microseconds time to transit from 0 to 0.1% of 10 Volts with $C = 0.001 \mu\text{f}$ [Ref. 4-10]. This implies that the control signals emanating from the central processor should allow at least 4 μs acquisition time prior to entering the hold mode. We note that the sample and hold subroutine (Appendix B) executes the instruction

IORI, R3 H'80' READY TO HOLD,

a two machine cycle instruction prior to sending the hold control signal. This instruction delays control signal transmission by $(2 \times 3 \mu\text{s}) = 6 \mu\text{s}$ allowing the sample and hold circuit ample time to settle with no appreciable error due to the acquisition time parameter.

2) Hold Mode Voltage Droop

The maximum change in output voltage as a function of time is specified to be 50 mv/sec maximum using a $0.001 \mu\text{f}$ polystyrene capacitor. Since the maximum total accumulated time to completion of the analog to digital conversion can be calculated as

5 Instructions (11 machine cycles)	= 33 μ s
1 Analog to Digital Conversion	= 20 μ s
3 Instructions if Conversion not synchronized with instructions (7 machine cycles)	= <u>21</u> μ s
	74 μ s

we can then compute droop error to be $50 \text{ mv/sec} \times (74 \times 10^{-6})$
 $\text{sec} = 3.73 \text{ mv.}$

3) Aperature Delay

The maximum time lapse between the time of hold signal receipt to opening of the switch is specified to be 50 nsec, an insignificant length of time in the instrument. There is therefore no error due to aperature delay.

4) Offset Error

Although the maximum offset error is specified to be 20 mv maximum [Ref. 4-10], the error was eliminated using the 100K trimpot offset adjustment. There was no appreciable offset error contribution due to the sample and hold circuit.

5) Gain Error

The gain error of a sample and hold circuit is apparent during the sample mode when the transfer function of the total amplifier deviates from the ideal unity slope condition (Fig. 4-12). In the noninverting unity gain mode, the specified gain error is $\pm 0.05\%$ maximum yielding a signal error of

$$(\pm 0.0005) \times 5.0 \text{ V} = 250 \text{ mV}$$

This error can, however, be eliminated with the gain

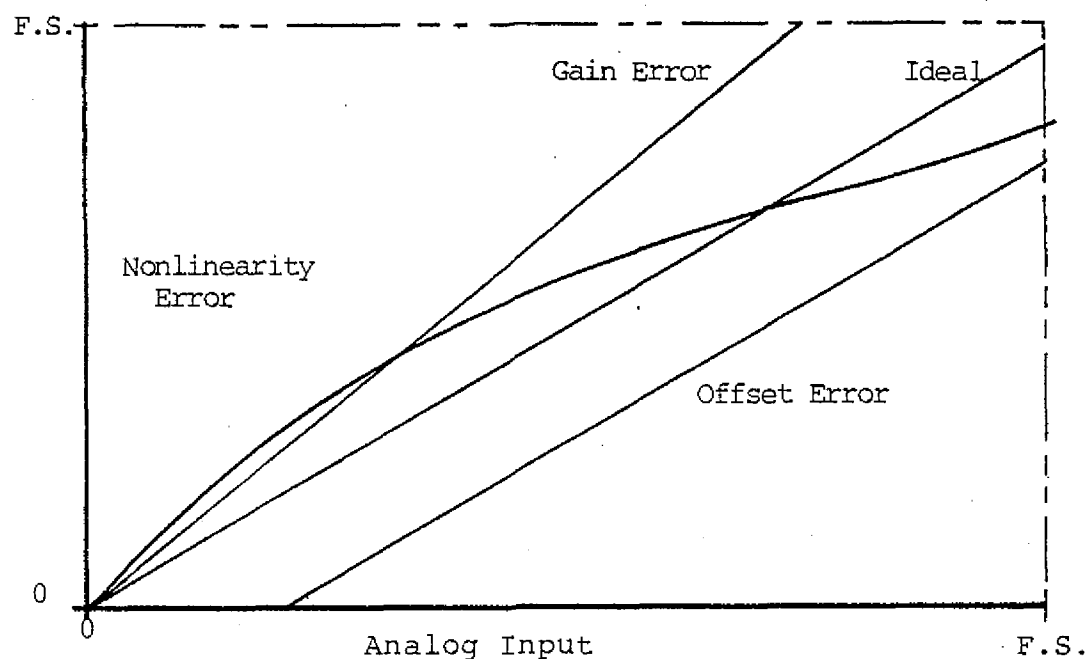


Fig. 4-12 GAIN, OFFSET AND LINEARITY ERRORS

adjustment available at the analog to digital converter. There will therefore be no appreciable net gain error due to the analog subsystem.

6) Nonlinearity Error

Nonlinearity error is apparent in the sample and hold circuit if the transfer function departs from a linear curve (Fig. 4-12). In the noninverting unity gain mode with a 0.001 μ f holding capacitor the maximum nonlinearity is 0.01% resulting in a worst case signal uncertainty of $(.0001) \times 2.5 \text{ Volts} = 25 \text{ mV}$.

7) Hold Mode Feedthrough

This error appears due to input signal appearing at the output when the unit is in the hold mode. Although the

feedthrough varies with signal frequency and the expected signal frequencies are substantially lower than the upper frequency limits of the sample and hold device (30 Hz max. versus several kiloHertz), we consider the worst case feedthrough of 0.01% [Ref. 4-10] or 25 mV.

D) Analog to Digital Converter Induced Errors

The A/D Converter selected for the solid state magnetic indicator instrument (Datel ADC-MA12B1B) [Ref. 4-11] uses the successive approximation technique to achieve excellent linearity and speed. Important parameters that potentially contribute errors are addressed below.

1) Resolution Error

The smallest analog change that can be distinguished by the A/D converter is

$$\text{Least Significant Bit (LSB)} = \frac{\text{Full Scale}}{2^n}$$

$$\text{LSB} = \frac{5}{2^{12}} = 1.22 \text{ mV}$$

this uncertainty manifests itself as an error in computing by limiting the precision of any calculation.

2) Linearity Error

The maximum deviation from a straight line drawn between the end points of the converter transfer function are specified in [Ref. 4-11] to be $\pm 1/2$ LSB (in our case ± 1.22 mV of analog signal).

3) Accuracy Error

The input to output error of the A/D converter is specified in [Ref. 4-11] to be $\pm 0.012\%$ F.S. $\pm 1/2$ LSB or

$$\pm (0.00012) \times 5.00V \pm 1.22 \text{ mV} = \pm 1.82 \text{ mV Worst Case}$$

In reality, the two error terms are unrelated and the

$$\text{Rss Error} = \pm [(.00012 \times 5V)^2 + (1.22\text{mV})^2]^{\frac{1}{2}}$$

$$\text{RSS Error} = \pm 1.36 \text{ mV}$$

4) Offset Error and Gain Error

Both the offset error and gain error were adjusted to zero using the trimming potentiometers (Fig. 4-7) and the calibration procedure outlined in Ref. 4-11. A reference signal of plus $1/2$ LSB (1.22 mV) was applied to the converter and the offset trimming potentiometer adjusted until the output flickered equally between logic "0" and logic "1". The gain was then adjusted by setting the converter input to full scale minus $1-1/2$ LSB (4.99817 Volts) and the gain trimming potentiometer was adjusted until the output flickered between logic "111...110" and logic "111...111". The above steps were repeated until no appreciable error in gain or offset was evident.

4-4 PROCESSING ERRORS

Errors in processing data accrue due to several sources including imprecision and truncation. Since the microprocessor selected for the instrument is inherently an eight bit device, single precision calculations are conducted with eight bits and double precision calculations are conducted with a total

of sixteen bits. This section addresses the effects of computational precision and truncation in the various subroutines and relates these to overall computational accuracy. The various subroutines are analyzed in chronological order as they appear in the main program.

A) Subroutine "SAMP"

The sample subroutine (delineated in Fig. 3-6a) selects and digitizes analog signals by controlling respective analog subsystem modules. During the first portion of this subroutine, A/D converter data bits are stored in two consecutive bytes⁷ in the computer memory. The A/D conversion precision of 12 bits is thereby preserved.

The second, third and fourth operations of the sample subroutine convert the unipolar binary format of the data to sign magnitude format, adds offset quantities and merely changes the signs of the Hx and Hy data. The operations are conducted in a double precision manner and precision of the data remains unaltered.

Correction of x axis orthogonality error is the final operation of the sample subroutine. Equation (3-1) is implemented at this point using a table lookup (for the sin function), multiplication and addition. The final result can be expressed as

$$Hx = Hx' + Hy \sin \epsilon$$

⁷A byte is accepted terminology for an eight bit data quantity.

where the respective quantities have the following forms

$$Hx^1 = x_1 + \sum_{i=1}^{11} a_i 2^i$$

$$Hy = x_2 + \sum_{j=1}^{11} a_j 2^j$$

$$\sin \epsilon = \sum_{k=1}^8 a_k 2^{-k}$$

and

x_1, x_2 are sign bits

$a_{i,j,k}$ equal 0 or 1 depending on whether the respective term is to exist or not

We can analyze the effects of imprecision and truncation by noting that the sin function has eight significant binary bits resulting in a resolution of $1/256$ or $90^\circ/256 = 0.352^\circ$.

The relative error in $\sin \epsilon$ is computed by Dahlquist [Ref. 4-12] as follows

let \tilde{a} = the approximate value of $\sin \epsilon$
 a = the exact value of $\sin \epsilon$

then the relative error in \tilde{a} is

$$(\tilde{a} - a)/a \text{ if } a \neq 0$$

Since data in the sin table has been truncated, maximum relative error can be as large as $\pm(1/2^{12})$ or $\pm 0.02\%$.

From the definition of relative error we obtain the following relationships between exact, estimate and estimated

relative error

$$\tilde{a} = a + ar = a(1 + r)$$

If a_1 , and a_2 have relative errors of $\pm 0.39\%$ and $\pm 0.02\%$, respectively, then

$$\begin{aligned}\tilde{a}_1 \tilde{a}_2 &= a_1(1 \pm 0.0039) a_2(1 \pm 0.00024) \\ &= a_1 a_2 (1 \pm 0.0039)(1 \pm 0.00024)\end{aligned}$$

Thus, the relative error in $\tilde{a}_1 \tilde{a}_2$ is

$$\begin{aligned}(1 \pm 0.0039)(1 \pm 0.00024) - 1 &= \\ \pm(0.0039) \pm(0.0039)(0.00024) \pm(0.00024) &= \\ \approx \pm(0.0041)\end{aligned}$$

Since the maximum value of $\sin \epsilon$ to be encountered occurs when the orthogonality error (ϵ) is 1 degree, $\sin \epsilon = 0.017$ maximum. The maximum value for H_y can be 0.6 gauss or 2048 units. Maximum error due to imprecision in the product $H_y \sin \epsilon$ is then

$$\begin{aligned}\text{Er Max} &= (2048 \times 0.017)(1 + .0041) - (2048 \times 0.017) \\ &= 0.1427 \text{ units}\end{aligned}$$

Since only the integer portion is retained in the final product, insignificant error can be attributed to imprecision of the $\sin \epsilon$ term in this case. Orthogonality error will be adequately corrected.

B) Subroutines ROTX and ROTY

These subroutines were developed in Chapter III and implement the equation of 2-11 required to compute horizontal

0-2 ✓

x and y magnetic field components. Equations to be implemented by the respective subroutines are

$$\begin{aligned} H_x = & H_{xm} \cos (\text{pitch}) + H_{ym} \sin (\text{pitch}) \sin (\text{roll}) \\ & + H_{zm} \sin (\text{pitch}) \cos (\text{roll}) \end{aligned} \quad (4-12)$$

and

$$H_y = H_{ym} \cos (\text{roll}) - H_{zm} \sin (\text{roll}) \quad (4-13)$$

where H_{xm} , H_{ym} and H_{zm} are measured field components made available from the magnetometer via the analog subsystem.

Since the transcendental functions are implemented using table lookup and are limited in precision to 8 bits, imprecision in these variables will dominate in generating error. In particular, the sin/cos terms will have relative error in the order of $\pm 1/256$ or $\pm 0.39\%$ while the measured field data has relative uncertainty of only $\pm 1/4096$ or $\pm 0.02\%$. Multiplications will result in addition of the bounds for the relative error as illustrated in section 4-4A above.

The transcendental terms above are limited in magnitude to 1.0 maximum while the field measurements can be 0.60 gauss max. In this case the individual product terms of (4-12) and (4-13) can have maximum errors of

$$E_r = (2048)(1 + 0.0041) - (2048) = 8.4 \text{ units}$$

Errors in H_y and H_x (4-12 and 4-13) will be maximum when roll and pitch are at 45 degrees and the fields are equal. In this case the error in H_y will be

$$EH_y = [(0.707)(2048)(1 + 0.0041) - (0.707)(2048)] - [(0.707)(2048)(1 - 0.0041) - (0.707)(2048)]$$

$$EH_y = 4.94 - 5.94 = 11.87 \text{ units}$$

Similarly, maximum error in H_x can be calculated as

$$EH_x \approx [(0.707)(2048)(1.0041) - (0.707)(2048)] \times 3$$

$$EH_x \approx 17.8 \text{ units maximum}$$

It should be noted that these error terms are worst case and peak at multiples of 45 degrees in yaw.

C) Subroutines COSY and SINY

These two subroutines compute the angle between the x axis sensor (when projected onto the horizontal plane) and the north-south horizontal vector of earth's magnetic field. The first two operations of these subroutines perform double precision multiplication and division. Since the data variables involved are 12 bits in length and the computations performed preserving 16 bits, no error is introduced.

The "ANGL" subroutine called by the above two subroutines computes the desired (x axis to horizontal vector) angle by completing an associative table look up procedure. The task required is to match a given data quantity either (H_x^2/H_h^2) or (H_y^2/H_h^2) with the contents of a memory cell. The address of this cell is then the required angle.

Since the table is limited in precision to 16 bits there are obviously cases where an interpolation is required to

ascertain the true address⁹. The function stored in tabular form is $\cos^2\theta$ where θ varies from 45 to 90 degrees. Maximum error will therefore be induced while attempting to locate solutions (angles near 90 degrees if inadequate precision is provided. Error in this region due to resolution of tabular data can be examined by noting the entries in Table 4-8

θ	$\cos^2\theta$	Most Significant Binary Bit (2^{-x})
90	0	-
89	0.000305	12
88	0.001218	9
87	0.00274	8

Table 4-8 $\cos^2\theta$ AND MOST SIGNIFICANT BINARY DIGITS

provided to indicate the relative magnitudes of $\cos^2\theta$ in the region of $\theta = 90$ degrees. We observe that the most significant binary digit affected at 89 degrees is binary decimal digit 12 implying that the resolution of H_x^2/H_h^2 or H_y^2/H_h^2 (the argument of $\cos^2\theta$) must be accurate to at least $1/2^{12}$ or 0.024%.

Considering the horizontal field of earth's magnetic vector as observed in laboratory experimentation at this latitude, we note that H_h is 730 units. At a heading of 89 degrees, $H_x = 730 \cos 89 = 12.7$ units. The argument would therefore be

$$\text{ARG} = H_x^2/H_h^2 = \frac{(12.7)^2}{(730)^2} = 0.000305$$

⁹The procedure determines the relative address by linear interpolation, then selects the closest address as the required angle for the solution.

Since, the squaring and division operations are conducted in double precision, precision is preserved and the algorithm should be able to resolve heading to at least one degree over all portions of the compass.

D) Errors Due to the Remaining Subroutines

Since all of the remaining subroutines work with data that has been rounded to a precision representing 1 degree or better and the computations involve addition or subtraction in double precision binary or binary coded decimal (BCD) format, we note that there will be no further appreciable error due to truncation or rounding.

4-5 MEASUREMENT ERROR SUMMARY

Errors due to sensors and measurement of their respective outputs were discussed in sections 4-2 and 4-3 above. Before proceeding with the analysis of errors, the total signal inaccuracy due to contribution from the many sources above will be summarized in Table 4-10. Total instrument error can then be computed by considering the propagation and enhancement of these errors during the computation process.

Since the errors in Table 4-9 are stochastically independent, we can compute error for any given signal level by finding the RSS of respective error sources. In this manner, the instrument error can be evaluated by considering all input signals with errors superimposed to produce an erroneous computation of heading.

PARAMETER	ERROR	COMMENT
1. Magnetometer		
Offset	≈ 0	Corrected by software
Orthogonality	≈ 0	Corrected by software
Noise	Negligible	
Gain	$\pm 0.01\%$	Proport. to signal level
Linearity	$\pm 0.01\%$	
2. Analog Subsystem		
Sampling	Negligible	Sampling rate & filtering adequate
Multiplexer		
Transfer Accuracy	$\pm 0.01\%$	Proport. to signal level
Settling Time	≈ 0	
Rate	≈ 0	
Input Leakage	≈ 0	
Sample and Hold		
Acquisition	≈ 0	
Hold	4mV	
Aperature Delay	≈ 0	
Offset	≈ 0	Corrected by software
Gain	≈ 0	Corrected by software
Nonlinearity	$\pm 0.01\%$	Proport. to signal level
Feedthrough	$\pm 0.01\%$	Proport. to signal level and frequency
A/D Converter		
Resolution	$\pm 1.2\text{mV}$	
Accuracy	$\pm 1.4\text{mV}$	
Offset	≈ 0	
Gain	≈ 0	

Table 4-9 SENSOR AND ANALOG SUBSYSTEM ERROR SUMMARY

4-6 SAMPLE ERROR ANALYSIS

Orthogonality correction using the algorithmic method can be verified by computing expected error prior to correction and comparing measured system output with the error prediction. Assuming that the angle between the x and y sensors exceeds 90 degrees as in Fig. 4-13, we can proceed to compute error by noting the following relationships

$$\begin{aligned} Hx &= Hh \cos (+\psi) \\ Hy &= Hh \sin (\psi) \\ Hx_1 &= Hx \cos \epsilon - Hy \sin \epsilon \\ \text{True Yaw} = \psi_T &= \cos^{-1} \left(\frac{Hx}{(Hx^2 + Hy^2)^{\frac{1}{2}}} \right) \end{aligned}$$

Computed yaw

$$\begin{aligned} \psi_m &= \cos^{-1} \left[\frac{Hx \cos \epsilon - Hy \sin \epsilon}{(Hx \cos \epsilon - Hy \sin \epsilon)^2 + Hy^2}^{\frac{1}{2}} \right] \\ &= \cos^{-1} \left[\frac{Hh \cos \psi \cos \epsilon - Hh \sin \psi \sin \epsilon}{[(Hh \cos \psi \cos \epsilon - Hh \sin \psi \sin \epsilon)^2 + H^2 h^2 \sin^2 \psi]}^{\frac{1}{2}} \right] \end{aligned}$$

Using small angle approximations with $\epsilon \approx 0.79^\circ$

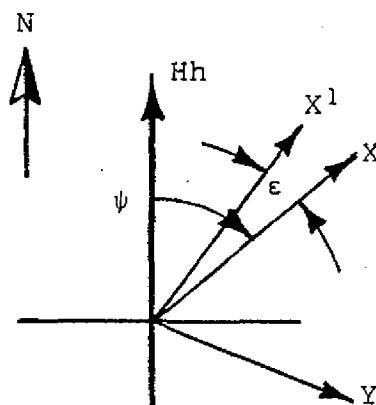
$$\cos \epsilon \approx 1 \text{ and } \sin \epsilon \approx 0.014$$

then

$$\psi_m = \cos^{-1} \left[\frac{Hh \cos \psi - 0.014 \sin \psi}{[Hh^2 (\cos \psi - 0.014 \sin \psi)^2 + Hh^2 \sin^2 \psi]}^{\frac{1}{2}} \right]$$

Computed error

$$\text{Error} = \psi_m - \psi$$

Fig. 4-13 ANGLE $(X - Y) > 90^\circ$

We can now evaluate computed yaw angle (ψ_m) given a particular yaw (ψ) and the horizontal field vector (Hh). Heading error for horizontal field vector of 730 units at various yaw angles with pitch and roll angles of zero degrees is tabulated in Table 4-10 and plotted along with actual measured yaw error (data taken during experimentation of Chapter V) in Fig. 4-14.

Heading (Degrees)	Computed Error (Degrees)	Heading (Degrees)	Computed Error (Degrees)
90	0.8	290	0.7
70	0.7	270	0.8
50	0.5	250	0.7
30	0.2	230	0.5
10	0.0	210	0.2
350	0.0	190	0.0
330	0.2	170	0.0
310	0.5	150	0.2
		130	0.5

Table 4-10 COMPUTED HEADING ERROR WITH $Hh = 730$ UNITS

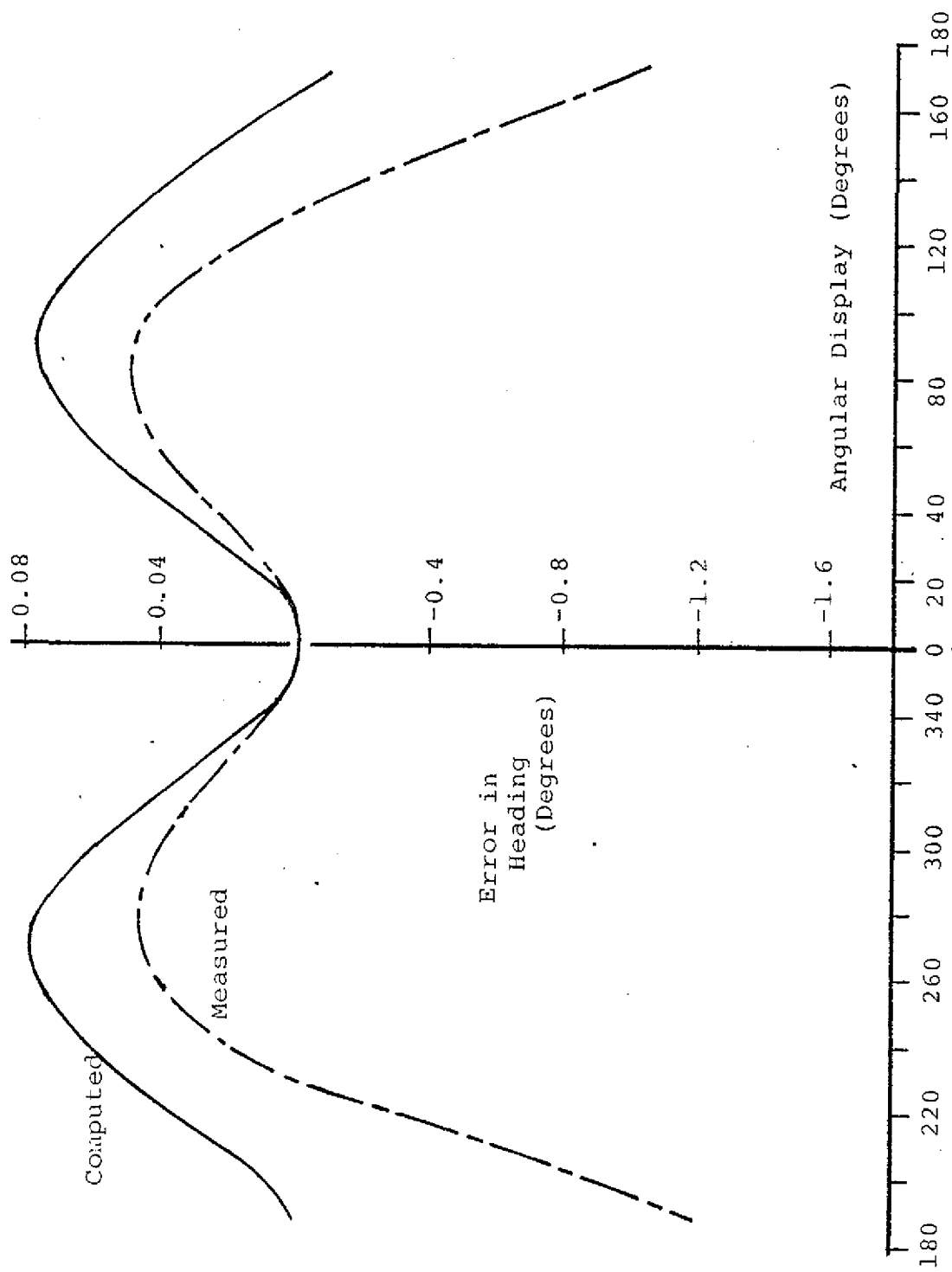


Fig. 4-14 COMPARISON OF COMPUTED AND MEASURED ORTHOGONALITY INDUCED ERROR

4-7 CONCLUSIONS

The preceeding error analysis has identified potential error sources along with relative magnitudes of error to be expected. Magnetometer sensor and analog subsystem errors were identified and analyzed individually. During this analysis it became apparent that errors due to sensor offset and nonorthogonality dominated and would severely limit total instrument performance. The relative magnitudes of these errors and their mode of contribution would have degraded system capacity.

By carefully characterizing the offset and orthogonality error it was determined that these systematic errors could be reduced by appropriate programming. A need to identify the extent of each error unique to the laboratory instrument imposed a need to evaluate the instrument empirically. Using earth's magnetic field and the laboratory test fixture (described in Chapter V) to provide control inputs each of the parameters was identified and measured. An algorithm with the empirically determined correction coefficients was included in the final system to reduce the error and to improve final system performance. The remaining potential error sources were tabulated and relative magnitudes noted.

Processing errors due to register precision and truncation were analyzed by considering pertinent subroutines individually. It was noted that the relative error bounds add when multiplying variables with relative error. In addition, it was noted that error accrued during processing is proportional to sensor signal levels involved. The final uncertainty is then proportional to actual aircraft attitude with error increasing as displacement from level flight occurs. Computational error is also noted to increase at particular headings causing the error function to peak at specific yaw angles.

The sample error analysis clearly shows that a correlation between sensor nonorthogonality induced error and measured (uncorrected) data exists. By predicting and computing an error function prior to experimentally verifying the result we gain confidence that the sensor characteristics derived empirically in previous sections are correct.

CHAPTER V

LABORATORY EVALUATION OF THE ATTITUDE INDEPENDENT
REMOTE MAGNETIC INDICATOR AND HEADING INSTRUMENT

5-1 INTRODUCTION

This chapter addresses laboratory evaluation of the microprocessor based computer designed to implement the heading measurement instrument. An integral part of this instrument was the three axis fluxgate magnetometer used to implement the attitude independent remote magnetic indicator of Chapter II. The laboratory evaluation was designed to investigate empirically the effects of physical parameters that would otherwise be impossible to assess.

Although phenomena such as noise, magnetic field gradient, sensor orthogonality errors and offset errors can be predicated, combined effects on the proposed instrument and remote magnetic indicator are best evaluated in the laboratory. In addition, it was noted that errors due to sensor offset and nonorthogonality could be corrected by software included with the sample subroutine. Determination of the effectiveness of this correction technique necessitated laboratory measurements of the errors (to determine correction constants) and comparison of data prior to and following corrections.

The chapter begins by discussing laboratory test apparatus designed to evaluate the instrument. Actual data measured and recorded during experimentation is then presented in both tabular and graphic form to facilitate comparison and evaluation. Finally, the laboratory data is discussed and it is concluded that the remote magnetic indicator used with the heading measurement instrument results in a viable alternative to conventional heading measurement systems. The microprocessor based

computer implementation of the instrument has added unique sensor measurement correction ability that enhances performance of otherwise marginal sensors. In this manner limitations in systems performance that now exist due to sensor inadequacy can be minimized without incurring the burden of using more expensive sensors.

5-2 TEST APPARATUS

A) Electronic Subsystem

The microprocessor based computer (illustrated in photos 5-1 and 5-2) was constructed on printed circuit boards consisting of a central processing card, two memory cards (2K bytes capacity each) and an output board. A separate analog subsystem card contained the multiplexer, sample and hold, analog to digital converter and trimming potentiometers. The circuit cards were all organized with edge connectors and mounted vertically into a hand wired backplane assembly as shown in photos 5-1 and 5-2.

The card in the left foreground of photo 5-1 served as the output display with three seven-segment displays displaying significant figures of system heading. A small printed circuit in the right foreground of photo 5-1 contained potentiometers used to generate analog signals proportional to roll and pitch signals (simulating gyroscope outputs). Cards shown vertically mounted in photo 5-2 can be identified from right to left as the analog subsystem, two memory cards and the central processing card. The large integrated circuit shown on the CPU card is the Signetics 2640 microprocessor.

B) Sensor Assembly

To evaluate the effects of combined aircraft pitch, roll

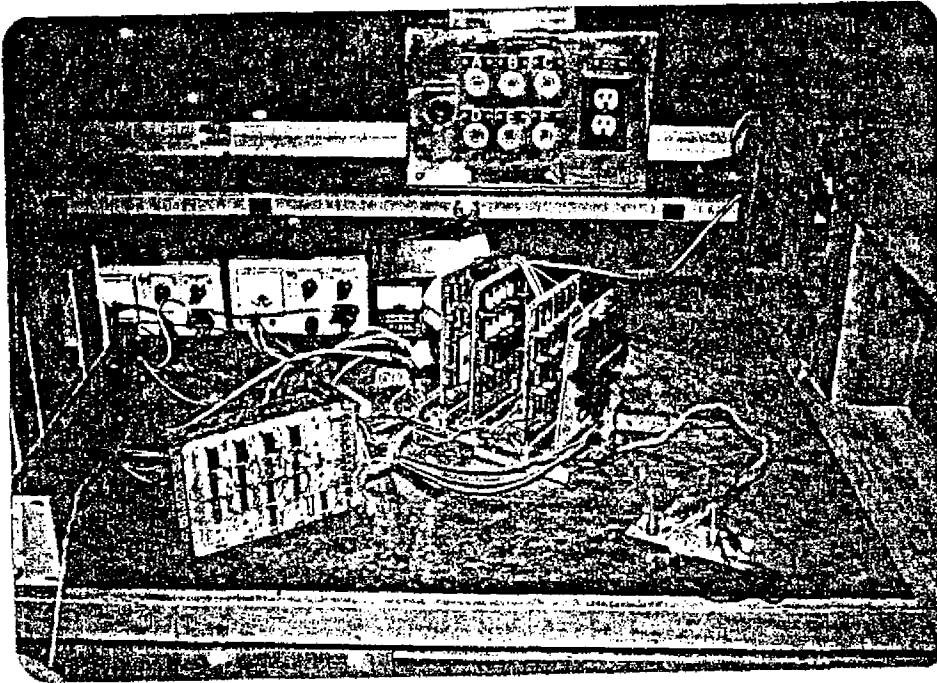


Photo 5-1 MICROPROCESSOR BASED HEADING COMPUTER

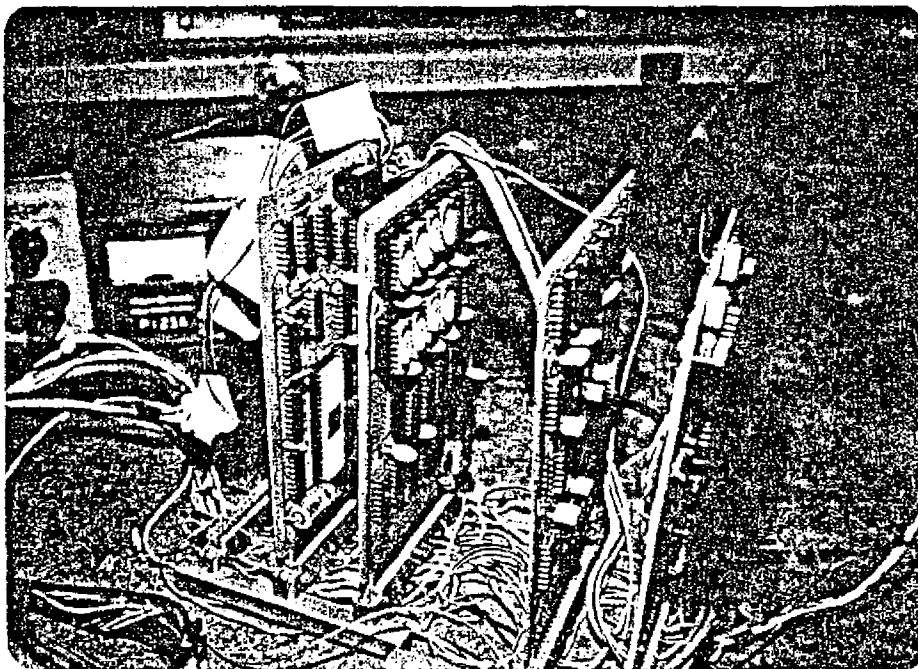


Photo 5-2 CENTRAL PROCESSOR, MEMORY AND
ANALOG SUBSYSTEM

and yaw a three axis gimbal apparatus was required. In addition, since angular measurements were required, a means of measuring angular rotation in each of the three axes was provided. The gimbal apparatus as illustrated in photos 5-3 and 5-4 was fitted with large protractors centered on the rotation axes. Pointers were provided to enable angular rotation measurements on the respective protractor scales. Since the angular precision on each protractor scale resolved angular position to 0.5 degrees, angular measurements to a resolution of at least 0.5 degrees were possible. Angular position was measured by estimating the decimal place of each measurement with accuracy to ± 0.5 degrees ensured.

Since the three axis magnetometer (housed in the rectangular block of photos 5-3 and 5-4) measured ambient magnetic fields the test apparatus was constructed of nonferrous material. This ensured that local fields due to residual magnetic fields in the test apparatus would be minimized. In addition, since the material had low permeability, there would be little deformation of the local field causing error due to changing field gradient.

The sensor package shown in photos 5-3 and 5-4 was physically mounted such that the sensors were centered as close to the center of the gimbal as possible. This precaution ensured that measurement error due to sensor translation was minimized¹. During instrument evaluation, the entire gimbal assembly and sensor were leveled and mounted in a Helmholtz coil assembly as illustrated in photo 5-5. Although the coils were not activated during experimentation, the rotations in heading were

¹Since the local magnetic field has a nonzero gradient, field measurements include a component due to translation of the sensor axes. This component of measurement produces unacceptable error in a system designed to measure field components that change due to rotation.

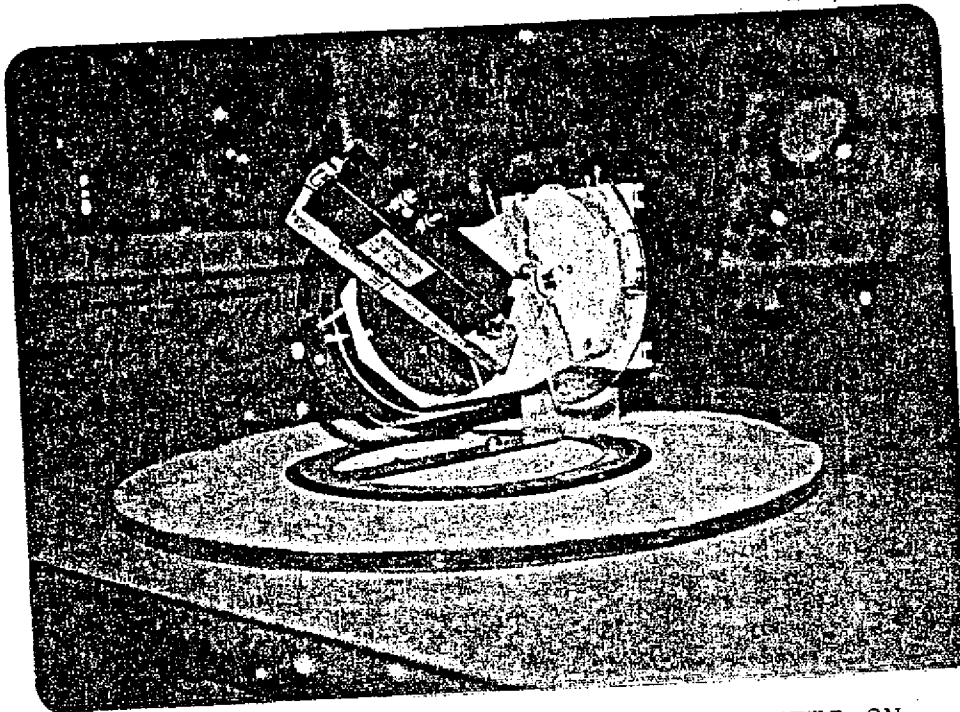


Photo 5-3 MAGNETOMETER SENSOR MOUNTED ON
GIMBALLED TEST FIXTURE

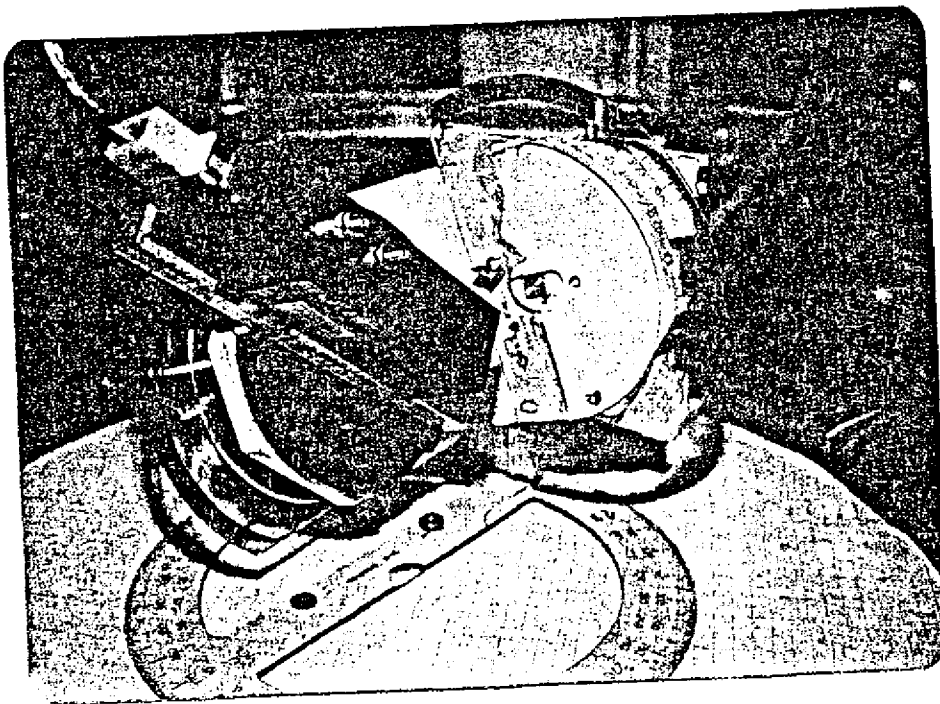


Photo 5-4 SENSOR AND GIMBAL ASSEMBLY WITH PROTRACTORS

carefully controlled since the gimbal assembly was an integral part of the Helmholtz coil fixture with the vertical rotation axis serving as the system yaw axis.

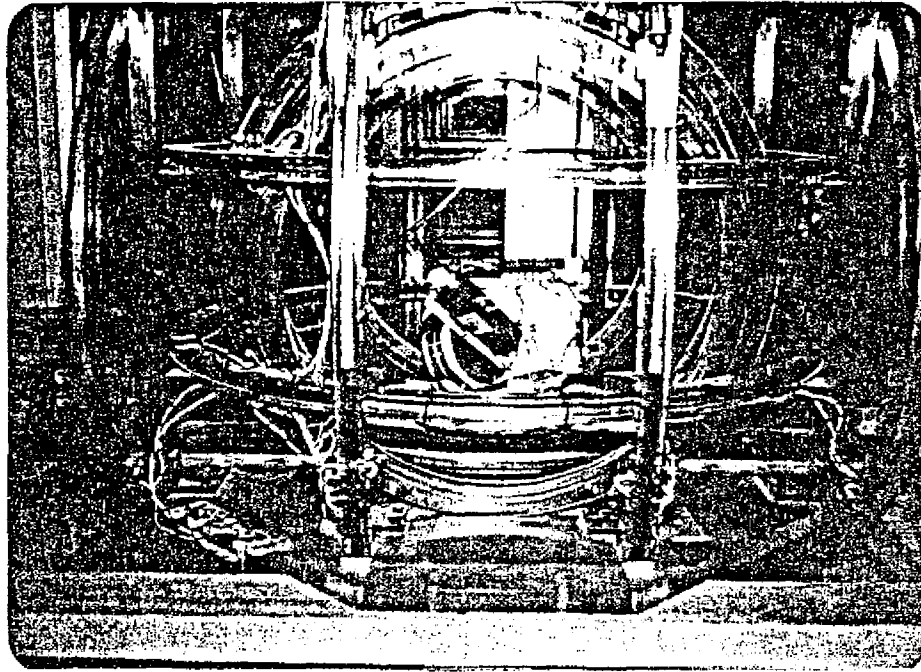


Photo 5-5 TEST FIXTURE MOUNTED IN HELMHOLTZ COIL ASSEMBLY

5-3 HEADING MEASUREMENTS WITH NO OFFSET CORRECTION

By maintaining heading of the test fixture constant (no rotation about the vertical axis) and varying both pitch and roll angle, the instrument display was observed to vary. This variation gave a direct measure of instrument error since a constant heading was maintained and a constant display was to be expected.

Data variations were recorded in Tables 5-1 and 5-2 and plotted on Figures 5-1 and 5-2. With only ± 10 degree variation in pitch combined with ± 30 degree variation in roll we note that the heading display varies 14 degrees. Obviously,

Roll Angle (Degrees)	$\theta = 0^\circ$	$\theta = 10^\circ$	$\theta = -10^\circ$
-30	000	353	4
-20	000	354	2
-10	359	357	0
0	359	359	358
10	359	000	355
20	358	002	354
30	358	004	353

Table 5-1 HEADING COMPUTED AT A FIXED YAW ANGLE
WITH NO OFFSET CORRECTION

Roll Angle (Degrees)	$\theta = 0^\circ$	$\theta = 10^\circ$	$\theta = -10^\circ$
-30	46	52	38
-20	45	49	41
-10	45	47	43
0	45	45	43
10	45	43	46
20	44	42	47
30	44	41	49

Table 5-2 HEADING COMPUTED AT A FIXED YAW ANGLE
WITH NO OFFSET CORRECTION

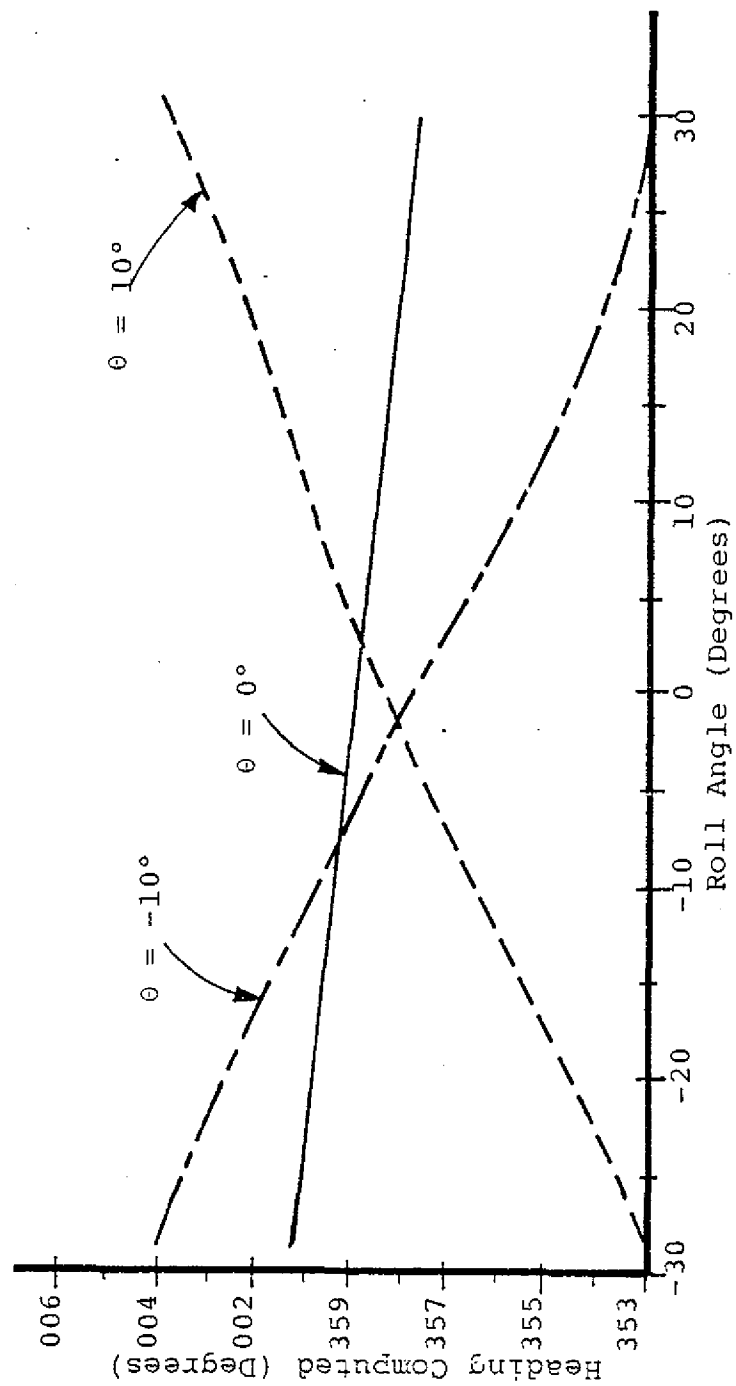


Fig. 5-1 HEADING COMPUTED AT A FIXED YAW ANGLE WITH VARYING θ AND ϕ (NO OFFSET CORRECTION)

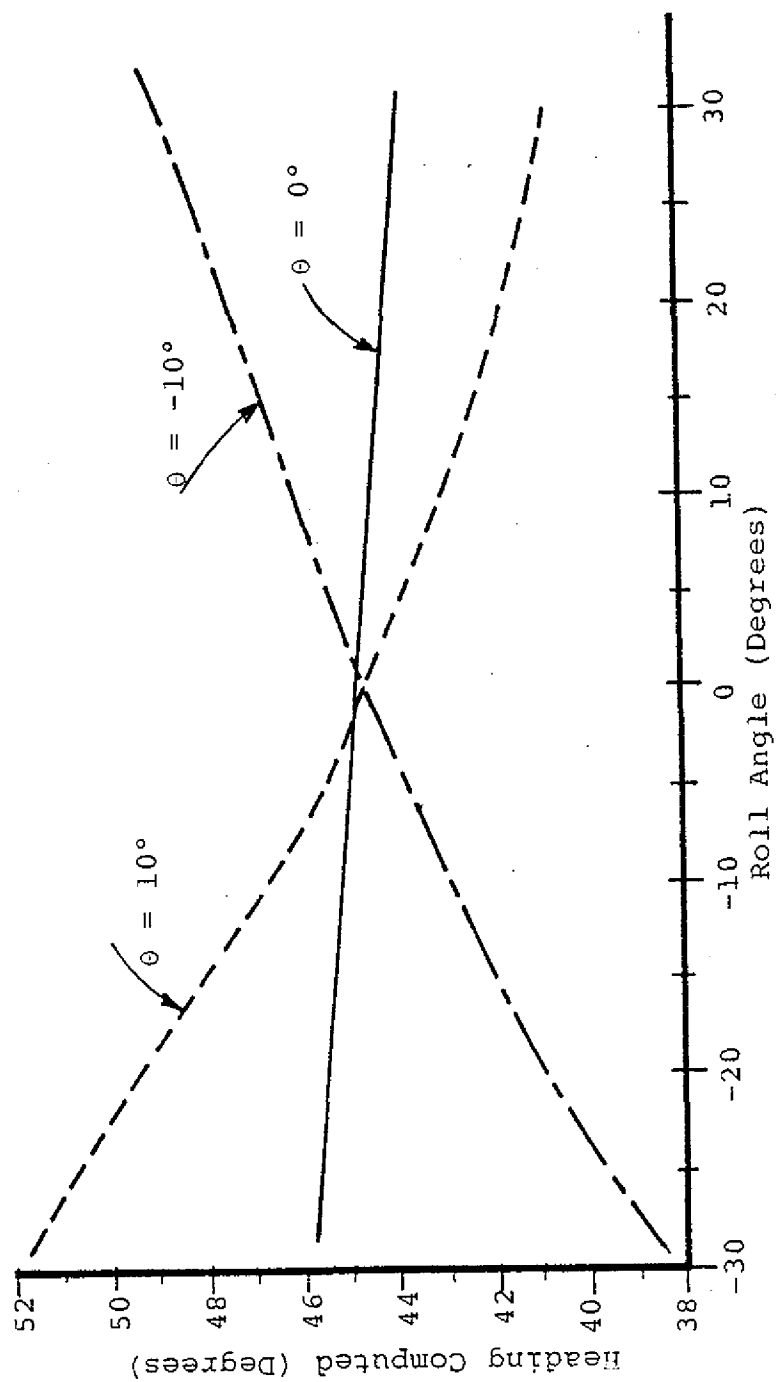


Fig. 5-2 HEADING COMPUTED AT A FIXED YAW ANGLE WITH VARYING
 θ AND ϕ (NO OFFSET CORRECTION)

instrument operation indicated excessive error requiring more elaborate sensors or correction of a sensor inadequacy.

5-4 HEADING MEASUREMENTS TO INVESTIGATE ORTHOGONALITY ERROR

System performance was evaluated by initially aligning the sensors with zero pitch and roll angle. Sensor Z was positioned vertically with positive direction downwards. By observing the Z axis output² as the test fixture was rotated about the vertical axis, adjustments were made in pitch and roll angle to minimize coning of the Z axis. Angular measurements on the respective roll and pitch axis protractors were then made to establish the initial reference attitude angles.

Heading measurement accuracy was evaluated by rotating the test fixture in the horizontal plane until the display flickered between (XX9) and (XX9+1). The rotation was then continued a very small amount until a steady display (multiple of 10 degrees) was observed³. Measurements ranging from 0 to 350 degrees were made by recording angular position required to produce specific heading data displays. Sets of data were recorded at various combinations of pitch and roll then tabulated in Tables 5-3 through 5-8. Relative error was computed by determining angular position expected at each display value and then computing the difference in angular positions. Errors at the roll extremes of ± 44 degrees are plotted for pitch angles of plus and minus 20 degrees on Fig. 5-3 through 5-6 inclusive.

²A special subroutine was used to display Z axis data directly in BCD format on the seven bar output display.

³This measurement technique ensured that all heading measurements were made identically. In addition, error due to system imprecision was reduced.

Data in Tables 5-5, 5-6 and Fig. 5-3, 5-4 were recorded with no sensor orthogonality error correction implemented. Data in Tables 5-7, 5-8 and Fig. 5-5, 5-6 was recorded with the sensor orthogonality correction implemented. Comparison of these data indicate that considerable improvement in accuracy is achieved by correcting sensor orthogonality error.

5-5 CONCLUSIONS

Laboratory evaluation of the heading measurement instrument has shown that the algorithms developed in previous chapters are viable. Operation of the device in a laboratory environment has enabled empirical evaluation of the system under adverse combinations of noise, field gradient and sensor plus instrument error sources.

Test apparatus described in section 5-2 served to enable controlled simulation of roll, pitch and yaw rotations. The apparatus was nonmagnetic in nature and contributed insignificant error due to field perturbation. Mounting of protractors and pointers on the test apparatus made angular measurements possible to a precision of at least ± 0.5 degrees.

Effects of sensor offsets were evaluated in section 5-3 by recording system heading computations when only roll and pitch varied. Since the variations in Figures 5-1 and 5-2 prior to offset correction exceed the maximum excursions of Figures 5-3 and 5-4 by at least a factor of two (angular excursions in first set also less than in the record) and we note that offset errors were corrected prior to recording data in the second set of data, we conclude that offset in magnetometers can be a

PITCH ANGLE 0 DEGREES
ROLL ANGLE 0 DEGREES

Heading Displayed (Degrees)	Angular Position (Degrees)	Relative Error (Degrees)
10	275.3	0.3
30	295.2	0.2
50	315.4	0.4
70	335.5	0.5
90	355.5	0.5
130	34.8	-0.2
150	54.3	-0.7
170	74.0	-1.0
190	94.0	-1.0
210	114.4	-0.6
230	135.0	0.0
250	155.5	0.5
270	174.7	-0.3
290	195.5	0.5
310	215.2	0.2
330	235.2	0.2
350	254.7	-0.3

Table 5-3 REFERENCE DATA MEASUREMENTS OF HEADING
TAKEN WITH NO ORTHOGONALITY CORRECTION

PITCH ANGLE 0 DEGREES

ROLL ANGLE 0 DEGREES

Heading Displayed (Degrees)	Angular Position (Degrees)	Relative Error (Degrees)
10	276.6	-0.4
30	296.6	-0.4
40	306.7	-0.3
50	316.7	-0.3
60	327.2	+0.2
70	337.0	0.0
90	355.9	-1.1
130	37.0	0.0
160	67.2	0.2
190	96.8	-0.2
220	126.9	-0.1
250	157.0	0.0
280	186.9	-0.1
310	216.6	-0.4
340	246.9	-0.1
350	256.4	-0.6

Table 5-4 HEADING MEASUREMENTS WITH OFFSET AND
ORTHOGONALITY CORRECTIONS MADE

Heading Displayed (Degrees)	Roll = 44°		Roll = 20°		Roll = -20°		Roll = -44°	
	Angular Position	Error	Angular Position	Error	Angular Position	Error	Angular Position	Error
10	276.3	1.3	276.5	1.5	275.0	0.0	274.0	-1.0
30	296.3	1.3					293.6	-1.4
40			306.1	1.1	304.0	-1.0		
50							313.8	-1.2
60	325.8	0.8						
70			335.6	1.6	334.3	-0.7	333.8	-1.2
90	355.0	0.0	354.0	-1.0	353.1	-1.9	353.0	-2.0
130	34.3	0.7	34.3	-0.7	34.6	-0.4	34.4	-0.6
160	64.5	-0.5	64.0	-1.0	65.0	0.0	65.0	0.0
190	94.3	-0.7	94.6	-0.4	95.0	0.0	95.5	0.5
220	125.2	0.2	125.3	0.3	126.0	1.0	126.5	1.5
250	156.6	1.6	156.2	1.2	156.7	1.7	157.0	2.0
280	186.6	1.6	186.8	1.8	186.5	1.5		
310	216.8	1.8	216.8	1.8	215.9	0.9	215.9	0.9
340	246.0	1.0	246.8	1.8	245.0	0.0		
350							224.9	-0.1

TABLE 5-5 HEADING MEASUREMENTS AT PITCH = 20° WITH NO
ORTHOgonALITY CORRECTION

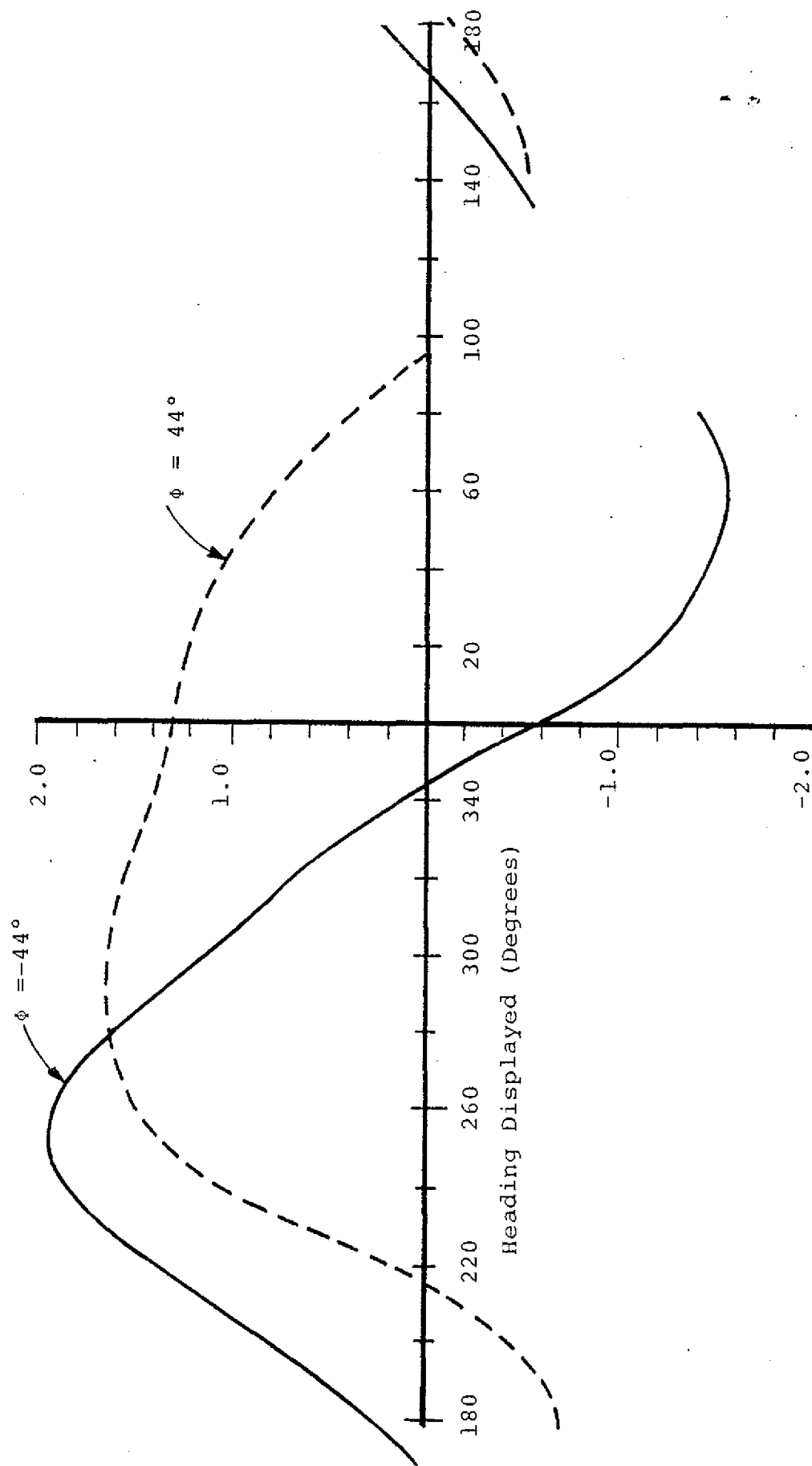


Fig. 5-3 HEADING MEASUREMENT ERROR AT PITCH = 20°
(NO ORTHOGONALITY CORRECTION)

Heading Displayed (Degrees)	Roll = 44°		Roll = 20°		Roll = -20°		Roll = -44°	
	Angular Position	Error	Angular Position	Error	Angular Position	Error	Angular Position	Error
10	276.1	1.1	275.1	0.1	274.2	-0.8	273.7	-1.3
30	296.2	1.2	295.9	0.9			293.6	-1.4
50	316.4	1.4	316.1	1.1			314.1	-0.9
70	336.5	1.5	336.4	1.4	335.5	0.5	334.6	-0.4
90	355.5	0.5	355.3	0.3	355.0	0.0	354.2	-0.8
130	36.0	1.0	36.4	1.4	135.7	0.7	135.7	0.7
150	55.3	0.3	55.9	0.9			55.8	0.8
170	74.5	-0.5	75.6	0.6			75.5	0.5
190	94.9	-0.1	95.3	0.3	95.5	0.5	95.5	0.5
210	115.0	0.0	115.4	0.4			115.6	0.6
220					125.5	0.5		
230	135.0	0.0	135.6	0.6			136.0	1.0
250	155.6	0.6	155.4	0.4	155.5	0.5	155.7	0.7
270	174.8	-0.2	174.8	-0.2			175.0	0.0
290	195.6	0.6	195.4	0.4			195.3	0.3
310	215.5	0.5	215.3	0.3	214.6	-0.4	214.5	-0.5
330	235.7	0.7	235.1	0.1			234.2	-0.8
350	255.6	0.6	255.2	0.2			253.8	-1.2

Table 5-6 HEADING MEASUREMENTS AT PITCH = -20°
WITH NO ORTHOGONALITY CORRECTION

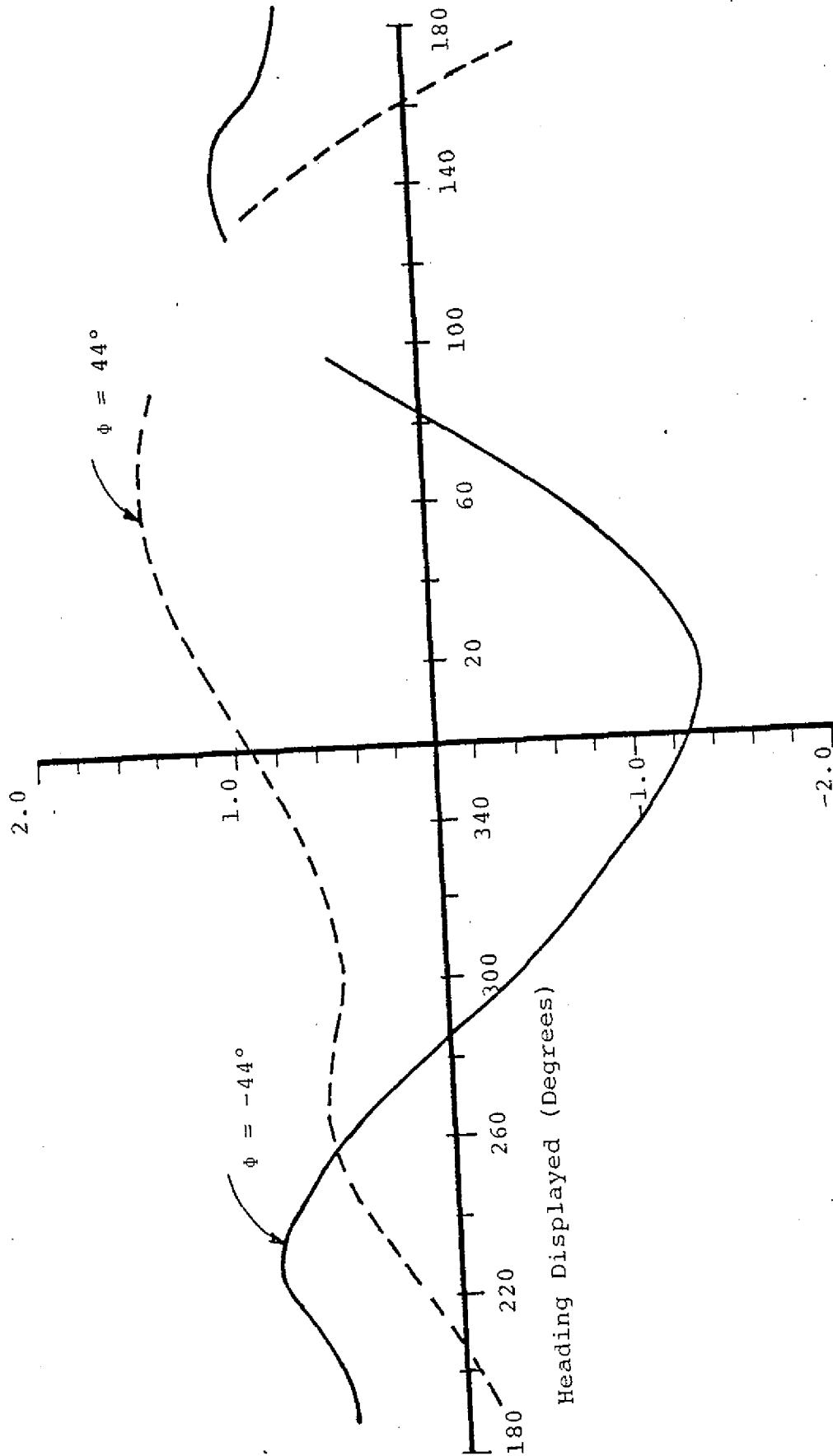


Fig. 5-4 HEADING MEASUREMENT ERROR AT PITCH = -20°
(NO ORTHOGONALITY CORRECTION)

Heading Displayed (Degrees)	Roll = 0°		Roll = 44°		Roll = -44°	
	Angular Position	Error	Angular Position	Error	Angular Position	Error
20	287.3	0.3	287.5	0.3	286.3	-0.7
40	307.2	0.2	307.5	0.3	306.0	-1.0
60	327.0	0.0	327.9	0.7	325.9	-1.1
80	346.3	-0.7	347.5	0.3	345.6	-1.4
90	355.9	-1.1	357.0	0.2	356.2	-1.8
140	46.9	-0.1	47.0	-0.2	46.5	-0.5
160	67.0	0.0	67.3	0.1	67.1	0.1
180	86.6	-0.4	86.5	-0.7	87.0	0.0
200	107.0	0.0	107.3	0.1	108.1	1.1
220	127.6	0.6	127.3	0.1	128.3	1.2
240	147.2	0.2	147.4	0.2	148.5	1.5
260	167.0	0.0	167.1	-0.1	168.5	1.5
280	187.3	0.3	187.1	-0.1	188.5	1.5
300	207.2	0.2	207.1	-0.1	208.0	1.0
320	227.3	0.3	227.0	-0.2	227.5	0.5
340	247.4	0.4	247.3	+0.1	247.4	0.4
0	266.4	-0.6	267.0	-0.2	266.0	-1.0

Table 5-7 HEADING MEASUREMENTS AT PITCH = 20°
 WITH OFFSET AND ORTHOGONALITY CORRECTION
 MADE

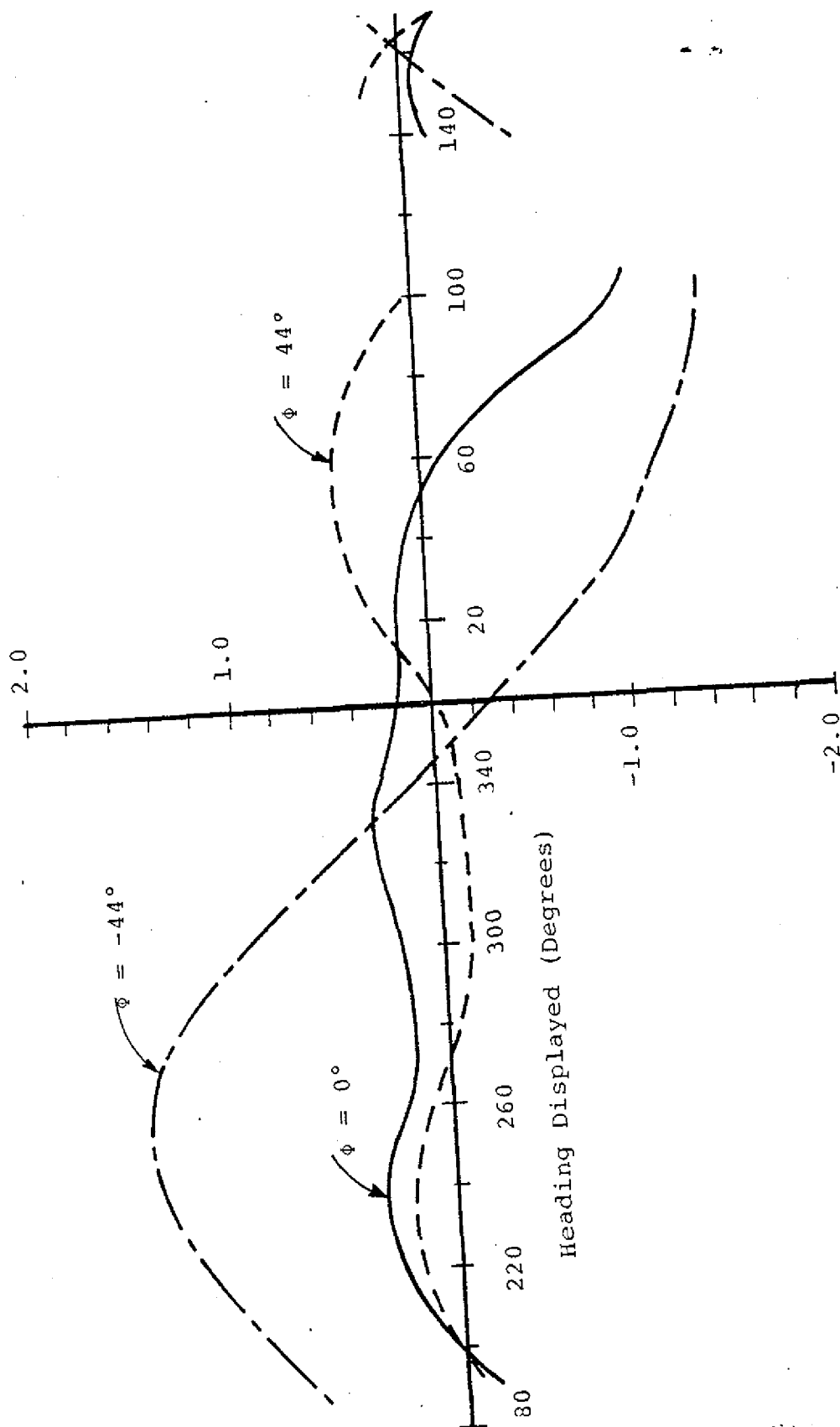


Fig. 5-5 HEADING MEASUREMENT ERROR AT PITCH $\sim 20^\circ$
(OFFSET AND ORTHOGONALITY ERROR CORRECTED)

Heading Displayed (Degrees)	Roll = 44°		Roll = -44°	
	Angular Position	Error	Angular Position	Error
20	287.0	-0.4	286.5	-0.3
40	307.0	-0.4	306.7	-0.1
60	327.0	-0.4	326.8	0.0
80	347.0	-0.4	346.8	0.0
90	356.7	-0.7	355.6	-0.2
140	47.8	0.4	48.0	1.2
160	67.7	0.3	68.0	1.2
180	87.0	-0.4	87.8	1.0
200	107.6	0.2	108.0	1.2
220	127.7	0.3	128.0	1.2
240	147.8	0.4	147.4	0.6
260	167.6	0.2	167.2	0.4
280	187.6	0.2	187.0	0.2
300	207.1	-0.3	206.5	-0.3
320	227.1	-0.3	226.6	-0.2
340	247.1	-0.3	246.9	0.1
0	266.3	-0.9	266.0	-0.8

TABLE 5-8 HEADING MEASUREMENTS AT PITCH = -20° WITH
 OFFSET AND ORTHOGONALITY ERROR CORRECTED

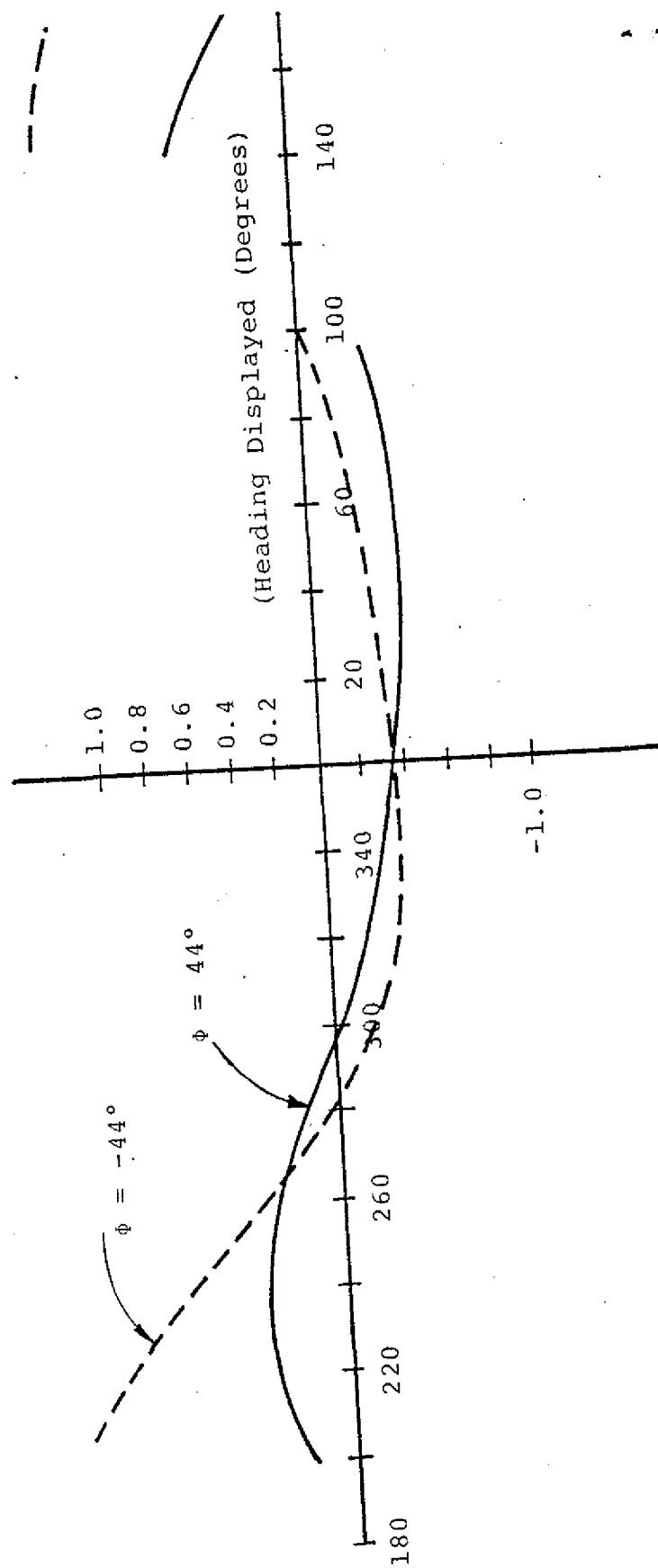


Fig. 5-6 HEADING MEASUREMENT ERROR AT PITCH = -20°
(OFFSET AND ORTHOGONALITY CORRECTED)

major error source⁴. Additionally, we note that the correction of offset error in sensors has been successful. Experimental results have verified that not only can offset errors be determined (Chapter IV), but a suitable algorithm can be implemented in the computer to improve system operation. It is postulated that offset error correction can be extended to include correction of varying offset values (functions of temperature and supply voltage) by monitoring error causing variables (example temperature) and computing correction constants prior to offset correction as above.

Errors induced by sensor nonorthogonality were predicted in Chapter IV section 4-2 and verified by plotting expected error along with measured error in Fig. 4-14. The curves of Fig. 4-14 were plotted for heading rotations with no pitch or roll angle. To evaluate system performance and the effect of orthogonality error with combined angular rotations, measurements of heading error were plotted in Fig. 5-3 through 5-6 inclusive.

Comparison of these data indicate that maximum excursions of error as a function of heading are significantly less when orthogonality corrections are made. It is also postulated that data could be improved further by similarly correcting orthogonality error in the Z axis sensor⁵.

In summary, the experimental evaluation has provided insight into the operation of an attitude independent remote magnetic indicator and heading computer in the "real world"

⁴This corroborates the observations predicted during error analysis in Chapter IV.

⁵We note that the error excursions are functions of pitch and roll and that Z axis data is used in the rotation algorithm.

environment complete with all contributing error sources. The error analysis evolved during development of the system has proven adequate in that an operational system was developed. Major error sources were measurable as predicted and the means of reducing their effects were successfully implemented. Correction of sensor offset and orthogonality error required an empirical evaluation of the respective sensor. These evaluations were performed, the errors characterized, correction coefficients determined, and correction algorithms implemented.

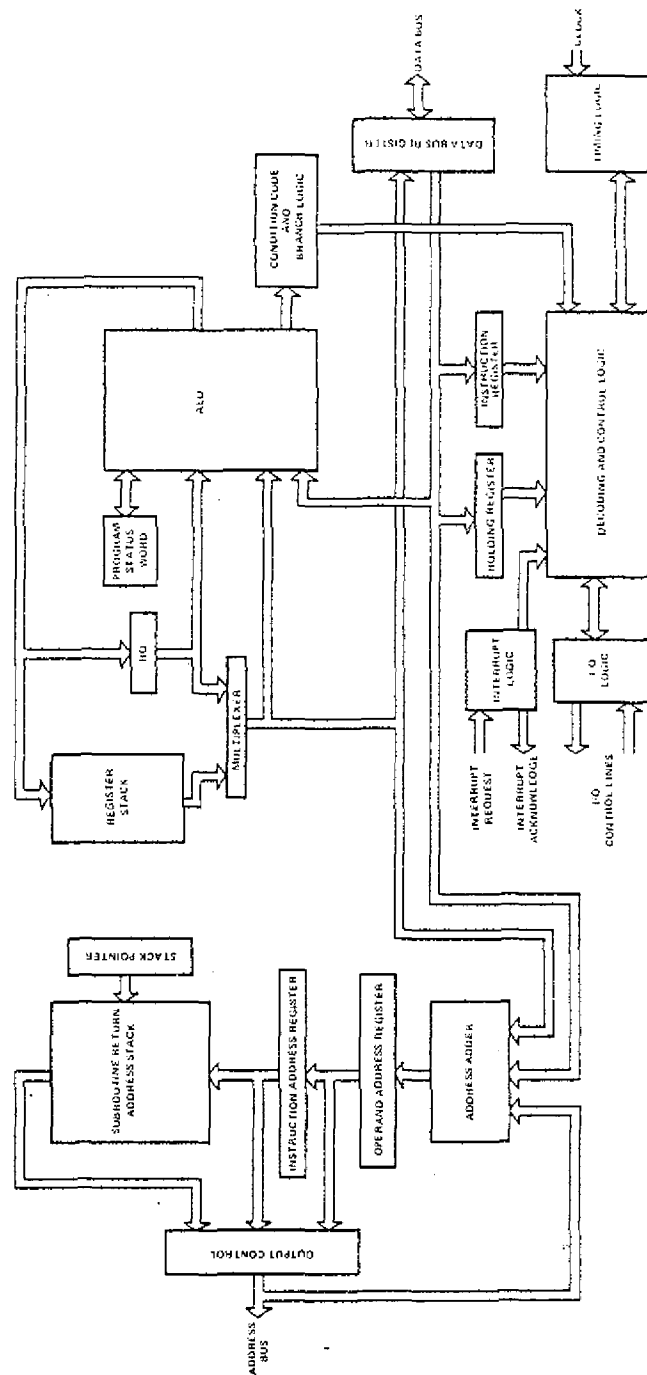
Successful implementation of these corrections was evidenced by significant reductions in system error. The correction methods presented can be extended in future with the net result that less demand is required of physical sensors if the sensor parameters can be established empirically prior to completion of instrument design. Utilization of a microprocessor in the instrument has added the computational flexibility required to facilitate accommodation of sensors with varying error magnitudes.

APPENDIX A

This appendix lists the instruction set of the Signetics 2650 microprocessor chip used to implement the heading instrument.

LOAD/STORE INSTRUCTIONS			Length (bytes)			
Instruction	Operation	Register				
LODZ	r	Load Register Zero	1			3
LODI	v	Load Immediate	2			2
LODR	(*)a	Load Relative	2			3
LODA	(*)a(X)	Load Absolute	3			2
STRZ	r	Store Register Zero	1			
STRI	v	Store Immediate	2			
STR	(*)a	Store Relative	2			
STRA	(*)a(X)	Store Absolute	3			
ARITHMETIC INSTRUCTIONS			Length (bytes)			
Instruction	Operation	Register				
ADDZ	r	Add to Register Zero	1			2
ADDI	v	Add Immediate	2			3
ADDR	(*)a	Add Relative	2			3
ADA	(*)a(X)	Add Absolute	3			2
SUBZ	r	Subtract from Register Zero	1			
SUBI	v	Subtract Immediate	2			
SUBR	(*)a	Subtract Relative	2			
SUBA	(*)a(X)	Subtract Absolute	3			
LOGICAL INSTRUCTIONS			Length (bytes)			
Instruction	Operation	Register				
ANDZ	r	And to Register Zero	1			3
ANDI	v	And Immediate	2			1
ANDR	(*)a	And Relative	2			1
AND	(*)a(X)	And Absolute	3			2
IORZ	r	Inclusive or to Register Zero	1			2
IORI	v	Inclusive or Immediate	2			1
IORR	(*)a	Inclusive or Relative	2			1
IORA	(*)a(X)	Inclusive or Absolute	3			2
EXRZ	r	Exclusive or to Register Zero	1			2
EXRI	v	Exclusive or Immediate	2			1
EXRR	(*)a	Exclusive or Relative	2			1
EXRA	(*)a(X)	Exclusive or Absolute	3			2
COMPARISON INSTRUCTIONS			Length (bytes)			
Instruction	Operation	Register				
CONZ	r	Compare to Register Zero	1			2
CONI	v	Compare Immediate	2			1
CONR	(*)a	Compare Relative	2			1
CON	(*)a(X)	Compare Absolute	3			2
ROTATE INSTRUCTIONS			Length (bytes)			
Instruction	Operation	Register				
RORR	r	Rotate Register Right	1			1
RRL	r	Rotate Register Left	1			1
BRANCH INSTRUCTIONS			Length (bytes)			
Instruction	Operation	Register				
BCTI	(*)a	Branch on Condition True Relative	2			1
BCFI	(*)a	Branch on Condition False Relative	2			1
BCTA	(*)a	Branch on Condition True Absolute	3			1
BCFA	(*)a	Branch on Condition False Absolute	3			1
BRNR	(*)a	Branch on Register Non-Zero Relative	2			1
BRNA	(*)a	Branch on Register Non-Zero Absolute	3			1
BIRR	(*)a	Branch on Incrementing Register Relative	2			1
BIRI	(*)a	Branch on Incrementing Register Absolute	3			1
BDRR	(*)a	Branch on Decrementing Register Relative	2			1
BDIR	(*)a	Branch on Decrementing Register Absolute	3			1
BXA	(*)a(X)	Branch Indexed Absolute, Unconditional	3			1
ZBR	(*)a	Zero Branch Relative, Unconditional	2			1
SUBROUTINE BRANCH/RETURN INSTRUCTIONS			Length (bytes)			
Instruction	Operation	Register				
BSIR	(*)a	Branch to Subroutine on Condition True, Relative	2			2
BSRI	(*)a	Branch to Subroutine on Condition True, Absolute	3			2
BSRR	(*)a	Branch to Subroutine on Condition True, Relative	2			2
BSRI	(*)a	Branch to Subroutine on Condition True, Absolute	3			2
BSNR	(*)a	Branch to Subroutine on Non-Zero Register, Relative	2			2
BSNA	(*)a	Branch to Subroutine on Non-Zero Register, Absolute	3			2
BSXA	(*)a(X)	Branch to Subroutine, Indexed, Unconditional	3			2
RETC	v	Return From Subroutine, Conditional	1			1
RETI	v	Return From Subroutine and Enable Interrupt, Conditional	1			1
ZBSR	(*)a	Zero Branch to Subroutine Relative, Unconditional	2			2
PROGRAM STATUS INSTRUCTIONS			Length (bytes)			
Instruction	Operation	Register				
LPSU		Load Program Status, Upper	1			1
LPSL		Load Program Status, Lower	1			1
SPSU		Store Program Status, Upper	1			1
SPSL		Store Program Status, Lower	1			1
CPSU	v	Clear Program Status, Upper, Selective	2			2
CPSL	v	Clear Program Status, Lower, Selective	2			2
PPSU	v	Preset Program Status, Upper, Selective	2			2
PPSL	v	Preset Program Status, Lower, Selective	2			2
TPSU	v	Test Program Status, Upper, Selective	2			2
TPSL	v	Test Program Status, Lower, Selective	2			2
INPUT/OUTPUT INSTRUCTIONS			Length (bytes)			
Instruction	Operation	Register				
WRDI		Write Data	1			1
REDD	r	Read Data	1			1
WRTC	r	Write Control	1			1
REDC	r	Read Control	1			1
WRTE	v	Write Extended	2			2
REDE	v	Read Extended	2			2
MISCELLANEOUS INSTRUCTIONS			Length (bytes)			
Instruction	Operation	Register				
HALT		Halt, Enter Wait State	1			1
DAR		Decimal Adjust Register	1			1
TML	v	Test Under Mask Immediate	2			1
NOP		No Operation	1			1

REPRODUCIBILITY OF THE
ORIGINAL PAGE IS POOR



BLOCK DIAGRAM

APPENDIX B

This appendix contains a listing of the assembly language program used to implement the remote magnetic indicator heading algorithm. The program was assembled on the A2650 cross assembler program operational on the HP 2100 computer at the University of Santa Clara.

REPRODUCIBILITY OF THE
ORIGINAL PAGE IS POOR

PIP ASSEMBLER DEFINITION SOURCE LEVEL 1 HEADLINE INSTRUMENT ASSEMBLY PROGRAM 1076 PAGE 2

```

LINE ADDR LABEL R1 R2 R3 R4 INCR SOURCE
3      0000      EQU 0
4      0001      EQU 1
5      0002      EQU 2
6      0003      EQU 3
7      0004      EQU 4
8      0005      EQU 5
9      0006      EQU 6
10     0007      EQU 7
11     0008      EQU 8
12     0009      EQU 9
13     0010      EQU 10
14     0011      EQU 11
15     0012      EQU 12
16     0013      EQU 13
17     0014      EQU 14
18     0015      EQU 15
19     0016      EQU 16
20     0017      EQU 17
21     0018      EQU 18
22     0019      EQU 19
23     0020      EQU 20
24     0021      EQU 21
25     0022      EQU 22
26     0023      EQU 23
27     0024      EQU 24
28     0025      EQU 25
29     0026      EQU 26
30     0027      EQU 27
31     0028      EQU 28
32     0029      EQU 29
33     0030      EQU 30
34     0031      EQU 31
35     0032      EQU 32
36     0033      EQU 33
37     0034      EQU 34
38     0035      EQU 35
39     0036      EQU 36
40     0037      EQU 37
41     0038      EQU 38
42     0039      EQU 39
43     0040      EQU 40
44     0041      EQU 41
45     0042      EQU 42
46     0043      EQU 43
47     0044      EQU 44
48     0045      EQU 45
49     0046      EQU 46
50     0047      EQU 47
51     0048      EQU 48
52     0049      EQU 49
53     0050      EQU 50
54     0051      EQU 51
55     0052      EQU 52
56     0053      EQU 53
57     0054      EQU 54
58     0055      EQU 55
59     0056      EQU 56
60     0057      EQU 57
61     0058      EQU 58
62     0059      EQU 59
63     0060      EQU 60
64     0061      EQU 61
65     0062      EQU 62
66     0063      EQU 63
67     0064      EQU 64
68     0065      EQU 65
69     0066      EQU 66
70     0067      EQU 67
71     0068      EQU 68
72     0069      EQU 69
73     0070      EQU 70
74     0071      EQU 71
75     0072      EQU 72
76     0073      EQU 73
77     0074      EQU 74
78     0075      EQU 75
79     0076      EQU 76
80     0077      EQU 77
81     0078      EQU 78
82     0079      EQU 79
83     0080      EQU 80
84     0081      EQU 81
85     0082      EQU 82
86     0083      EQU 83
87     0084      EQU 84
88     0085      EQU 85
89     0086      EQU 86
90     0087      EQU 87
91     0088      EQU 88
92     0089      EQU 89
93     0090      EQU 90
94     0091      EQU 91
95     0092      EQU 92
96     0093      EQU 93
97     0094      EQU 94
98     0095      EQU 95
99     0096      EQU 96
100    0097      EQU 97
101    0098      EQU 98
102    0099      EQU 99
103    0100      EQU 100
104    0101      EQU 101
105    0102      EQU 102
106    0103      EQU 103
107    0104      EQU 104
108    0105      EQU 105
109    0106      EQU 106
110    0107      EQU 107
111    0108      EQU 108
112    0109      EQU 109
113    0110      EQU 110
114    0111      EQU 111
115    0112      EQU 112
116    0113      EQU 113
117    0114      EQU 114
118    0115      EQU 115
119    0116      EQU 116
120    0117      EQU 117
121    0118      EQU 118
122    0119      EQU 119
123    0120      EQU 120
124    0121      EQU 121
125    0122      EQU 122
126    0123      EQU 123
127    0124      EQU 124
128    0125      EQU 125
129    0126      EQU 126
130    0127      EQU 127
131    0128      EQU 128
132    0129      EQU 129
133    0130      EQU 130
134    0131      EQU 131
135    0132      EQU 132
136    0133      EQU 133
137    0134      EQU 134
138    0135      EQU 135
139    0136      EQU 136
140    0137      EQU 137
141    0138      EQU 138
142    0139      EQU 139
143    0140      EQU 140
144    0141      EQU 141
145    0142      EQU 142
146    0143      EQU 143
147    0144      EQU 144
148    0145      EQU 145
149    0146      EQU 146
150    0147      EQU 147
151    0148      EQU 148
152    0149      EQU 149
153    0150      EQU 150
154    0151      EQU 151
155    0152      EQU 152
156    0153      EQU 153
157    0154      EQU 154
158    0155      EQU 155
159    0156      EQU 156
160    0157      EQU 157
161    0158      EQU 158
162    0159      EQU 159
163    0160      EQU 160
164    0161      EQU 161
165    0162      EQU 162
166    0163      EQU 163
167    0164      EQU 164
168    0165      EQU 165
169    0166      EQU 166
170    0167      EQU 167
171    0168      EQU 168
172    0169      EQU 169
173    0170      EQU 170
174    0171      EQU 171
175    0172      EQU 172
176    0173      EQU 173
177    0174      EQU 174
178    0175      EQU 175
179    0176      EQU 176
180    0177      EQU 177
181    0178      EQU 178
182    0179      EQU 179
183    0180      EQU 180
184    0181      EQU 181
185    0182      EQU 182
186    0183      EQU 183
187    0184      EQU 184
188    0185      EQU 185
189    0186      EQU 186
190    0187      EQU 187
191    0188      EQU 188
192    0189      EQU 189
193    0190      EQU 190
194    0191      EQU 191
195    0192      EQU 192
196    0193      EQU 193
197    0194      EQU 194
198    0195      EQU 195
199    0196      EQU 196
200    0197      EQU 197
201    0198      EQU 198
202    0199      EQU 199
203    0200      EQU 200
204    0201      EQU 201
205    0202      EQU 202
206    0203      EQU 203
207    0204      EQU 204
208    0205      EQU 205
209    0206      EQU 206
210    0207      EQU 207
211    0208      EQU 208
212    0209      EQU 209
213    0210      EQU 210
214    0211      EQU 211
215    0212      EQU 212
216    0213      EQU 213
217    0214      EQU 214
218    0215      EQU 215
219    0216      EQU 216
220    0217      EQU 217
221    0218      EQU 218
222    0219      EQU 219
223    0220      EQU 220
224    0221      EQU 221
225    0222      EQU 222
226    0223      EQU 223
227    0224      EQU 224
228    0225      EQU 225
229    0226      EQU 226
230    0227      EQU 227
231    0228      EQU 228
232    0229      EQU 229
233    0230      EQU 230
234    0231      EQU 231
235    0232      EQU 232
236    0233      EQU 233
237    0234      EQU 234
238    0235      EQU 235
239    0236      EQU 236
240    0237      EQU 237
241    0238      EQU 238
242    0239      EQU 239
243    0240      EQU 240
244    0241      EQU 241
245    0242      EQU 242
246    0243      EQU 243
247    0244      EQU 244
248    0245      EQU 245
249    0246      EQU 246
250    0247      EQU 247
251    0248      EQU 248
252    0249      EQU 249
253    0250      EQU 250
254    0251      EQU 251
255    0252      EQU 252
256    0253      EQU 253
257    0254      EQU 254
258    0255      EQU 255
259    0256      EQU 256
260    0257      EQU 257
261    0258      EQU 258
262    0259      EQU 259
263    0260      EQU 260
264    0261      EQU 261
265    0262      EQU 262
266    0263      EQU 263
267    0264      EQU 264
268    0265      EQU 265
269    0266      EQU 266
270    0267      EQU 267
271    0268      EQU 268
272    0269      EQU 269
273    0270      EQU 270
274    0271      EQU 271
275    0272      EQU 272
276    0273      EQU 273
277    0274      EQU 274
278    0275      EQU 275
279    0276      EQU 276
280    0277      EQU 277
281    0278      EQU 278
282    0279      EQU 279
283    0280      EQU 280
284    0281      EQU 281
285    0282      EQU 282
286    0283      EQU 283
287    0284      EQU 284
288    0285      EQU 285
289    0286      EQU 286
290    0287      EQU 287
291    0288      EQU 288
292    0289      EQU 289
293    0290      EQU 290
294    0291      EQU 291
295    0292      EQU 292
296    0293      EQU 293
297    0294      EQU 294
298    0295      EQU 295
299    0296      EQU 296
300    0297      EQU 297
301    0298      EQU 298
302    0299      EQU 299
303    0300      EQU 300
304    0301      EQU 301
305    0302      EQU 302
306    0303      EQU 303
307    0304      EQU 304
308    0305      EQU 305
309    0306      EQU 306
310    0307      EQU 307
311    0308      EQU 308
312    0309      EQU 309
313    0310      EQU 310
314    0311      EQU 311
315    0312      EQU 312
316    0313      EQU 313
317    0314      EQU 314
318    0315      EQU 315
319    0316      EQU 316
320    0317      EQU 317
321    0318      EQU 318
322    0319      EQU 319
323    0320      EQU 320
324    0321      EQU 321
325    0322      EQU 322
326    0323      EQU 323
327    0324      EQU 324
328    0325      EQU 325
329    0326      EQU 326
330    0327      EQU 327
331    0328      EQU 328
332    0329      EQU 329
333    0330      EQU 330
334    0331      EQU 331
335    0332      EQU 332
336    0333      EQU 333
337    0334      EQU 334
338    0335      EQU 335
339    0336      EQU 336
340    0337      EQU 337
341    0338      EQU 338
342    0339      EQU 339
343    0340      EQU 340
344    0341      EQU 341
345    0342      EQU 342
346    0343      EQU 343
347    0344      EQU 344
348    0345      EQU 345
349    0346      EQU 346
350    0347      EQU 347
351    0348      EQU 348
352    0349      EQU 349
353    0350      EQU 350
354    0351      EQU 351
355    0352      EQU 352
356    0353      EQU 353
357    0354      EQU 354
358    0355      EQU 355
359    0356      EQU 356
360    0357      EQU 357
361    0358      EQU 358
362    0359      EQU 359
363    0360      EQU 360
364    0361      EQU 361
365    0362      EQU 362
366    0363      EQU 363
367    0364      EQU 364
368    0365      EQU 365
369    0366      EQU 366
370    0367      EQU 367
371    0368      EQU 368
372    0369      EQU 369
373    0370      EQU 370
374    0371      EQU 371
375    0372      EQU 372
376    0373      EQU 373
377    0374      EQU 374
378    0375      EQU 375
379    0376      EQU 376
380    0377      EQU 377
381    0378      EQU 378
382    0379      EQU 379
383    0380      EQU 380
384    0381      EQU 381
385    0382      EQU 382
386    0383      EQU 383
387    0384      EQU 384
388    0385      EQU 385
389    0386      EQU 386
390    0387      EQU 387
391    0388      EQU 388
392    0389      EQU 389
393    0390      EQU 390
394    0391      EQU 391
395    0392      EQU 392
396    0393      EQU 393
397    0394      EQU 394
398    0395      EQU 395
399    0396      EQU 396
400    0397      EQU 397
401    0398      EQU 398
402    0399      EQU 399
403    0400      EQU 400
404    0401      EQU 401
405    0402      EQU 402
406    0403      EQU 403
407    0404      EQU 404
408    0405      EQU 405
409    0406      EQU 406
410    0407      EQU 407
411    0408      EQU 408
412    0409      EQU 409
413    0410      EQU 410
414    0411      EQU 411
415    0412      EQU 412
416    0413      EQU 413
417    0414      EQU 414
418    0415      EQU 415
419    0416      EQU 416
420    0417      EQU 417
421    0418      EQU 418
422    0419      EQU 419
423    0420      EQU 420
424    0421      EQU 421
425    0422      EQU 422
426    0423      EQU 423
427    0424      EQU 424
428    0425      EQU 425
429    0426      EQU 426
430    0427      EQU 427
431    0428      EQU 428
432    0429      EQU 429
433    0430      EQU 430
434    0431      EQU 431
435    0432      EQU 432
436    0433      EQU 433
437    0434      EQU 434
438    0435      EQU 435
439    0436      EQU 436
440    0437      EQU 437
441    0438      EQU 438
442    0439      EQU 439
443    0440      EQU 440
444    0441      EQU 441
445    0442      EQU 442
446    0443      EQU 443
447    0444      EQU 444
448    0445      EQU 445
449    0446      EQU 446
450    0447      EQU 447
451    0448      EQU 448
452    0449      EQU 449
453    0450      EQU 450
454    0451      EQU 451
455    0452      EQU 452
456    0453      EQU 453
457    0454      EQU 454
458    0455      EQU 455
459    0456      EQU 456
460    0457      EQU 457
461    0458      EQU 458
462    0459      EQU 459
463    0460      EQU 460
464    0461      EQU 461
465    0462      EQU 462
466    0463      EQU 463
467    0464      EQU 464
468    0465      EQU 465
469    0466      EQU 466
470    0467      EQU 467
471    0468      EQU 468
472    0469      EQU 469
473    0470      EQU 470
474    0471      EQU 471
475    0472      EQU 472
476    0473      EQU 473
477    0474      EQU 474
478    0475      EQU 475
479    0476      EQU 476
480    0477      EQU 477
481    0478      EQU 478
482    0479      EQU 479
483    0480      EQU 480
484    0481      EQU 481
485    0482      EQU 482
486    0483      EQU 483
487    0484      EQU 484
488    0485      EQU 485
489    0486      EQU 486
490    0487      EQU 487
491    0488      EQU 488
492    0489      EQU 489
493    0490      EQU 490
494    0491      EQU 491
495    0492      EQU 492
496    0493      EQU 493
497    0494      EQU 494
498    0495      EQU 495
499    0496      EQU 496
500    0497      EQU 497
501    0498      EQU 498
502    0499      EQU 499
503    0500      EQU 500
504    0501      EQU 501
505    0502      EQU 502
506    0503      EQU 503
507    0504      EQU 504
508    0505      EQU 505
509    0506      EQU 506
510    0507      EQU 507
511    0508      EQU 508
512    0509      EQU 509
513    0510      EQU 510
514    0511      EQU 511
515    0512      EQU 512
516    0513      EQU 513
517    0514      EQU 514
518    0515      EQU 515
519    0516      EQU 516
520    0517      EQU 517
521    0518      EQU 518
522    0519      EQU 519
523    0520      EQU 520
524    0521      EQU 521
525    0522      EQU 522
526    0523      EQU 523
527    0524      EQU 524
528    0525      EQU 525
529    0526      EQU 526
530    0527      EQU 527
531    0528      EQU 528
532    0529      EQU 529
533    0530      EQU 530
534    0531      EQU 531
535    0532      EQU 532
536    0533      EQU 533
537    0534      EQU 534
538    0535      EQU 535
539    0536      EQU 536
540    0537      EQU 537
541    0538      EQU 538
542    0539      EQU 539
543    0540      EQU 540
544    0541      EQU 541
545    0542      EQU 542
546    0543      EQU 543
547    0544      EQU 544
548    0545      EQU 545
549    0546      EQU 546
550    0547      EQU 547
551    0548      EQU 548
552    0549      EQU 549
553    0550      EQU 550
554    0551      EQU 551
555    0552      EQU 552
556    0553      EQU 553
557    0554      EQU 554
558    0555      EQU 555
559    0556      EQU 556
560    0557      EQU 557
561    0558      EQU 558
562    0559      EQU 559
563    0560      EQU 560
564    0561      EQU 561
565    0562      EQU 562
566    0563      EQU 563
567    0564      EQU 564
568    0565      EQU 565
569    0566      EQU 566
570    0567      EQU 567
571    0568      EQU 568
572    0569      EQU 569
573    0570      EQU 570
574    0571      EQU 571
575    0572      EQU 572
576    0573      EQU 573
577    0574      EQU 574
578    0575      EQU 575
579    0576      EQU 576
580    0577      EQU 577
581    0578      EQU 578
582    0579      EQU 579
583    0580      EQU 580
584    0581      EQU 581
585    0582      EQU 582
586    0583      EQU 583
587    0584      EQU 584
588    0585      EQU 585
589    0586      EQU 586
590    0587      EQU 587
591    0588      EQU 588
592    0589      EQU 589
593    0590      EQU 590
594    0591      EQU 591
595    0592      EQU 592
596    0593      EQU 593
597    0594      EQU 594
598    0595      EQU 595
599    0596      EQU 596
600    0597      EQU 597
601    0598      EQU 598
602    0599      EQU 599
603    0600      EQU 600
604    0601      EQU 601
605    0602      EQU 602
606    0603      EQU 603
607    0604      EQU 604
608    0605      EQU 605
609    0606      EQU 606
610    0607      EQU 607
611    0608      EQU 608
612    0609      EQU 609
613    0610      EQU 610
614    0611      EQU 611
615    0612      EQU 612
616    0613      EQU 613
617    0614      EQU 614
618    0615      EQU 615
619    0616      EQU 616
620    0617      EQU 617
621    0618      EQU 618
622    0619      EQU 619
623    0620      EQU 620
624    0621      EQU 621
625    0622      EQU 622
626    0623      EQU 623
627    0624      EQU 624
628    0625      EQU 625
629    0626      EQU 626
630    0627      EQU 627
631    0628      EQU 628
632    0629      EQU 629
633    0630      EQU 630
634    0631      EQU 631
635    0632      EQU 632
636    0633      EQU 633
637    0634      EQU 634
638    0635      EQU 635
639    0636      EQU 636
640    0637      EQU 637
641    0638      EQU 638
642    0639      EQU 639
643    0640      EQU 640
644    0641      EQU 641
645    0642      EQU 642
646    0643      EQU 643
647    0644      EQU 644
648    0645      EQU 645
649    0646      EQU 646
650    0647      EQU 647
651    0648      EQU 648
652    0649      EQU 649
653    0650      EQU 650
654    0651      EQU 651
655    0652      EQU 652
656    0653      EQU 653
657    0654      EQU 654
658    0655      EQU 655
659    0656      EQU 656
660    0657      EQU 657
661    0658      EQU 658
662    0659      EQU 659
663    0660      EQU 660
664    0661      EQU 661
665    0662      EQU 662
666    0663      EQU 663
667    0664      EQU 664
668    0665      EQU 665
669    0666      EQU 666
670    0667      EQU 667
671    0668      EQU 668
672    0669      EQU 669
673    0670      EQU 670
674    0671      EQU 671
675    0672      EQU 672
676    0673      EQU 673
677    0674      EQU 674
678    0675      EQU 675
679    0676      EQU 676
680    0677      EQU 677
681    0678      EQU 678
682    0679      EQU 679
683    0680      EQU 680
684    0681      EQU 681
685    0682      EQU 682
686    0683      EQU 683
687    0684      EQU 684
688    0685      EQU 685
689    0686      EQU 686
690    0687      EQU 687
691    0688      EQU 688
692    0689      EQU 689
693    0690      EQU 690
694    0691      EQU 691
695    0692      EQU 692
696    0693      EQU 693
697    0694      EQU 694
698    0695      EQU 695
699    0696      EQU 696
700    0697      EQU 697
701    0698      EQU 698
702    0699      EQU 699
703    0700      EQU 700
704    0701      EQU 701
705    0702      EQU 702
706    0703      EQU 703
707    0704      EQU 704
708    0705      EQU 705
709    0706      EQU 706
710    0707      EQU 707
711    0708      EQU 708
712    0709      EQU 709
713    0710      EQU 710
714    0711      EQU 711
715    0712      EQU 712
716    0713      EQU 713
717    0714      EQU 714
718    0715      EQU 715
719    0716      EQU 716
720    0717      EQU 717
721    0718      EQU 718
722    0719      EQU 719
723    0720      EQU 720
724    0721      EQU 721
725    0722      EQU 722
726    0723      EQU 723
727    0724      EQU 724
728    0725      EQU 725
729    0726      EQU 726
730    0727      EQU 727
731    0728      EQU 728
732    0729      EQU 729
733    0730      EQU 730
734    0731      EQU 731
735    0732      EQU 732
736    0733      EQU 733
737    0734      EQU 734
738    0735      EQU 735
739    0736      EQU 736
740    0737      EQU 737
741    0738      EQU 738
742    0739      EQU 739
743    0740      EQU 740
744    0741      EQU 741
745    0742      EQU 742
746    0743      EQU 743
747    0744      EQU 744
748    0745      EQU 745
749    0746      EQU 746
750    0747      EQU 747
751    0748      EQU 748
752    0749      EQU 749
753    0750      EQU 750
754    0751      EQU 751
755    0752      EQU 752
756    0753      EQU 753
757    0754      EQU 754
758    0755      EQU 755
759    0756      EQU 756
760    0757      EQU 757
761    0758      EQU 758
762    0759      EQU 759
763    0760      EQU 760
764    0761      EQU 761
765    0762      EQU 762
766    0763      EQU 763
767    0764      EQU 764
768    0765      EQU 765
769    0766      EQU 766
770    0767      EQU 767
771    0768      EQU 768
772    0769      EQU 769
773    0770      EQU 770
774    0771      EQU 771
775    0772      EQU 772
776    0773      EQU 773
777    0774      EQU 774
778    077
```


REPRODUCIBILITY OF THE
ORIGINAL PAGE IS POOR

LINE ADDR LARL B1 B2 B3 B4 ERROR SOURCE

82	0598		CE CF 00 01	DATA	HICE,CF,00,01,02,03,04,05,06,07
			02 03 03 04		
			05 06 07		
83	05A3		08 09 09 0A	DATA	HID8,09,09,0A,0B,0C,0D,0E,0F,EO
			08 0C 0D 0D		
			0E 0F E0		
84	05AE		E1 E1 E2 E3	DATA	HIE1,E1,E2,E3,E4,E5,E6,E7,EB
			E3 E4 E5 E6		
			E6 E7 F8		
85	05H9	05H9	FF FF FF FF	CUS	H1FF,FF,FF,FF,FF,FF,FF,FF,FF
			FF FF FF FF		
			FF FF FF FF	DATA	H1FF,FF,FF,FF,FF,FF,FF,FF,FE
			FF FF FE FF		
86	05C3		FE FE FE FE	DATA	H1FE,FD,FD,FD,FD,FC,FC,FC,FB
			FE FE FD FD		
87	05C0		FD FC FC FC	DATA	H1FB,FB,FB,FA,FA,FA,FA,FA,FA
			FC FA FA FA		
88	05D7		FA FA FA FA	DATA	H1FB,FB,FB,FA,FA,FA,FA,FA,FA
			FA FA FA FA		
89	05E1		FA FA FA FA	DATA	H1FB,FB,FB,FA,FA,FA,FA,FA,FA
			FA FA FA FA		
90	05E8		F4 F3 F3 F2	DATA	H1F4,F3,F3,F2,F2,F1,F1,F0,EF,EF
			F2 F1 F1 F0		
			EF EF EF EF	DATA	H1EE,FE,ED,ED,ED,ED,ED,ED,EA,EA,EA,EA
91	05F5		EE EF FD ED	DATA	H1E7,E6,E6,E5,E4,E3,E3,E2,E1,E1
			EC EF EB EA		
			EA E9 EB EA		
92	0601		E7 E6 E6 E5	DATA	H1E0,0F,0F,0D,0D,0C,0B,0A,09,09
			E4 E3 E3 E2		
			E1 E1 E1 E1		
93	0608		E0 0F 0E 0D	DATA	H1D8,07,06,05,04,03,03,02,01,00
			0D 0C 0B 0A		
			09 09 09 09		
94	0615		08 07 06 05	DATA	H1CF,CE,CD,CC,CC,CC,CC,CC,CC,CC
			04 03 03 02		
			01 00 00 00	DATA	H1C5,C4,C3,C2,C1,C0,BF,BE,BD,AC
95	061F		CF CE CD CC	DATA	H1B4,BA,B9,B8,B7,H6,H5,H3,H2,H1
			CB CA C9 C8		
			C7 C6 C5 C4		
96	0629		C5 C4 C3 C2	DATA	H1B0,AF,AE,AD,AB,AA,AA,AA,AA,AA
			C1 C0 BF BE		
			BD BC BA BB		
97	0633		BD BA B9 BA	DATA	H1A3,A2,A1,9F,9E,9D,9C,9B,9A,98,97,95
			B7 B6 B5 B3		
			B2 B1 B0 AF		
98	063D		AE AD AB AA		
			AA A9 AA A7		
			A6 A5 A4 A3		
99	0648		A2 A1 9F		
			9E 9D 9C 9B		
			99 98 97 95		

REPRODUCIBILITY OF THE
ORIGINAL PAGE IS POOR

PIP ASSEMBLER VERSION SCU LEVEL 1 HEADING INSTRUMENT ASSEMBLY PROGRAM 1976 PAGE 5

LINE	ADDR	1AHL	B1	B2	B3	B4	ERROR	SOURCE
100	0054		94	93	92	90		DATA
			8F	8E	8C	88		H194,93,92,90,8F,8E,8C,88,8A,88,
			8A	84				
101	005F		87	86	84	83		DATA
			82	80	7F	7E		H187,86,84,83,82,80,7F,7E,7C,78,
			7C	78				
102	0068		7A	78	77	75		DATA
			74	73	71	70		H17A,78,77,75,74,73,71,70,6E,6D,6C,
			6E	60	6C			
103	0073		6A	69	67	66		DATA
			64	63	61	60		H16A,69,67,66,64,63,61,60,5F,5D,5C,
			5F	50	5C			
104	007E		5A	59	57	56		DATA
			54	53	51	50		H15A,59,57,56,54,53,51,50,4E,4D,
			4E	40				
105	008H		44	44	44	47		DATA
			45	44	42	41		H144,44,44,47,45,44,42,41,3F,3E,3C,
			3F	3C				
106	0093		3B	39	38	3A		DATA
			35	33	31	30		H13B,39,38,36,35,33,31,30,2E,2D,
			2E	20				
107	0090		2B	24	28	27		DATA
			25	24	22	20		H12B,24,24,27,25,24,22,20,1F,1D,
			1F	10				
108	00A7		1C	1A	19	17		DATA
			15	14	12	11		H11C,1A,19,17,15,14,12,11,0F,0E,
			0F	0F				
109	00A1		0C	0A	09	07		DATA
			06	04	03	01		H10C,0A,09,07,06,04,03,01,00,
			00					
110	00BA	00BA	7F	74	77	72		COSH DATA
			6E	69	65	61		H17F,78,77,72,6E,69,65,61,5C,58,54,
			5C	54				
111	00C5		50	46	47	43		DATA
			3F	3C	38	34		H150,48,47,43,3F,3C,38,34,31,2D,2A,
			31	20	2A			
112	00D0		27	23	20	10		DATA
			1B	1A	15	13		H127,23,20,1D,18,15,13,11,0E,0C,
			11	0F	0C			
113	00DB		08	09	07	0A		DATA
			04	03	02	01		H104,09,07,06,04,03,02,01,01,00,00,00,00,
			01	00	00	00		
			00					
114	00EB	00EB	FF	88	12	9F		COSH DATA
			2F	C5	63	64		H1FF,68,12,9F,2F,C5,63,64,67,72,38,0C,
			47	72	38	0C		
115	00F4		F0	E3	FB	FF		DATA
			28	6C	C3	32		H1F0,E3,EB,FF,28,6C,C3,32,B9,59,15,EC,
			B9	59	15	EC		
116	0700		F0	F2	22	72		DATA
			F2	73	26	FA		H1E0,12,22,72,E2,73,26,FA,FA,10,52,18,
			F4	1	52	BA		

REPRODUCIBILITY OF THE
ORIGINAL PAGE IS POOR

P/P ASSEMBLER VERSION 500 LEVEL 1 HEADING INSTRUMENT ASSEMBLY PROGRAM 1976 PAGE 6

LINE ADDR LAML B1 B2 B3 B4 B5 B6 B7 B8 B9 B10 B11 B12 B13 B14 B15 B16 B17 B18 B19 B20 B21 B22 B23 B24 B25 B26 B27 B28 B29 B30 B31 B32 B33 B34 B35 B36 B37 B38 B39 B40 B41 B42 B43 B44 B45 B46 B47 B48 B49 B50 B51 B52 B53 B54 B55 B56 B57 B58 B59 B60 B61 B62 B63 B64 B65 B66 B67 B68 B69 B70 B71 B72 B73 B74 B75 B76 B77 B78 B79 B80 B81 B82 B83 B84 B85 B86 B87 B88 B89 B90 B91 B92 B93 B94 B95 B96 B97 B98 B99 B100 B101 B102 B103 B104 B105 B106 B107 B108 B109 B110 B111 B112 B113 B114 B115 B116 B117 B118 B119 B120 B121 B122 B123 B124 B125 B126 B127 B128 B129 B130 B131 B132 B133 B134 B135 B136 B137 B138 B139 B140 B141 B142 B143 B144 B145 B146 B147 B148 B149 B150 B151 B152 B153 B154 B155 B156

```

117 070C 43 F5 CD CC DATA H143.F5.C0.CC.F1.3E.H3.4F.13.00
118 0716 0716 01 02 04 08 HCD DATA H101.02.04.08.16.32.64.00
119 071E 071E 03 SINE DATA H103
120 0720 0720 05 ORG H1750
121 0721 0721 06 * * * * *
122 0722 0722 07 * * * * *
123 0723 0723 08 * * * * *
124 0724 0724 09 * * * * *
125 0725 0725 0A * * * * *
126 0726 0726 0B * * * * *
127 0727 0727 0C * * * * *
128 0728 0728 0D * * * * *
129 0729 0729 0E * * * * *
130 0730 0730 0F * * * * *
131 0731 0731 10 * * * * *
132 0732 0732 11 * * * * *
133 0733 0733 12 * * * * *
134 0734 0734 13 * * * * *
135 0735 0735 14 * * * * *
136 0736 0736 15 * * * * *
137 0737 0737 16 * * * * *
138 0738 0738 17 * * * * *
139 0739 0739 18 * * * * *
140 0740 0740 19 * * * * *
141 0741 0741 1A * * * * *
142 0742 0742 1B * * * * *
143 0743 0743 1C * * * * *
144 0744 0744 1D * * * * *
145 0745 0745 1E * * * * *
146 0746 0746 1F * * * * *
147 0747 0747 20 * * * * *
148 0748 0748 21 * * * * *
149 0749 0749 22 * * * * *
150 0750 0750 23 * * * * *
151 0751 0751 24 * * * * *
152 0752 0752 25 * * * * *
153 0753 0753 26 * * * * *
154 0754 0754 27 * * * * *
155 0755 0755 28 * * * * *
156 0756 0756 29 * * * * *
157 0757 0757 2A * * * * *
158 0758 0758 2B * * * * *
159 0759 0759 2C * * * * *
160 0760 0760 2D * * * * *
161 0761 0761 2E * * * * *
162 0762 0762 2F * * * * *
163 0763 0763 30 * * * * *
164 0764 0764 31 * * * * *
165 0765 0765 32 * * * * *
166 0766 0766 33 * * * * *
167 0767 0767 34 * * * * *
168 0768 0768 35 * * * * *
169 0769 0769 36 * * * * *
170 0770 0770 37 * * * * *
171 0771 0771 38 * * * * *
172 0772 0772 39 * * * * *
173 0773 0773 3A * * * * *
174 0774 0774 3B * * * * *
175 0775 0775 3C * * * * *
176 0776 0776 3D * * * * *
177 0777 0777 3E * * * * *
178 0778 0778 3F * * * * *
179 0779 0779 40 * * * * *
180 0780 0780 41 * * * * *
181 0781 0781 42 * * * * *
182 0782 0782 43 * * * * *
183 0783 0783 44 * * * * *
184 0784 0784 45 * * * * *
185 0785 0785 46 * * * * *
186 0786 0786 47 * * * * *
187 0787 0787 48 * * * * *
188 0788 0788 49 * * * * *
189 0789 0789 4A * * * * *
190 0790 0790 4B * * * * *
191 0791 0791 4C * * * * *
192 0792 0792 4D * * * * *
193 0793 0793 4E * * * * *
194 0794 0794 4F * * * * *
195 0795 0795 50 * * * * *
196 0796 0796 51 * * * * *
197 0797 0797 52 * * * * *
198 0798 0798 53 * * * * *
199 0799 0799 54 * * * * *
200 0800 0800 55 * * * * *
201 0801 0801 56 * * * * *
202 0802 0802 57 * * * * *
203 0803 0803 58 * * * * *
204 0804 0804 59 * * * * *
205 0805 0805 5A * * * * *
206 0806 0806 5B * * * * *
207 0807 0807 5C * * * * *
208 0808 0808 5D * * * * *
209 0809 0809 5E * * * * *
210 0810 0810 5F * * * * *
211 0811 0811 60 * * * * *
212 0812 0812 61 * * * * *
213 0813 0813 62 * * * * *
214 0814 0814 63 * * * * *
215 0815 0815 64 * * * * *
216 0816 0816 65 * * * * *
217 0817 0817 66 * * * * *
218 0818 0818 67 * * * * *
219 0819 0819 68 * * * * *
220 0820 0820 69 * * * * *
221 0821 0821 6A * * * * *
222 0822 0822 6B * * * * *
223 0823 0823 6C * * * * *
224 0824 0824 6D * * * * *
225 0825 0825 6E * * * * *
226 0826 0826 6F * * * * *
227 0827 0827 70 * * * * *
228 0828 0828 71 * * * * *
229 0829 0829 72 * * * * *
230 0830 0830 73 * * * * *
231 0831 0831 74 * * * * *
232 0832 0832 75 * * * * *
233 0833 0833 76 * * * * *
234 0834 0834 77 * * * * *
235 0835 0835 78 * * * * *
236 0836 0836 79 * * * * *
237 0837 0837 7A * * * * *
238 0838 0838 7B * * * * *
239 0839 0839 7C * * * * *
240 0840 0840 7D * * * * *
241 0841 0841 7E * * * * *
242 0842 0842 7F * * * * *
243 0843 0843 80 * * * * *
244 0844 0844 81 * * * * *
245 0845 0845 82 * * * * *
246 0846 0846 83 * * * * *
247 0847 0847 84 * * * * *
248 0848 0848 85 * * * * *
249 0849 0849 86 * * * * *
250 0850 0850 87 * * * * *
251 0851 0851 88 * * * * *
252 0852 0852 89 * * * * *
253 0853 0853 8A * * * * *
254 0854 0854 8B * * * * *
255 0855 0855 8C * * * * *
256 0856 0856 8D * * * * *
257 0857 0857 8E * * * * *
258 0858 0858 8F * * * * *
259 0859 0859 90 * * * * *
260 0860 0860 91 * * * * *
261 0861 0861 92 * * * * *
262 0862 0862 93 * * * * *
263 0863 0863 94 * * * * *
264 0864 0864 95 * * * * *
265 0865 0865 96 * * * * *
266 0866 0866 97 * * * * *
267 0867 0867 98 * * * * *
268 0868 0868 99 * * * * *
269 0869 0869 9A * * * * *
270 0870 0870 9B * * * * *
271 0871 0871 9C * * * * *
272 0872 0872 9D * * * * *
273 0873 0873 9E * * * * *
274 0874 0874 9F * * * * *
275 0875 0875 A0 * * * * *
276 0876 0876 A1 * * * * *
277 0877 0877 A2 * * * * *
278 0878 0878 A3 * * * * *
279 0879 0879 A4 * * * * *
280 0880 0880 A5 * * * * *
281 0881 0881 A6 * * * * *
282 0882 0882 A7 * * * * *
283 0883 0883 A8 * * * * *
284 0884 0884 A9 * * * * *
285 0885 0885 AA * * * * *
286 0886 0886 AB * * * * *
287 0887 0887 AC * * * * *
288 0888 0888 AD * * * * *
289 0889 0889 AE * * * * *
290 0890 0890 AF * * * * *
291 0891 0891 B0 * * * * *
292 0892 0892 B1 * * * * *
293 0893 0893 B2 * * * * *
294 0894 0894 B3 * * * * *
295 0895 0895 B4 * * * * *
296 0896 0896 B5 * * * * *
297 0897 0897 B6 * * * * *
298 0898 0898 B7 * * * * *
299 0899 0899 B8 * * * * *
300 0900 0900 B9 * * * * *
301 0901 0901 BA * * * * *
302 0902 0902 BB * * * * *
303 0903 0903 BC * * * * *
304 0904 0904 BD * * * * *
305 0905 0905 BE * * * * *
306 0906 0906 BF * * * * *
307 0907 0907 C0 * * * * *
308 0908 0908 C1 * * * * *
309 0909 0909 C2 * * * * *
310 0910 0910 C3 * * * * *
311 0911 0911 C4 * * * * *
312 0912 0912 C5 * * * * *
313 0913 0913 C6 * * * * *
314 0914 0914 C7 * * * * *
315 0915 0915 C8 * * * * *
316 0916 0916 C9 * * * * *
317 0917 0917 CA * * * * *
318 0918 0918 CB * * * * *
319 0919 0919 CC * * * * *
320 0920 0920 CD * * * * *
321 0921 0921 CE * * * * *
322 0922 0922 CF * * * * *
323 0923 0923 D0 * * * * *
324 0924 0924 D1 * * * * *
325 0925 0925 D2 * * * * *
326 0926 0926 D3 * * * * *
327 0927 0927 D4 * * * * *
328 0928 0928 D5 * * * * *
329 0929 0929 D6 * * * * *
330 0930 0930 D7 * * * * *
331 0931 0931 D8 * * * * *
332 0932 0932 D9 * * * * *
333 0933 0933 DA * * * * *
334 0934 0934 DB * * * * *
335 0935 0935 DC * * * * *
336 0936 0936 DD * * * * *
337 0937 0937 DE * * * * *
338 0938 0938 DF * * * * *
339 0939 0939 E0 * * * * *
340 0940 0940 E1 * * * * *
341 0941 0941 E2 * * * * *
342 0942 0942 E3 * * * * *
343 0943 0943 E4 * * * * *
344 0944 0944 E5 * * * * *
345 0945 0945 E6 * * * * *
346 0946 0946 E7 * * * * *
347 0947 0947 E8 * * * * *
348 0948 0948 E9 * * * * *
349 0949 0949 EA * * * * *
350 0950 0950 EB * * * * *
351 0951 0951 EC * * * * *
352 0952 0952 ED * * * * *
353 0953 0953 EE * * * * *
354 0954 0954 EF * * * * *
355 0955 0955 F0 * * * * *
356 0956 0956 F1 * * * * *
357 0957 0957 F2 * * * * *
358 0958 0958 F3 * * * * *
359 0959 0959 F4 * * * * *
360 0960 0960 F5 * * * * *
361 0961 0961 F6 * * * * *
362 0962 0962 F7 * * * * *
363 0963 0963 F8 * * * * *
364 0964 0964 F9 * * * * *
365 0965 0965 FA * * * * *
366 0966 0966 FB * * * * *
367 0967 0967 FC * * * * *
368 0968 0968 FD * * * * *
369 0969 0969 FE * * * * *
370 0970 0970 FF * * * * *
371 0971 0971 00 * * * * *
372 0972 0972 01 * * * * *
373 0973 0973 02 * * * * *
374 0974 0974 03 * * * * *
375 0975 0975 04 * * * * *
376 0976 0976 05 * * * * *
377 0977 0977 06 * * * * *
378 0978 0978 07 * * * * *
379 0979 0979 08 * * * * *
380 0980 0980 09 * * * * *
381 0981 0981 0A * * * * *
382 0982 0982 0B * * * * *
383 0983 0983 0C * * * * *
384 0984 0984 0D * * * * *
385 0985 0985 0E * * * * *
386 0986 0986 0F * * * * *
387 0987 0987 10 * * * * *
388 0988 0988 11 * * * * *
389 0989 0989 12 * * * * *
390 0990 0990 13 * * * * *
391 0991 0991 14 * * * * *
392 0992 0992 15 * * * * *
393 0993 0993 16 * * * * *
394 0994 0994 17 * * * * *
395 0995 0995 18 * * * * *
396 0996 0996 19 * * * * *
397 0997 0997 1A * * * * *
398 0998 0998 1B * * * * *
399 0999 0999 1C * * * * *
400 1000 1000 1D * * * * *
401 1001 1001 1E * * * * *
402 1002 1002 1F * * * * *
403 1003 1003 20 * * * * *
404 1004 1004 21 * * * * *
405 1005 1005 22 * * * * *
406 1006 1006 23 * * * * *
407 1007 1007 24 * * * * *
408 1008 1008 25 * * * * *
409 1009 1009 26 * * * * *
410 1010 1010 27 * * * * *
411 1011 1011 28 * * * * *
412 1012 1012 29 * * * * *
413 1013 1013 2A * * * * *
414 1014 1014 2B * * * * *
415 1015 1015 2C * * * * *
416 1016 1016 2D * * * * *
417 1017 1017 2E * * * * *
418 1018 1018 2F * * * * *
419 1019 1019 30 * * * * *
420 1020 1020 31 * * * * *
421 1021 1021 32 * * * * *
422 1022 1022 33 * * * * *
423 1023 1023 34 * * * * *
424 1024 1024 35 * * * * *
425 1025 1025 36 * * * * *
426 1026 1026 37 * * * * *
427 1027 1027 38 * * * * *
428 1028 1028 39 * * * * *
429 1029 1029 3A * * * * *
430 1030 1030 3B * * * * *
431 1031 1031 3C * * * * *
432 1032 1032 3D * * * * *
433 1033 1033 3E * * * * *
434 1034 1034 3F * * * * *
435 1035 1035 40 * * * * *
436 1036 1036 41 * * * * *
437 1037 1037 42 * * * * *
438 1038 1038 43 * * * * *
439 1039 1039 44 * * * * *
440 1040 1040 45 * * * * *
441 1041 1041 46 * * * * *
442 1042 1042 47 * * * * *
443 1043 1043 48 * * * * *
444 1044 1044 49 * * * * *
445 1045 1045 4A * * * * *
446 1046 1046 4B * * * * *
447 1047 1047 4C * * * * *
448 1048 1048 4D * * * * *
449 1049 1049 4E * * * * *
450 1050 1050 4F * * * * *
451 1051 1051 50 * * * * *
452 1052 1052 51 * * * * *
453 1053 1053 52 * * * * *
454 1054 1054 53 * * * * *
455 1055 1055 54 * * * * *
456 1056 1056 55 * * * * *
457 1057 1057 56 * * * * *
458 1058 1058 57 * * * * *
459 1059 1059 58 * * * * *
460 1060 1060 59 * * * * *
461 1061 1061 5A * * * * *
462 1062 1062 5B * * * * *
463 1063 1063 5C * * * * *
464 1064 1064 5D * * * * *
465 1065 1065 5E * * * * *
466 1066 1066 5F * * * * *
467 1067 1067 60 * * * * *
468 1068 1068 61 * * * * *
469 1069 1069 62 * * * * *
470 1070 1070 63 * * * * *
471 1071 1071 64 * * * * *
472 1072 1072 65 * * * * *
473 1073 1073 66 * * * * *
474 1074 1074 67 * * * * *
475 1075 1075 68 * * * * *
476 1076 1076 69 * * * * *
477 1077 1077 6A * * * * *
478 1078 1078 6B * * * * *
479 1079 1079 6C * * * * *
480 1080 1080 6D * * * * *
481 1081 1081 6E * * * * *
482 1082 1082 6F * * * * *
483 1083 1083 70 * * * * *
484 1084 1084 71 * * * * *
485 1085 1085 72 * * * * *
486 1086 1086 73 * * * * *
487 1087 1087 74 * * * * *
488 1088 1088 75 * * * * *
489 1089 1089 76 * * * * *
490 1090 1090 77 * * * * *
491 1091 1091 78 * * * * *
492 1092 1092 79 * * * * *
493 1093 1093 7A * * * * *
494 1094 1094 7B * * * * *
495 1095 1095 7C * * * * *
496 1096 1096 7D * * * * *
497 1097 1097 7E * * * * *
498 1098 1098 7F * * * * *
499 1099 1099 80 * * * * *
500 1100 1100 81 * * * * *
501 1101 1101 82 * * * * *
502 1102 1102 83 * * * * *
503 1103 1103 84 * * * * *
504 1104 1104 85 * * * * *
505 1105 1105 86 * * * * *
506 1106 1106 87 * * * * *
507 1107 1107 88 * * * * *
508 1108 1108 89 * * * * *
509 1109 1109 8A * * * * *
510 1110 1110 8B * * * * *
511 1111 1111 8C * * * * *
512 1112 1112 8D * * * * *
513 1113 1113 8E * * * * *
514 1114 1114 8F * * * * *
515 1115 1115 90 * * * * *
516 1116 1116 91 * * * * *
517 1117 1117 92 * * * * *
518 1118 1118 93 * * * * *
519 1119 1119 94 * * * * *
520 1120 1120 95 * * * * *
521 1121 1121 96 * * * * *
522 1122 1122 97 * * * * *
523 1123 1123 98 * * * * *
524 1124 1124 99 * * * * *
525 1125 1125 A0 * * * * *
526 1126 1126 A1 * * * * *
527 1127 1127 A2 * * * * *
528 1128 1128 A3 * * * * *
529 1129 1129 A4 * * * * *
530 1130 1130 A5 * * * * *
531 1131 1131 A6 * * * * *
532 1132 1132 A7 * * * * *
533 1133 1133 A8 * * * * *
534 1134 1134 A9 * * * * *
535 1135 1135 AA * * * * *
536 1136 1136 AB * * * * *
537 1137 1137 AC * * * * *
538 1138 1138 AD * * * * *
539 1139 1139 AE * * * * *
540 1140 1140 AF * * * * *
541 1141 1141 B0 * * * * *
542 1142 1142 B1 * * * * *
543 1143 1143 B2 * * * * *
544 1144 1144 B3 * * * * *
545 1145 1145 B4 * * * * *
546 1146 1146 B5 * * * * *
547 1147 1147 B6 * * * * *
548 1148 1148 B7 * * * * *
549 1149 1149 B8 * * * * *
550 1150 1150 B9 * * * * *
551 1151 1151 BA * * * * *
552 1152 1152 BB * * * * *
553 1153 1153 BC * * * * *
554 1154 1154 BD * * * * *
555 1155 1155 BE * * * * *
556 1156 1156 BF * * * * *
557 1157 1157 C0 * * * * *
558 1158 1158 C1 * * * * *
559 1159 1159 C2 * * * * *
560 1160 1160 C3 * * * * *
561 1161 1161 C4 * * * * *
562 1162 1162 C5 * * * * *
563 1163 1163 C6 * * * * *
564 1164 1164 C7 * * * * *
565 1165 1165 C8 * * * * *
566 1166 1166 C9 * * * * *
567 1167 1167 CA * * * * *
568 1168 1168 CB * * * * *
569 1169 1169 CC * * * * *
570 1170 1170 CD * * * * *
571 1171 1171 CE * * * * *
572 1172 1172 CF * * * * *
573 1173 1173 D0 * * * * *
574 1174 1174 D1 * * * * *
575 1175 1175 D2 * * * * *
576 1176 1176 D3 * * * * *
577 1177 1177 D4 * * * * *
578 1178 1178 D5 * * * * *
579 1179 1179 D6 * * * * *
580 1180 1180 D7 * * * * *
581 1181 1181 D8 * * * * *
582 1182 1182 D9 * * * * *
583 1183 1183 DA * * * * *
584 1184 1184 DB * * * * *
585 1185 1185 DC * * * * *
586 1186 1186 DD * * * * *
587 1187 1187 DE * * * * *
588 1188 1188 DF * * * * *
589 1189 1189 E0 * * * * *
590 1190 1190 E1 * * * * *
591 1191 1191 E2 * * * * *
592 1192 1192 E3 * * * * *
593 1193 1193 E4 * * * * *
594 1194 1194 E5 * * * * *
595 1195 1195 E6 * * * * *
596 1196 1196 E7 * * * * *
597 1197 1197 E8 * * * * *
598 1198 1198 E9 * * * * *
599 1199 1199 EA * * * * *
600 1200 1200 EB * * * * *
601 1201 1201 EC * * * * *
602 1202 1202 ED * * * * *
603 1203 1203 EE * * * * *
604 1204 1204 EF * * * * *
605 1205 1205 F0 * * * * *
606 1206 1206 F1 * * * * *
607 1207 1207 F2 * * * * *
608 1208 1208 F3 * * * * *
609 1209 1209 F4 * * * * *
610 1210 1210 F5 * * * * *
611 1211 1211 F6 * * * * *
612 1212 1212 F7 * * * * *
613 1213 1213 F8 * * * * *
614 1214 1214 F9 * * * * *
615 1215 1215 FA * * * * *
616 1216 1216 FB * * * * *
617 1217 1217 FC * * * * *
618 1218 1218 FD * * * * *
619 1219 1219 FE * * * * *
620 1220 1220 FF * * * * *
621 1221 1221 00 * * * * *
622 1222 1222 01 * * * * *
623 1223 1223 02 * * * * *
624 1224 1224 03 * * * * *
625 1225 1225 04 * * * * *
626 1226 1226 05 * * * * *
627 1227 1227 06 * * * * *
628 1228 1228 07 * * * * *
629 1229 1229 08 * * * * *
630 1230 1230 09 * * * * *
631 1231 1231 0A * * * * *
632 1232 1232 0B * * * * *
633 1233 1233 0C * * * * *
634 1234 1234 0D * * * * *
635 1235 1235 0E * * * * *
636 1236 1236 0F * * * * *
637 1237 1237 10 * * * * *
638 1238 1238 11 * * * * *
639 1239 1239 12 * * * * *
640 1240 1240 13 * * * * *
641 1241 1241 14 * * * * *
642 1242 1242 15 * * * * *
643 1243 1243 16 * * * * *
644 1244 1244 17 * * * * *
645 1245 1245 18 * * * * *
646 1246 1246 19 * * * * *
647 1247 1247 1A * * * * *
648 1248 1248 1B * * * * *
649 1249 1249 1C * * * * *
650 1250 1250 1D * * * * *
651 1251 1251 1E * * * * *
652 1252 1252 1F * * * * *
653 1253 1253 20 * * * * *
654 1254 1254 21 * * * * *
655 1255 1255 22 * * * * *
656 1256 1256 23 * * * * *
657 1257 
```

REPRODUCIBILITY OF THE
ORIGINAL PAGE IS POOR

```

P/P ASSEMBLER VERSION SCU LEVEL 1 HEADING INSTRUMENT ASSEMBLY PROGRAM 1976 PAGE 1
LINE ADDR LABEL B1 B2 B3 B4 B5 B6 B7 B8 B9 B10 B11 B12 B13 B14 B15 B16 B17 B18 B19 B20 B21 B22 B23 B24 B25 B26 B27 B28 B29 B30 B31 B32 B33 B34 B35 B36 B37 B38 B39 B40 B41 B42 B43 B44 B45 B46 B47 B48 B49 B50 B51 B52 B53 B54 B55 B56 B57 B58 B59 B60 B61 B62 B63 B64 B65 B66 B67 B68 B69 B70 B71 B72 B73 B74 B75 B76 B77 B78 B79 B80 B81 B82 B83 B84 B85 B86 B87 B88 B89 B90 B91 B92 B93 B94 B95 B96 B97 B98 B99 B100 B101 B102 B103 B104 B105 B106 B107 B108 B109 B110 B111 B112 B113 B114 B115 B116 B117 B118 B119 B120 B121 B122 B123 B124 B125 B126 B127 B128 B129 B130 B131 B132 B133 B134 B135 B136 B137 B138 B139 B140 B141 B142 B143 B144 B145 B146 B147 B148 B149 B150 B151 B152 B153 B154 B155 B156 B157 B158 B159 B160 B161 B162 B163 B164 B165 B166 B167 B168 B169 B170 B171 B172 B173 B174 B175 B176 B177 B178 B179 B180 B181 B182 B183 B184 B185 B186 B187 B188 B189 B190 B191 B192 B193 B194 B195 B196 B197 B198 B199 B200 B201 B202 B203 B204 B205 B206 B207 B208 B209 B210 B211 B212 B213 B214 B215 B216 B217 B218 B219 B220 B221 B222 B223 B224 B225 B226 B227 B228 B229 B230 B231 B232 B233 B234 B235 B236 B237 B238 B239 B240 B241 B242 B243 B244 B245 B246 B247 B248 B249 B250 B251 B252 B253 B254 B255 B256 B257 B258 B259 B260 B261 B262 B263 B264 B265 B266 B267 B268 B269 B270 B271 B272 B273 B274 B275 B276 B277 B278 B279 B280 B281 B282 B283 B284 B285 B286 B287 B288 B289 B290 B291 B292 B293 B294 B295 B296 B297 B298 B299 B300 B301 B302 B303 B304 B305 B306 B307 B308 B309 B310 B311 B312 B313 B314 B315 B316 B317 B318 B319 B320 B321 B322 B323 B324 B325 B326 B327 B328 B329 B330 B331 B332 B333 B334 B335 B336 B337 B338 B339 B340 B341 B342 B343 B344 B345 B346 B347 B348 B349 B350 B351 B352 B353 B354 B355 B356 B357 B358 B359 B360 B361 B362 B363 B364 B365 B366 B367 B368 B369 B370 B371 B372 B373 B374 B375 B376 B377 B378 B379 B380 B381 B382 B383 B384 B385 B386 B387 B388 B389 B390 B391 B392 B393 B394 B395 B396 B397 B398 B399 B400 B401 B402 B403 B404 B405 B406 B407 B408 B409 B410 B411 B412 B413 B414 B415 B416 B417 B418 B419 B420 B421 B422 B423 B424 B425 B426 B427 B428 B429 B430 B431 B432 B433 B434 B435 B436 B437 B438 B439 B440 B441 B442 B443 B444 B445 B446 B447 B448 B449 B450 B451 B452 B453 B454 B455 B456 B457 B458 B459 B460 B461 B462 B463 B464 B465 B466 B467 B468 B469 B470 B471 B472 B473 B474 B475 B476 B477 B478 B479 B480 B481 B482 B483 B484 B485 B486 B487 B488 B489 B490 B491 B492 B493 B494 B495 B496 B497 B498 B499 B500 B501 B502 B503 B504 B505 B506 B507 B508 B509 B510 B511 B512 B513 B514 B515 B516 B517 B518 B519 B520 B521 B522 B523 B524 B525 B526 B527 B528 B529 B530 B531 B532 B533 B534 B535 B536 B537 B538 B539 B540 B541 B542 B543 B544 B545 B546 B547 B548 B549 B550 B551 B552 B553 B554 B555 B556 B557 B558 B559 B560 B561 B562 B563 B564 B565 B566 B567 B568 B569 B570 B571 B572 B573 B574 B575 B576 B577 B578 B579 B580 B581 B582 B583 B584 B585 B586 B587 B588 B589 B590 B591 B592 B593 B594 B595 B596 B597 B598 B599 B600 B601 B602 B603 B604 B605 B606 B607 B608 B609 B610 B611 B612 B613 B614 B615 B616 B617 B618 B619 B620 B621 B622 B623 B624 B625 B626 B627 B628 B629 B630 B631 B632 B633 B634 B635 B636 B637 B638 B639 B640 B641 B642 B643 B644 B645 B646 B647 B648 B649 B650 B651 B652 B653 B654 B655 B656 B657 B658 B659 B660 B661 B662 B663 B664 B665 B666 B667 B668 B669 B670 B671 B672 B673 B674 B675 B676 B677 B678 B679 B680 B681 B682 B683 B684 B685 B686 B687 B688 B689 B690 B691 B692 B693 B694 B695 B696 B697 B698 B699 B700 B701 B702 B703 B704 B705 B706 B707 B708 B709 B710 B711 B712 B713 B714 B715 B716 B717 B718 B719 B720 B721 B722 B723 B724 B725 B726 B727 B728 B729 B730 B731 B732 B733 B734 B735 B736 B737 B738 B739 B740 B741 B742 B743 B744 B745 B746 B747 B748 B749 B750 B751 B752 B753 B754 B755 B756 B757 B758 B759 B760 B761 B762 B763 B764 B765 B766 B767 B768 B769 B770 B771 B772 B773 B774 B775 B776 B777 B778 B779 B780 B781 B782 B783 B784 B785 B786 B787 B788 B789 B790 B791 B792 B793 B794 B795 B796 B797 B798 B799 B800 B801 B802 B803 B804 B805 B806 B807 B808 B809 B810 B811 B812 B813 B814 B815 B816 B817 B818 B819 B820 B821 B822 B823 B824 B825 B826 B827 B828 B829 B830 B831 B832 B833 B834 B835 B836 B837 B838 B839 B840 B841 B842 B843 B844 B845 B846 B847 B848 B849 B850 B851 B852 B853 B854 B855 B856 B857 B858 B859 B860 B861 B862 B863 B864 B865 B866 B867 B868 B869 B870 B871 B872 B873 B874 B875 B876 B877 B878 B879 B880 B881 B882 B883 B884 B885 B886 B887 B888 B889 B890 B891 B892 B893 B894 B895 B896 B897 B898 B899 B900 B901 B902 B903 B904 B905 B906 B907 B908 B909 B910 B911 B912 B913 B914 B915 B916 B917 B918 B919 B920 B921 B922 B923 B924 B925 B926 B927 B928 B929 B930 B931 B932 B933 B934 B935 B936 B937 B938 B939 B940 B941 B942 B943 B944 B945 B946 B947 B948 B949 B950 B951 B952 B953 B954 B955 B956 B957 B958 B959 B960 B961 B962 B963 B964 B965 B966 B967 B968 B969 B970 B971 B972 B973 B974 B975 B976 B977 B978 B979 B980 B981 B982 B983 B984 B985 B986 B987 B988 B989 B990 B991 B992 B993 B994 B995 B996 B997 B998 B999

```



```

LINE ADDR LABEL 01 02 03 04 FROM SOURCE
290 0889 0889 05 FE .
291 0888 0888 00 63 79
292 088E 50
293 084F C0 63 79
294 0882 09 77
295 0894 F0 61
296
297 0896 17
298
299
300
301
302
303 0897 0C 04 00
304 089A C3
305 089A 44 00
306 089D 1A 10
307 089F 2C 04 62
308 08A2 1A 06
309 08A4 0A 07
310 08A6 0A 1A
311 08A8 1B 1A
312 08AA 08AA 20
313 08AB 1B 0F
314 08AD 04 10
315 08AF 2C 04 42
316 08B2 19 0A
317 08B4 04 01
318 08B6 04 10
319 08B8 1B 0A
320 08BA 04 0A
321 08BC 04 10
322 08BE 0A 0E 0F 04 CC
323 08C1 05 0A
324 08C3 0F 0A 02
325 08C6 0F 0A CC
326 08C9 05 0A
327 08CA 17
328
329 08CC 08CC 47 7F
330 08CE CF 04 7C
331 08D1 CC 04 74
332 08D2 0A 5A
333 08D5 CC 04 7A
334 08D7 0F 0A 06
335 08DA 0C 04 7B
336 08DB 0F 0C 04
337 08DE 25 FF
338 08E3
339 08E5 17
340

```

 * A SUBROUTINE TO JUMP TO THE PRODUCT
 * CALLED BY MAIN PROG. * FETCHES CONVERTED DATA
 * FROM TABLE "DATA" THEN O/P'S BCD ANGLE * SIGN*

 DATA LODA,MO DATA,6 FETCH THETA (MSR)
 STRZ K3
 ANDI,K0 M'80> SAVE SIGN
 BCTR,M NTH BR, ON NEG THETA
 EOR,M0 DATA,6 COMPARE SIGNS
 BCTR,M NPHI
 LODI,M0 7
 WTE,M0 SKIT BOTH POSITIVE
 BCTR,M UN AGL
 EORZ K0
 WTE,M0 SRIT PHI NEG.
 BCTR,M UN AGL
 EOR,M0 DATA,6
 BCTR,M UN
 LODI,M0 3
 WTE,M0 SRIT PITCH NEG.& ROLL POS.
 BCTR,M UN AGL
 LODI,K0 8
 WTE,M0 SRIT BOTH NEGATIVE
 BCTR,M UN LOF FORM ANGLE (BCD)
 WTE,M0 1-1A OUTPUT PITCH
 LODA,M3 DATA,6 FETCH ROLL
 BCTR,M UN LOD ANGLE (BCD)
 WTE,M0 PHI OUTPUT PHI
 RETL,UN

 LOD ANDI,K3 M'7F
 STRA,K3 08R2+1 MULTIPLICATION
 EORZ R0
 STRA,M0 08R2 CLEAR L5 BYTE
 LODI,M0 M'53 FACTOR(1.35156)
 STRA,M0 M'K1+1 MULTIPLIER
 BCTR,M UN SOPY BINARY ANGLE
 LODA,M0 MSLI+1 ANGLE
 BCTR,M UN BCD ANGLE (BCD)
 WTE,M0 M'FF
 RETL,UN

TOP ASSEMBLER V0.05 [ON SCREEN] INST-MENT ASSEMBLY PROGRAM 1476 PAGE 11

LINE	ADDR	LABL	IN	OP	OUT	FRQ	SOURCE
342	05E6		77	06			
343	05E8		0C	04	00		
344	05EA		F3				
345	05EC		05	7F			
346	05ED		01	00			
347	05EF		0F	04	07		
348	05F1		00	65	00		
349	05F4		0C	04	08		
350	05FA		00	64	08		
351	05FD		0C	04	05		
352	0500		0C	04	7A		
353	0503		0C	04	5A		
354	0506		F3				
355	0508		44	7F			
356	050A		45	80			
357	050C		0C	04	7B		
358	050E		0C	04	46		
359	0511		0C	04	5B		
360	0514		0C	04	7C		
361	0517		0F	04	66		
362	051A		0C	04	77		
363	051D		0C	04	44		
364	0520		0C	04	7H		
365	0523		0C	04	4C		
366	0526		3F	0F	40		
367	0529		0C	04	68		
368	052C		0C	04	7A		
369	052F		0F	04	66		
370	0532		0C	04	67		
371	0535		0C	04	7E		
372	0538		00	06	46		
373	053B		00	06	70		
374	053E		0C	04	4B		
375	0541		0C	04	4C		
376	0544		0C	04	4D		
377	0547		0C	04	4E		
378	054A		0C	04	4F		
379	054D		0F	04	6A		
380	054F		0F	04	6B		
381	0552		0C	04	67		
382	0555		0C	04	7E		
383	0558		00	06	46		
384	055B		00	06	70		
385	055E		0C	04	4B		
386	0561		0C	04	4C		
387	0564		0C	04	4D		
388	0567		0C	04	4E		
389	056A		0C	04	4F		
390	056D		0F	04	6A		
391	056F		0C	04	7B		
392	0572		0C	04	70		
393	0575		0C	04	77		

REPRODUCIBILITY OF THE
ORIGINAL PAGE IS POOR

LINE	ADDR	LABL	INSTR	CC	OP	IF	DATA
394	0958						STRA,R0 DATA
395	0958						RETC,UN
396							***** SUBROUTINE TO SQUARE TWO 2 BYTE VALUES *****
397							* ENTER WITH VALUE IN R1(MSB) & R2(LSB)
398							* EXIT WITH 2 MSB IN RSLT & RSLT+1
399							*****
400							***** BEGIN *****
401	095C						SQU
402	095C						FORZ
403	095E						STRA,R0 R0
404	095F						STRA,R0 RSLT
405	0962						STRA,R0 RSLT+1
406	0965						LDDI,R3 16
407	0967						ANDI,R1 16
408	0969						STRA,R1 OPR2
409	096C						STRA,R2 OPR2+1
410	096F						RRR,R3
411	0970						RRR,R2
412	0971						FORZ
413	0972						R0
414	0973						NOAD
415	0975						NOAD
416	0978						RSLT+1
417	0978						OPR2+1
418	097F						RSLT+1
419	0981						RSLT
420	0984						NOAD+3
421	0987						RSLT
422	098A						NOAD
423	098A						RSLT
424	098F						RSLT
425	0991						RSLT+1
426	0992						RSLT+1
427	0995						RSLT+1
428							CONF. MUL. IF JED.
429	0997						END OF SUBROUTINE

LINE ADDR LABEL M1 M2 M3 M4 FROM SOURCE

```

431      SADD PPST 0000 77 00      * S.R. SADD TO PERFORM DOUBLE PRECISION *
432      0000 00 00      * SIGN & MAGNITUDE AND SUBT *
433      0000 00 00      * ADDEND (SUBTRACTEND) IN TEMP, TEMP+1 *
434      0000 00 00      * ADDEND (MULTIPLY) IN RSLT, RSLT+1 *
435      0000 00 00      * STEM = SIGN IF TEMP IN TEMP SHES = SIG *
436      0000 00 00      * CUM HLT IS FLAG (10=ADD1) = SUBT *
437      0000 00 00      * SIGNED TOTAL LEFT IN RSLT, RSLT+1 *
438      0000 00 00      * *****
439      SADD PPST 0000 77 00      * *****
440      0000 00 00      * *****
441      0000 00 00      * *****
442      0000 00 00      * *****
443      0000 00 00      * *****
444      0000 00 00      * *****
445      0000 00 00      * *****
446      0000 00 00      * *****
447      0000 00 00      * *****
448      0000 00 00      * *****
449      0000 00 00      * *****
450      0000 00 00      * *****
451      0000 00 00      * *****
452      0000 00 00      * *****
453      0000 00 00      * *****
454      0000 00 00      * *****
455      0000 00 00      * *****
456      0000 00 00      * *****
457      0000 00 00      * *****
458      0000 00 00      * *****
459      0000 00 00      * *****
460      0000 00 00      * *****
461      0000 00 00      * *****
462      0000 00 00      * *****
463      0000 00 00      * *****
464      0000 00 00      * *****
465      0000 00 00      * *****
466      0000 00 00      * *****
467      0000 00 00      * *****
468      0000 00 00      * *****
469      0000 00 00      * *****
470      0000 00 00      * *****
471      0000 00 00      * *****
472      0000 00 00      * *****
473      0000 00 00      * *****
474      0000 00 00      * *****
475      0000 00 00      * *****
476      0000 00 00      * *****
477      0000 00 00      * *****
478      0000 00 00      * *****
479      0000 00 00      * *****
480      0000 00 00      * *****
481      0000 00 00      * *****
482      0000 00 00      * *****

```

REPRODUCIBILITY OF THE
ORIGINAL PAGE IS POOR

REPRODUCIBILITY OF THE
ORIGINAL PAGE IS POOR

LINE ADDR L A L M1 M2 M3 M4 FROM SOURCE

```

483 09F0      RETC,UN
484 09FE      17
485 0A00      IOW1,R0 M:80*
      BCTR,UN
      * START HERE IF TEMP IN "TEMP" IS NEGATIVE
      XNEG
      LODA,R0 RSLT-1,R2
      SUBA,R0 TEMP-1,R2
      STRA,R0 RSLT-1,R2
      BDRR,R2 XNEG
      TPSL
      HCFB,UN
      TZER AND1,R0 M:7F*
      STRA,R0 RSLT
      RETC,UN
      * START HERE IF SUBTRACTION IS REQUIRED
      * I.E. INSLT,RSLT+11 - 11TEMP, TEMP+11
      SSUB LODA,R0 SRES
      STR2 R3
      LOD1,R2 2
      EDRA,R0 STEM
      BCFB,N SUBA
      CPBL C
      SLUP LODA,R0 TEMP-1,R2
      ADDA,R0 RSLT-1,R2
      STRA,R0
      BDRR,R2 SLUP
      LONZ R3
      STRA,R0 RSLT
      RETC,UN

```

REPRODUCIBILITY OF THE
ORIGINAL PAGE IS PO

PIP ASSEMBLER VERSION SCU LEVEL 1 HEADJING INSTRUMENT ASSEMBLY PROGRAM 1976 PAGE 15

LINE ADDR LABEL B1 B2 B3 B4 FROM SOURCE

```

513      0A36 0A16 77 01      * START HERE IF BOTH TERMS SAME SIGN
514      0A38 0A18 0E 64 76      C=1
515      0A3A 0A1A 0E 64 76      RSLT = TEMP - RSLT
516      0A3C 0A1C 0E 64 76      RSLT = TEMP - RSLT
517      0A3E 0A1E 0E 64 76      RSLT = TEMP - RSLT
518      0A40 0A20 0E 64 76      RSLT = TEMP - RSLT
519      0A42 0A22 0E 64 76      RSLT = TEMP - RSLT
520      0A44 0A24 0E 64 76      RSLT = TEMP - RSLT
521      0A46 0A26 0E 64 76      RSLT = TEMP - RSLT
522      0A48 0A28 0E 64 76      RSLT = TEMP - RSLT
523      0A4A 0A2A 0E 64 76      RSLT = TEMP - RSLT
524      0A4C 0A2C 0E 64 76      RSLT = TEMP - RSLT
525      0A4E 0A2E 0E 64 76      RSLT = TEMP - RSLT
526      0A50 0A30 0E 64 76      RSLT = TEMP - RSLT
527      0A52 0A32 0E 64 76      RSLT = TEMP - RSLT
528      0A54 0A34 0E 64 76      RSLT = TEMP - RSLT
529      0A56 0A36 0E 64 76      RSLT = TEMP - RSLT
530      0A58 0A38 0E 64 76      RSLT = TEMP - RSLT
531      0A5A 0A3A 0E 64 76      RSLT = TEMP - RSLT
532      0A5C 0A3C 0E 64 76      RSLT = TEMP - RSLT
533      0A5E 0A3E 0E 64 76      RSLT = TEMP - RSLT
534      0A60 0A40 0E 64 76      RSLT = TEMP - RSLT
535      0A62 0A42 0E 64 76      RSLT = TEMP - RSLT
536      0A64 0A44 0E 64 76      RSLT = TEMP - RSLT
537      0A66 0A46 0E 64 76      RSLT = TEMP - RSLT
538      0A68 0A48 0E 64 76      RSLT = TEMP - RSLT
539      0A6A 0A4A 0E 64 76      RSLT = TEMP - RSLT
540      0A6C 0A4C 0E 64 76      RSLT = TEMP - RSLT
541      0A6E 0A4E 0E 64 76      RSLT = TEMP - RSLT

```

REPRODUCIBILITY OF THE
ORIGINAL PAGE IS POOR

REP ASSEMBLER VERSION SCULFVEI 1 HEADING INSTRUMENT ASSEMBLY PROGRAM 1976 PAGE 16

LINE ADDR L'IL B1 B2 B3 B4 B5 B6 B7 B8 B9 B10 B11 B12 B13 B14 B15 B16 B17 B18 B19 B20 B21 B22 B23 B24 B25 B26 B27 B28 B29 B30 B31 B32 B33 B34 B35 B36 B37 B38 B39 B40 B41 B42 B43 B44 B45 B46 B47 B48 B49 B50 B51 B52 B53 B54 B55 B56 B57 B58 B59 B60 B61 B62 B63 B64 B65 B66 B67 B68 B69 B70 B71 B72 B73 B74 B75 B76 B77 B78 B79 B80 B81 B82 B83 B84 B85 B86 B87 B88 B89 B90 B91 B92 B93 B94 B95 B96 B97 B98 B99 B100 B101 B102 B103 B104 B105 B106 B107 B108 B109 B110 B111 B112 B113 B114 B115 B116 B117 B118 B119 B120 B121 B122 B123 B124 B125 B126 B127 B128 B129 B130 B131 B132 B133 B134 B135 B136 B137 B138 B139 B140 B141 B142 B143 B144 B145 B146 B147 B148 B149 B150 B151 B152 B153 B154 B155 B156 B157 B158 B159 B160 B161 B162 B163 B164 B165 B166 B167 B168 B169 B170 B171 B172 B173 B174 B175 B176 B177 B178 B179 B180 B181 B182 B183 B184 B185 B186 B187 B188 B189 B190 B191 B192 B193 B194 B195 B196 B197 B198 B199 B200 B201 B202 B203 B204 B205 B206 B207 B208 B209 B210 B211 B212 B213 B214 B215 B216 B217 B218 B219 B220 B221 B222 B223 B224 B225 B226 B227 B228 B229 B230 B231 B232 B233 B234 B235 B236 B237 B238 B239 B240 B241 B242 B243 B244 B245 B246 B247 B248 B249 B250 B251 B252 B253 B254 B255 B256 B257 B258 B259 B260 B261 B262 B263 B264 B265 B266 B267 B268 B269 B270 B271 B272 B273 B274 B275 B276 B277 B278 B279 B280 B281 B282 B283 B284 B285 B286 B287 B288 B289 B290 B291 B292 B293 B294 B295 B296 B297 B298 B299 B300 B301 B302 B303 B304 B305 B306 B307 B308 B309 B310 B311 B312 B313 B314 B315 B316 B317 B318 B319 B320 B321 B322 B323 B324 B325 B326 B327 B328 B329 B330 B331 B332 B333 B334 B335 B336 B337 B338 B339 B340 B341 B342 B343 B344 B345 B346 B347 B348 B349 B350 B351 B352 B353 B354 B355 B356 B357 B358 B359 B360 B361 B362 B363 B364 B365 B366 B367 B368 B369 B370 B371 B372 B373 B374 B375 B376 B377 B378 B379 B380 B381 B382 B383 B384 B385 B386 B387 B388 B389 B390 B391 B392 B393 B394 B395 B396 B397 B398 B399 B400 B401 B402 B403 B404 B405 B406 B407 B408 B409 B410 B411 B412 B413 B414 B415 B416 B417 B418 B419 B420 B421 B422 B423 B424 B425 B426 B427 B428 B429 B430 B431 B432 B433 B434 B435 B436 B437 B438 B439 B440 B441 B442 B443 B444 B445 B446 B447 B448 B449 B450 B451 B452 B453 B454 B455 B456 B457 B458 B459 B460 B461 B462 B463 B464 B465 B466 B467 B468 B469 B470 B471 B472 B473 B474 B475 B476 B477 B478 B479 B480 B481 B482 B483 B484 B485 B486 B487 B488 B489 B490 B491 B492 B493 B494 B495 B496 B497 B498 B499 B500 B501 B502 B503 B504 B505 B506 B507 B508 B509 B510 B511 B512 B513 B514 B515 B516 B517 B518 B519 B520 B521 B522 B523 B524 B525 B526 B527 B528 B529 B530 B531 B532 B533 B534 B535 B536 B537 B538 B539 B540 B541 B542 B543 B544 B545 B546 B547 B548 B549 B550 B551 B552 B553 B554 B555 B556 B557 B558 B559 B560 B561 B562 B563 B564 B565 B566 B567 B568 B569 B570 B571 B572 B573 B574 B575 B576 B577 B578 B579 B580 B581 B582 B583 B584 B585 B586 B587 B588 B589 B590 B591 B592 B593 B594 B595 B596 B597 B598 B599 B600 B601 B602 B603 B604 B605 B606 B607 B608 B609 B610 B611 B612 B613 B614 B615 B616 B617 B618 B619 B620 B621 B622 B623 B624 B625 B626 B627 B628 B629 B630 B631 B632 B633 B634 B635 B636 B637 B638 B639 B640 B641 B642 B643 B644 B645 B646 B647 B648 B649 B650 B651 B652 B653 B654 B655 B656 B657 B658 B659 B660 B661 B662 B663 B664 B665 B666 B667 B668 B669 B670 B671 B672 B673 B674 B675 B676 B677 B678 B679 B680 B681 B682 B683 B684 B685 B686 B687 B688 B689 B690 B691 B692 B693 B694 B695 B696 B697 B698 B699 B700 B701 B702 B703 B704 B705 B706 B707 B708 B709 B710 B711 B712 B713 B714 B715 B716 B717 B718 B719 B720 B721 B722 B723 B724 B725 B726 B727 B728 B729 B730 B731 B732 B733 B734 B735 B736 B737 B738 B739 B740 B741 B742 B743 B744 B745 B746 B747 B748 B749 B750 B751 B752 B753 B754 B755 B756 B757 B758 B759 B760 B761 B762 B763 B764 B765 B766 B767 B768 B769 B770 B771 B772 B773 B774 B775 B776 B777 B778 B779 B780 B781 B782 B783 B784 B785 B786 B787 B788 B789 B790 B791 B792 B793 B794 B795 B796 B797 B798 B799 B800 B801 B802 B803 B804 B805 B806 B807 B808 B809 B810 B811 B812 B813 B814 B815 B816 B817 B818 B819 B820 B821 B822 B823 B824 B825 B826 B827 B828 B829 B830 B831 B832 B833 B834 B835 B836 B837 B838 B839 B840 B841 B842 B843 B844 B845 B846 B847 B848 B849 B850 B851 B852 B853 B854 B855 B856 B857 B858 B859 B860 B861 B862 B863 B864 B865 B866 B867 B868 B869 B870 B871 B872 B873 B874 B875 B876 B877 B878 B879 B880 B881 B882 B883 B884 B885 B886 B887 B888 B889 B890 B891 B892 B893 B894 B895 B896 B897 B898 B899 B900 B901 B902 B903 B904 B905 B906 B907 B908 B909 B910 B911 B912 B913 B914 B915 B916 B917 B918 B919 B920 B921 B922 B923 B924 B925 B926 B927 B928 B929 B930 B931 B932 B933 B934 B935 B936 B937 B938 B939 B940 B941 B942 B943 B944 B945 B946 B947 B948 B949 B950 B951 B952 B953 B954 B955 B956 B957 B958 B959 B960 B961 B962 B963 B964 B965 B966 B967 B968 B969 B970 B971 B972 B973 B974 B975 B976 B977 B978 B979 B980 B981 B982 B983 B984 B985 B986 B987 B988 B989 B990 B991 B992 B993 B994 B995 B996 B997 B998 B999

```

*****
* S.R. ROTY TO ADJUST HY DATA USING ALGORITHM *
* HY=HY+COR(MOLL)-MZM*SIN(MOLL) *
* USES SIGN AND MAGNITUDE DATA FROM TABLE DATM *
* STORES NEW DATA INTO DATY, DATY+1 *
* CALLS S.R.S. "SAUD" & "SHPY" TO PERFORM SIGNED *
* MAGNITUDE ARITHMETIC *
*****
MOY PPSL WC-C GET MOLL ANGLE PHI
LODA,R0 DATM+H
STRZ R1 STRIP OFF SIGN
ANDI,M1 STRIP OFF SIGN
EOR,R0 DATM+4 DETERMINE SIGN OF PROD.
ANDI,R0 M+80+
STRZ,M0 CUS (PHI)
LODA,R0 COS,M1 SIN (PHI)
STRZ,M0 COSM MULTIPLIER
LODA,R0 SIN,M1 GET MZ
STRZ,M0 OPRI+1 STRIP SIGN
LODA,R0 DATM+4 MULTIPLICAND
ANDI,M0 M+7F+ FORM 226SIN(PHI)
STRZ,R0 OPRI+1 MOVE PRODUCT
LODA,R0 DATM+5
STRZ,M0 OPRI+1
HSTA,UN SHPY
LODA,R0 RSLT FORM 226SIN(PHI)
STRZ,M0 TRMP MOVE PRODUCT
LODA,R0 RSLT+1
STRZ,M0 TRMP+1
*****
* BEGIN FORMING 2ND TERM *
LODA,R0 DATI+2
STRZ R1
ANDI,M1 M+7F+
STRZ,M1 OPRI+1
ANDI,M0 M+80+
STRZ,M0 SHES
LODA,R0 DATM+3
STRZ,M0 OPRI+1
LODA,R0 COSM
STRZ,M0 OPRI+1
HSTA,UN SHPY
*****
* NOW FORM NEW HY *
PPSL COM
HSTA,UN SAUD
LODA,R0 RSLT
STRZ,M0 DATY
LODA,R0 RSLT+1
STRZ,M0 DATY+1
HSTA,UN

```


PJP ASSEMBLER VERSION 500 LEVEL 1 MEASURING INSTRUMENT ASSEMBLY PROGRAM 1976 PAGE 16

LINE ADDR L4HL R1 R2 R3 R4 ERROR SOURCE

```

641 *****
642 * A SUBROUTINE TO COMPUTE HEADING WHEN
643 * ( 7-1135 < YAW < (17-145 DEGREES
644 *****
645 SINY L001,R1 2 INDEX
646 LUP L002,R0 HY2-1,R1 LOAD OPRI-1,OPRI
647 STRA,R0 OPRI-1,R1
648 BDRR,R1 LUP
649 EORZ R0
650 BSTA,UN WY1
651 BSTA,UN ANGL
652 BSTA,UN BCDA
653 L001,R0 H*90
654 PPSL C*WC
655 SURZ K1
656 LAR,R0
657 STRZ R1
658 BSTA,UN HDG
659 RETC,UN
660 *****

```

```

PIP ASSEMBLER VERSION SCU LEVEL 1 MEASURING INSTRUMENT ASSEMBLY PROGRAM 1976 PAGE 19
LINE ADDR LABEL M1 M2 M3 M4 ENCODE SOURCE

```

[illegible]

LINE ADDR L4 L3 L2 L1 B4 B3 B2 B1 B0 SOURCE

714	0B9D	0E 04 77	LSLT	MS BYTE OF ARG.
715	0BA0	05 17	LOUT,R1 23	1ST ESTIMATE
716	0BA2	07 17	LOUT,R3 23	TWICE 1ST INCREMENT
717	0BA4	00 6A 0A	LODA,R0 COSM,R1	COS(EST.)
718	0BA7	05 01	CPSL C	MODIFY & TEST CTR.
719	0BA9	53	RRR,R3	
720	0BAA	1B 1F	BCTR,R2 LAST	
721	0BAC	E2	COMZ R2	
722	0BAD	19 00	BCTR,GT ELTA	BR, IF EST. < ANGLE
723	0BAF	1A 12	BCTR,LT EGTA	BR, IF EST. > ANGLE
724	0BB1	E4 01	COMI,R0 1	
725	0BB3	1D 0C 43	BCTA,GT QUIT	
726	0BB6	1C 0C 49	BCTA,EQ ONE	
727	0BB9	1F 0C 27	BCTR,UN ITLS	MS BITS ARE END. & < 1
728	0BBC	05 01	CPSL C	INCR. EST.
729	0BBE	R1	LOUZ R1	
730	0BBF	R3	ADDZ R3	
731	0BC0	C1	STNZ R1	
732	0BC1	1B 61	BCTR,UN LUPA	CONTINUE LOOPING
733	0BC3	77 01	PPSL C	DECR. EST.
734	0BC5	R1	LOUZ R1	
735	0BC6	A3	SUBZ R3	
736	0BC7	C1	STNZ R1	
737	0BCA	1B 5A	BCTR,UN LUPA	LOOP HACK
738	0BCA	07 0A	LOUT,R3 10	LAST ITERATIONS
739	0BCC	00 6A 0A	LODA,R0 COSM,R1	
740	0BCF	F2	COMZ R2	
741	0BD0	19 05	BCTR,GT EIT	
742	0BD2	1A 09	BCTR,LT EGF	
743	0BD4	1F 0A 61	BCTA,UN EOL1	TEST VS QUTY 1
744	0BD7	75 01	CPSL C	
745	0BD9	R5 01	ADDI,R1 1	
746	0BDH	1A 04	BCTR,UN 15FH	
747	0BD0	77 01	PPSL C	
748	0BDF	A5 01	SUBI,R1 1	
749	0BE1	F6 69	BCTR,R3 LUPH	LOOP IF R1=0
750			* REGIN INTERPOLATING USING MSBITS	
751	0BE3	00 6A 0A	LODA,R0 COSM,R1	
752	0BE6	E2	COMZ R2	
753	0BE7	19 1A	BCTR,GT 101	
754			* START IF COS(EST.) < ARG. TEMP ST. COS(EST.)	
755	0BE9	C3	STNZ R3	
756	0BEA	00 6A 0A	LODA,R0 COSM,R1	
757	0BED	77 01	PPSL C	
758	0BEF	A3	SUBZ R3	
759	0BF0	75 01	CPSL C	
760	0BF2	50	RRR,R0	
761	0BF3	75 01	CPSL C	
762	0BF5	63	ADDZ R3	
763	0BF6	F2	COMZ R2	
764	0BF7	1F 0C 27	BCTR,UN 101	1-TEMP. VALUE VS ARG
765	0BFA	77 01	PPSL C	

VIP ASSEMBLER VERSION 500 LEVEL 1 HEADLINE INSTRUMENT ASSEMBLY PROGRAM 1976 PAGE 23

```

LINE ADDR LABEL IN 32 13 14 FROM SOURCE
843
844
845
846
847 UC7C 77 09 AC-L SIGN OF HX ?
848 UC7E 0C 04 IF LODA,R0 DATA BH, IF NEG
849 UC7I 1A 1A BCTN,N YAW0
850 UC83 0C 04 K1 * SOLVE FOR HEADING (HCL) FORM
851 UC86 1A 1A LODA,R0 DATY GET MY
852
853
854
855 UC88 45 00 * START HERE D- POS, HY & HX
856 UC8A 1B 0C COMI,M1 D
857 UC8C 04 6A BCTN,R0 MYN
858 UC8E 01 SUBZ K1
859 UC8F 04 6A DASH,R0 K1
860 UC90 03 SINZ K1
861 UC91 06 04 LODI,M2 H*0J1
862 UC93 06 00 SUBI,M2 0
863 UC95 76 DAR,R2
864 UC96 1B 27 ACI,M1,N FINR
865
866
867 UC9A 0C 0B * ENTER HERE IF HX=POS. & MY=NEG.
868 UC9B 01 LODI,M2 H*0J1
869 UC9C 03 LODZ M1
870 UC9D 1A 27 SINZ R2
871
872
873
874 UC9E 0C 04 K1 * ENTER HERE HX=NEG & MY= +/- TEST SIGN OF MY
875 UC9F 1A 27 BCTN,N MY

```

REPRODUCIBILITY OF THE
ORIGINAL PAGE IS POOR

PHIP ASSEMBLER VERSION 500 LEVEL 1 HEADING INSTRUMENT ASSEMBLY PROGRAM 1976 PAGE 24

LINE	ADDR	DATA	PC	PC+1	PC+2	PC+3	PC+4	PC+5	PC+6	PC+7	PC+8	PC+9	PC+10	PC+11	PC+12	PC+13	PC+14	PC+15	PC+16	PC+17	PC+18	PC+19	PC+20	PC+21	PC+22	PC+23	PC+24	PC+25	PC+26	PC+27	PC+28	PC+29	PC+30	PC+31	PC+32	PC+33	PC+34	PC+35	PC+36	PC+37	PC+38	PC+39	PC+40	PC+41	PC+42	PC+43	PC+44	PC+45	PC+46	PC+47	PC+48	PC+49	PC+50	PC+51	PC+52	PC+53	PC+54	PC+55	PC+56	PC+57	PC+58	PC+59	PC+60	PC+61	PC+62	PC+63	PC+64	PC+65	PC+66	PC+67	PC+68	PC+69	PC+70	PC+71	PC+72	PC+73	PC+74	PC+75	PC+76	PC+77	PC+78	PC+79	PC+80	PC+81	PC+82	PC+83	PC+84	PC+85	PC+86	PC+87	PC+88	PC+89	PC+90	PC+91	PC+92	PC+93	PC+94	PC+95	PC+96	PC+97	PC+98	PC+99	PC+100	PC+101	PC+102	PC+103	PC+104	PC+105	PC+106	PC+107	PC+108	PC+109	PC+110	PC+111	PC+112	PC+113	PC+114	PC+115	PC+116	PC+117	PC+118	PC+119	PC+120	PC+121	PC+122	PC+123	PC+124	PC+125	PC+126	PC+127	PC+128	PC+129	PC+130	PC+131	PC+132	PC+133	PC+134	PC+135	PC+136	PC+137	PC+138	PC+139	PC+140	PC+141	PC+142	PC+143	PC+144	PC+145	PC+146	PC+147	PC+148	PC+149	PC+150	PC+151	PC+152	PC+153	PC+154	PC+155	PC+156	PC+157	PC+158	PC+159	PC+160	PC+161	PC+162	PC+163	PC+164	PC+165	PC+166	PC+167	PC+168	PC+169	PC+170	PC+171	PC+172	PC+173	PC+174	PC+175	PC+176	PC+177	PC+178	PC+179	PC+180	PC+181	PC+182	PC+183	PC+184	PC+185	PC+186	PC+187	PC+188	PC+189	PC+190	PC+191	PC+192	PC+193	PC+194	PC+195	PC+196	PC+197	PC+198	PC+199	PC+200	PC+201	PC+202	PC+203	PC+204	PC+205	PC+206	PC+207	PC+208	PC+209	PC+210	PC+211	PC+212	PC+213	PC+214	PC+215	PC+216	PC+217	PC+218	PC+219	PC+220	PC+221	PC+222	PC+223	PC+224	PC+225	PC+226	PC+227	PC+228	PC+229	PC+230	PC+231	PC+232	PC+233	PC+234	PC+235	PC+236	PC+237	PC+238	PC+239	PC+240	PC+241	PC+242	PC+243	PC+244	PC+245	PC+246	PC+247	PC+248	PC+249	PC+250	PC+251	PC+252	PC+253	PC+254	PC+255	PC+256	PC+257	PC+258	PC+259	PC+260	PC+261	PC+262	PC+263	PC+264	PC+265	PC+266	PC+267	PC+268	PC+269	PC+270	PC+271	PC+272	PC+273	PC+274	PC+275	PC+276	PC+277	PC+278	PC+279	PC+280	PC+281	PC+282	PC+283	PC+284	PC+285	PC+286	PC+287	PC+288	PC+289	PC+290	PC+291	PC+292	PC+293	PC+294	PC+295	PC+296	PC+297	PC+298	PC+299	PC+300	PC+301	PC+302	PC+303	PC+304	PC+305	PC+306	PC+307	PC+308	PC+309	PC+310	PC+311	PC+312	PC+313	PC+314	PC+315	PC+316	PC+317	PC+318	PC+319	PC+320	PC+321	PC+322	PC+323	PC+324	PC+325	PC+326	PC+327	PC+328	PC+329	PC+330	PC+331	PC+332	PC+333	PC+334	PC+335	PC+336	PC+337	PC+338	PC+339	PC+340	PC+341	PC+342	PC+343	PC+344	PC+345	PC+346	PC+347	PC+348	PC+349	PC+350	PC+351	PC+352	PC+353	PC+354	PC+355	PC+356	PC+357	PC+358	PC+359	PC+360	PC+361	PC+362	PC+363	PC+364	PC+365	PC+366	PC+367	PC+368	PC+369	PC+370	PC+371	PC+372	PC+373	PC+374	PC+375	PC+376	PC+377	PC+378	PC+379	PC+380	PC+381	PC+382	PC+383	PC+384	PC+385	PC+386	PC+387	PC+388	PC+389	PC+390	PC+391	PC+392	PC+393	PC+394	PC+395	PC+396	PC+397	PC+398	PC+399	PC+400	PC+401	PC+402	PC+403	PC+404	PC+405	PC+406	PC+407	PC+408	PC+409	PC+410	PC+411	PC+412	PC+413	PC+414	PC+415	PC+416	PC+417</
------	------	------	----	------	------	------	------	------	------	------	------	------	-------	-------	-------	-------	-------	-------	-------	-------	-------	-------	-------	-------	-------	-------	-------	-------	-------	-------	-------	-------	-------	-------	-------	-------	-------	-------	-------	-------	-------	-------	-------	-------	-------	-------	-------	-------	-------	-------	-------	-------	-------	-------	-------	-------	-------	-------	-------	-------	-------	-------	-------	-------	-------	-------	-------	-------	-------	-------	-------	-------	-------	-------	-------	-------	-------	-------	-------	-------	-------	-------	-------	-------	-------	-------	-------	-------	-------	-------	-------	-------	-------	-------	-------	-------	-------	-------	-------	-------	-------	-------	--------	--------	--------	--------	--------	--------	--------	--------	--------	--------	--------	--------	--------	--------	--------	--------	--------	--------	--------	--------	--------	--------	--------	--------	--------	--------	--------	--------	--------	--------	--------	--------	--------	--------	--------	--------	--------	--------	--------	--------	--------	--------	--------	--------	--------	--------	--------	--------	--------	--------	--------	--------	--------	--------	--------	--------	--------	--------	--------	--------	--------	--------	--------	--------	--------	--------	--------	--------	--------	--------	--------	--------	--------	--------	--------	--------	--------	--------	--------	--------	--------	--------	--------	--------	--------	--------	--------	--------	--------	--------	--------	--------	--------	--------	--------	--------	--------	--------	--------	--------	--------	--------	--------	--------	--------	--------	--------	--------	--------	--------	--------	--------	--------	--------	--------	--------	--------	--------	--------	--------	--------	--------	--------	--------	--------	--------	--------	--------	--------	--------	--------	--------	--------	--------	--------	--------	--------	--------	--------	--------	--------	--------	--------	--------	--------	--------	--------	--------	--------	--------	--------	--------	--------	--------	--------	--------	--------	--------	--------	--------	--------	--------	--------	--------	--------	--------	--------	--------	--------	--------	--------	--------	--------	--------	--------	--------	--------	--------	--------	--------	--------	--------	--------	--------	--------	--------	--------	--------	--------	--------	--------	--------	--------	--------	--------	--------	--------	--------	--------	--------	--------	--------	--------	--------	--------	--------	--------	--------	--------	--------	--------	--------	--------	--------	--------	--------	--------	--------	--------	--------	--------	--------	--------	--------	--------	--------	--------	--------	--------	--------	--------	--------	--------	--------	--------	--------	--------	--------	--------	--------	--------	--------	--------	--------	--------	--------	--------	--------	--------	--------	--------	--------	--------	--------	--------	--------	--------	--------	--------	--------	--------	--------	--------	--------	--------	--------	--------	--------	--------	--------	--------	--------	--------	--------	--------	--------	--------	--------	--------	--------	--------	--------	--------	--------	--------	--------	--------	--------	--------	--------	--------	--------	--------	--------	--------	--------	--------	--------	--------	--------	--------	--------	--------	--------	--------	--------	--------	--------	--------	--------	--------	--------	--------	--------	--------	--------	--------	----------

REPRODUCIBILITY OF THE
ORIGINAL PAGE IS POOR

```

LINE ADDR LABEL M1 M2 M3 M4 ERROR SOURCE
956
957
958
959
960
961
962
963
964 0EAB 75 01
965 0EBA 0C 04 5C
966 0EBD 0D 04 5D
967 0EC0 0E 07 1E
968 0EC3 C3
969 0EC4 44 7F
970 0EC6 47 80
971 0EC8 CC 04 78
972 0ECB CC 04 7C
973 0ECE CE 04 7A
974 0ED1 CF 04 7E
975 0ED4 3F 08 A6
976 0ED7 0C 04 5A
977 0EDA 0D 04 5H
978 0EDD C2
979 0EE0 44 7F
980 0EE0 45 80
981 0EE2 CC 04 A5
982 0EE5 CD 04 B6
983 0EE8 CE 04 7D
984 0EEB 75 02
985 0EED 3F 09 98
986 0EF0 0C 04 77
987 0EF3 0D 04 78
988 0EF6 CC 04 5A
989 0EF9 CD 04 5B
990 0EFC 77 02
991 0EFE 17
992
993
*****
* S.R. TO CORRECT NONORTHOGONALITY ERRORS IN HX *
* ENTER ONCE EACH SAMPLE CORRECTING HX SAMPLE *
* HX=HX(MEAS)+HY(MEAS)*SIN(ERRO) *
* LOCATE SIN(ERRO) IN SINE *
* USES "SMPLY" TO FORM PRODUCT & "SAODD" TO SUM *
* EXIT WITH MODIFIED HX IN DATA,DATA+1 *
*****
ORTH CPSL C
LODA,R0 DATA+2 HY HSB
LODA,R1 DATA+3 HY LSB
LODA,R2 SINE SIN(ERRO)
STRZ R3
ANDI,R0 017F1 STRIP SIGN
ANDI,R3 01801 SAVE SIGN
STRA,R0 00R2
STRA,R1 00R2+1
STRA,R2 00R1+1
STRA,R3 SINES
BSTA,UN SMPLY
LODA,R0 DATA
LODA,R1 DATA+1
STRZ R2
ANDI,R0 017F1
ANDI,R2 01801
STRA,R0 TEMP
STRA,R1 TEMP+1
STRA,R2 STEM
CPSL COM
BSTA,UN SAODD
LODA,R0 RSLT
LODA,R1 RSLT+1
STRA,R0 DATA
STRA,R1 DATA+1
PPSL COM
RELOC,UN
*****
END

```

TOTAL ASSEMBLY ERRORS = 0

APPENDIX C

The transcendental functions used throughout the heading computation algorithm were implemented using a table look up procedure. To generate the respective look up tables in computer memory data was first generated using algol programs. This technique expedited modifications to tabular data and provided output data in a convenient (hexadecimal) format.

Programs that calculated $\cos(\theta)$ and $\cos^2(\theta)$ to eight bit and sixteen bit resolution respectively are included.

REPRODUCIBILITY OF THE
ORIGINAL PAGE IS POOR

REPRODUCIBILITY OF THE
ORIGINAL PAGE IS POOR

PAGE 001

```

001 00000 HPAI 11,"RP"
002 00000 BFG11
003 00001 A*****
004 00001 A A PROGRAM TO GENERATE A COS-COS TABLE FOR A
005 00001 A MICROPROCESSOR BASED SYSTEM
006 00001 A ADDRESS: ANGLE = COS(ANGLE), AND DATA IN
007 00001 A BITH BINARY AND HEX FORMAT IS TABULATED
008 00001 A*****
009 00001 INTEGER A,B,C,D,E,F
010 00010 REAL THETA,SINETHA,AR,HSTH1
011 00020 REAL ARRAY AN(0:255,0:15)
012 21070 INTEGER ARRAY VAL(0:15):="0","1","2","3","4","5",
013 21102 "6","7","8","9","A","B",
014 21107 "C","D","E","F"
015 21114 INTEGER ARRAY MULT(0:1):="B.4,2.1"
016 21124 INTEGER ARRAY HEX(0:255,0:15)
017 23136 WRITE (A,*(1:1))
018 23175 WRITE (A,*(//,9X,"A",5X,"THETA",4X,"COS-COS",5X,
019 23226 "BINARY",14X,"HEX",//))
020 23242 WRITE (A,*(5X,"(ADDRESS)",3X,"(DEG)",18X," DATA ",//))
021 23276 FOR A:= 45 TO 90 DO
022 23304 BEGIN
023 23304 AN:=A
024 23310 THETA:= AN*PI/180
025 23316 SINETHA:=(COS(THETA))^2
026 23330 H:=0
027 23332 HSTH:=SINETHA
028 23336 WHILE H<17 DO
029 23341 BEGIN
030 23342 HSTH:= 2*HSTH
031 23350 IF HSTH>1 THEN
032 23355 BEGIN
033 23355 AN(A,H):=1
034 23367 HSTH:=HSTH-1
035 23375 END ELSE AN(A,H):=0
036 23405 H:=H+1
037 23440 END
038 23441 H:=0
039 23443 FOR C:=0 TO 3 DO
040 23451 BEGIN
041 23451 F:=4*PI
042 23455 F:=0
043 23457 FOR F:=0 TO 3 DO
044 23465 BEGIN
045 23465 F:=F+MULT(F)*AN(A,H)
046 23470 HEX(A,C):= VAL(F)
047 23513 END
048 23517 END
049 23543 THETA:= THETA*180/PI
050 23553 WRITE (B,*(15X,15.2(3X,FA,6)+3X,16(1,15X,4A2),A,
051 23604 THETA,SINETHA, FOR H:= 0 TO 15 DO
052 23620 AN(A,H), FOR C:= 0 TO 3 DO HEX(A,C))
053 23653 ENDD
054 23657 ENDA

```

PROGRAM= 0236A3 ERRORS=000

REPRODUCIBILITY OF THE
ORIGINAL PAGE IS POOR

Δ	ΔLTA	CUS-COS	BINARY	DATA	HEX
45	45.00000	.500000	0111111111111111	0111111111111111	7 F F
46	46.00000	.482550	0111101110001000	0111101110001000	7 8 8
47	47.00000	.465122	0111011100010010	0111011100010010	7 7 1
48	48.00000	.447736	0111001010011110	0111001010011110	7 2 9
49	49.99999	.430413	0110111000101111	0110111000101111	6 E 2
50	50.00000	.411176	0110100111001011	0110100111001011	6 9 C
51	51.00000	.396046	0110101010110001	0110101010110001	6 5 6
52	52.00001	.379039	0110001000010001	0110001000010001	6 1 0
53	53.00000	.362181	0101110010110111	0101110010110111	5 C B
54	54.00000	.345491	0101100001110010	0101100001110010	5 8 7
55	55.00000	.328940	0101010000111000	0101010000111000	5 4 J
56	56.00000	.312697	0101000000001100	0101000000001100	5 0 C
57	57.00000	.296632	0101011111110000	0101011111110000	4 B F
58	58.00000	.280814	0100011111110001	0100011111110001	4 7 E
59	59.99999	.265244	0100011111101000	0100011111101000	4 3 F
60	60.00001	.250000	0011111111111111	0011111111111111	3 F F
61	61.00000	.235040	0011110000101011	0011110000101011	3 C 8
62	62.00000	.220403	0011100001101100	0011100001101100	3 8 6
63	63.00000	.206107	0011010011000011	0011010011000011	3 4 C
64	64.00000	.192169	0011000100110010	0011000100110010	3 1 J
65	65.00000	.178606	0010110110111100	0010110110111100	2 D 8
66	66.00000	.165435	0010101010010101	0010101010010101	2 A 5
67	66.99999	.152671	0010011100010101	0010011100010101	2 7 1
68	68.00000	.140330	0010001111101100	0010001111101100	2 3 C
69	69.00000	.128427	0010000011100000	0010000011100000	2 0 E
70	70.00000	.116978	0001110111110010	0001110111110010	1 0 F
71	71.00000	.105945	0001101100010001	0001101100010001	1 8 2
72	72.00000	.095491	0001100001110010	0001100001110010	1 8 2
73	73.00000	.085481	0001010101110001	0001010101110001	1 5 E
74	73.99998	.075976	0001001101110011	0001001101110011	1 3 J
75	75.00000	.066987	0001000100100110	0001000100100110	1 2 6
76	76.00000	.058596	0000111011110111	0000111011110111	0 E F
77	77.00002	.050603	0000110011110100	0000110011110100	0 C F
78	78.00000	.043227	0000101110001000	0000101110001000	0 B 1
79	79.00000	.036408	0000100101010010	0000100101010010	0 9 5
80	80.00000	.030154	0000011011111000	0000011011111000	0 7 8
81	81.00000	.024472	0000010010001001	0000010010001001	0 4 J
82	82.00000	.019349	0000010011110101	0000010011110101	0 4 J
83	83.00000	.014852	0000001111001101	0000001111001101	0 3 C
84	84.00000	.010296	0000001011001100	0000001011001100	0 3 C
85	85.99998	.007500	0000000111110001	0000000111110001	0 1 F
86	86.00000	.002739	0000000010110011	0000000010110011	0 0 H
87	87.00000	.000212	0000000000010011	0000000000010011	0 0 1
88	88.00000	.000000	0000000000000000	0000000000000000	0 0 0
89	89.00000	.000000	0000000000000000	0000000000000000	0 0 0
90	90.00000	.000000	0000000000000000	0000000000000000	0 0 0

REPRODUCIBILITY OF THE
ORIGINAL PAGE IS POOR

PAGE 001

```

001 00000 HPAI .I, "RPM"
002 00000 HPGIN
003 00001 &*****
004 00001 & A PROGRAM TO GENERATE A COS TABLE FOR A
005 00001 & MICROPROCESSOR BASED SYSTEM
006 00001 & ADDRESS, ANGLE, COS(ANGLE), AND DATA IN
007 00001 & BOTH BINARY AND HEX FORMAT IS TABULATED
008 00001 &*****
009 00001 INTEGER A,B,C,D,E,F;
010 00010 RFAI THETA,STHETA,AR,HSTH;
011 00020 RFAI ARRAY AN(0:255,0:15);
012 21070 INTEGER ARRAY VAL(0:15):="0","1","2","3","4","5",
013 21102 "6","7","8","9","A","B",
014 21107 "C","D","E","F";
015 21114 INTEGER ARRAY MULT(0:3):="8.4.2.1";
016 21124 INTEGER ARRAY HEX(0:255,0:3);
017 21136 WRITE (A,*(H1));
018 23175 WRITE (6,*(//,9X,"AR",5X,"THETA",4X,"COS(THETA)",2X, "BINARY",6X,"HEX",
019 23240 /));
020 23243 WRITE (6,*(5X,"(ADDR)",3X,"(DEG)",18X," DATA ",//));
021 23277 FOR A:= 45 TO 90 DO
022 23305 BEGIN
023 23305 AR:=A;
024 23311 THETA:= AR*PI/180;
025 23317 STHETA:= COS(THETA);
026 23323 H:=0;
027 23325 RSTH:=STHETA;
028 23331 WHILE B<9 DO
029 23334 BEGIN
030 23335 RSTH:= 2*BSTH;
031 23343 IF RSTH>1 THEN
032 23350 BEGIN
033 23350 AN(A,B):=1;
034 23362 RSTH:=RSTH-1;
035 23370 END; ELSE AN(A,B):=0;
036 23403 H:=B+1;
037 23406 B:=0;
038 23407 B:=0;
039 23411 FOR C:=0 TO 3 DO
040 23417 BEGIN
041 23417 D:=4*C;
042 23450 E:=0;
043 23452 FOR F:=0 TO 3 DO
044 23460 BEGIN
045 23460 F:=F*MULT[F]*AN(A,D+E);
046 23513 HEX(A,C):= VAL(F);
047 23526 END;
048 23532 END;
049 23536 THETA:= THETA*10/PI;
050 23546 WRITE (6,*(5X,15,2(3X,AR,6),3X,BF1.0,5X,242),A,THETA,STHETA,
051 23505 FOR A:=0 TO 7 DO AN(A,8),FOR D:=0 TO 1 DO HEX(A,D));
052 23546 END;
053 23552 END;

```

PROGRAM= 027656 ERRORS=000

REPRODUCIBILITY OF THE
ORIGINAL PAGE IS POOR
ORIGINAL PAGE IS POOR

A	THETA	COS(THETA)	BINARY	HEX
(ADDR.)	(DEG)		DATA	
45	45.00000	.707107	1.11.1.1	8 5
46	46.00000	.694659	1.11...1	8 1
47	47.00000	.681998	1.1.111.	4 E
48	48.00000	.669131	1.1.1.11	A 8
49	49.99999	.656049	1.1.1.11	A 7
50	50.00000	.642788	1.1.1.1.	A 4
51	51.00000	.629320	1.1....1	A 1
52	52.00001	.615662	1..111.1	9 0
53	53.00000	.601815	1..11.1.	9 A
54	54.00000	.587785	1..1.11.	9 6
55	55.00000	.573576	1..1..1.	9 2
56	56.00000	.559193	1...1111	8 F
57	57.00000	.544639	1...1.11	8 8
58	58.00000	.529919	1....111	8 7
59	59.99999	.515038	1....1.1	8 3
60	60.00001	.500000	.111111	7 F
61	61.00000	.484610	.11111..	7 C
62	62.00000	.469471	.1111...	7 8
63	63.00000	.453991	.111.1..	7 4
64	64.00000	.438371	.111....	7 0
65	65.00100	.422618	.11.11..	6 C
66	66.00000	.406737	.11.1...	6 8
67	66.99998	.390731	.11.1.1.	6 4
68	68.00000	.374607	.1.11111	5 F
69	69.00000	.358348	.1.11.11	5 8
70	70.00000	.342020	.1.1.111	5 7
71	71.00000	.325568	.1.1..11	5 3
72	72.00000	.309017	.1..1111	4 F
73	73.00000	.292372	.1..1.1.	4 A
74	73.99998	.275637	.1...11.	4 6
75	75.00000	.258819	.1....1.	4 2
76	76.00000	.241922	.1111.1	3 0
77	77.00002	.224951	.1111..	3 9
78	78.00000	.207912	.11.1.1	3 5
79	79.00000	.190809	.11....	3 0
80	80.00000	.173648	.1.11..	2 C
81	81.00000	.156475	.1.1...	2 8
82	82.00000	.139173	.1...11	2 J
83	83.00000	.121849	...1111	1 F
84	84.00002	.104528	...11.1.	1 A
85	84.99998	.087156	...1.11.	1 6
86	86.00000	.069757	...1...1	1 1
87	87.00000	.052336	...11.1	0 0
88	88.00000	.034900	...1...1	0 8
89	89.00000	.0174521...1	0 4
90	90.00000	.000000	0 0

BIBLIOGRAPHY

- [1-1] C. C. Kalweit, "The ESRO 1 attitude measurement system," *IEEE Trans. Aerosp. Electron. Syst.*, vol. AES-7, pp. 132-141, Jan. 1971.
- [1-2] G. A. Korn and T. M. Korn, *Mathematical Handbook for Scientists and Engineers*. New York: McGraw-Hill, 1961, sec. 14.10-2.
- [1-3] E. V. Condon and H. Odishaw, *Handbook of Physics*, 2nd ed., 1967, ch. 2-3.
- [1-4] S. H. Crandall, *Dynamics of Mechanical and Electromechanical Systems*. New York: McGraw-Hill, 1968, pp. 42-152.
- [1-5] M. Kayton and W. Fried, *Avionics Navigation Systems*. New York: Wiley, 1969.
- [1-6] S. Chapman and J. Bartel, *Geomagnetism*, vol. II, New York: Oxford Univ. Press, 1940.
- [1-7] Vestine *et al.*, "The geomagnetic field, its description and analysis," Dept. Terrestrial Magnetism, Carnegie Inst. Technol., Pittsburgh, PA., publ. 580, ch. 2, 1947.
- [1-8] E. Irving, *Paleomagnetism and Its Application to Geology and Geophysical Problems*. New York: Wiley, 1964, ch. 3.
- [1-9] F. D. Stacey, *Physics of the Earth*. New York: Wiley, 1969, ch. 5.
- [1-10] D. R. Hartman, D. J. Tskey, and G. L. Friedberg, "A system for digital aeromagnetic interpretation," *Geophysics*, vol. 36, pp. 891-918, Oct. 1971.
- [1-11] M. L. Hill, "Introducing the electrostatic autopilot", *Astronaut. Aeronaut.*, pp. 24-31, Nov. 1972.
- [1-12] R. Markson, "Practical aspects of electrostatic stabilization," *Astronaut. Aeronaut.*, pp. 44-49, Apr. 1974.

BIBLIOGRAPHY (Continued)

- [2-1] R. Pietila and W. R. Dunn, Jr., "A Vector Autopilot System," *IEEE Transactions on Aerospace and Electronic Systems*, vol. AES-12, No. 3, May, 1976.
- [2-2] G. A. Korn and T. M. Korn, *Electronic Analog Computer*, McGraw-Hill, 2nd ed., 1956.
- [2-3] E. A. Parrish, Jr., and Y. C. Lee, "A microcomputer preprocessor/postprocessor for analog signals," *IEEE Trans. on Industrial Electronics and Control Instrumentation*, vol. IECI-21, No. 1, Feb. 1974, pp. 38-41.

- [3-1] R. Allan, "Components: Microprocessors Galore," *IEEE Spectrum*, vol. 13, no. 1, Jan. 1976, pp. 50-56.
- [3-2] G. Kaplon, "Industrial Electronics to Boost Productivity," *IEEE Spectrum*, vol. 13, no. 1, Jan. 1976, pp. 87-90.
- [3-3] H. Falk, "Computers: Poised for Progress", *IEEE Spectrum*, vol. 13, no. 1, Jan. 1976, pp 44-49.
- [3-4] D. Christianson, "Technology '76", *IEEE Spectrum*, vol. 13, no. 1, Jan. 1976, pp 42-43.
- [3-5] W. Myers, "Key Developments in Computer Technology: A Survey", *Computer, IEEE Computer Society*, vol 9, no. 11, Nov. 1976, pp 48-77.
- [3-6] E. A. Terrero, "Focus on Microprocessors", *Electronic Design* 7, March 29, 1976, pp 58-64.
- [3-7] R. Noyce, "From Relays to MPU's", *Computer, IEEE Computer Society*, vol. 9, no. 12, Dec. 1976, pp 26-29.
- [3-8] E. R. Garren, "Applying Microprocessors and Microcomputers", *Modern Data*, Feb. 1975, pp. 54-57.
- [3-9] D. N. Kaye, "How to Pick a Microprocessor, a Mini or Anything in Between", *Electronic Design* 16, Aug. 1975, pp. 26-30.

BIBLIOGRAPHY (Continued)

- [3-10] T. A. Seim, "Microprocessors Aid Experimentation in Scientific Laboratory", *Computer Design*, Sept. 1976, pp. 83-89.
- [3-11] M. Teener and W. Liles, "Microcomputers, Where the Action Really is", *Modern Data*, Feb. 1975, pp. 49-53.
- [3-12] H. D. Scott and R. A. Smoak, "A Microcomputer Controller for a Nuclear Pool Reactor", *IEEE Trans. on Industrial Electronics and Control Instrumentation*, vol. IECI-22, no. 1, Feb. 1975, pp. 15-18.
- [3-13] A. Osbourne and Associates, "An Introduction to Microcomputers", Adam Osbourne and Associates, Inc., Berkeley, CA. 1975.
- [3-14] M. H. Lewin, "Integrated Microprocessors", *IEEE Trans. on Circuits and Systems*, Vol. CAS-22, no. 7, July 1975, pp. 577-585.
- [3-15] R. K. Jurgen, "The Microprocessor: In the Driver's Seat", *IEEE Spectrum*, vol. 12, no. 6, June 1975, pp. 73-77.
- [3-16] C. Newcombe, "How to Evaluate Microprocessor Instruments", *IEEE Spectrum*, vol. 13, no. 4, April 1976, pp. 38-55.
- [3-17] S. Sheikh, "A Programmable Digital Control System for Copying Machines", *IEEE Trans. on Industrial Electronics and Control Instrumentation*, vol. IECI-21, no. 1, Feb. 1974, pp. 25-33.
- [3-18] D. L. Smith, "The Problem with Programmable Controllers", *IEEE Trans. on Industrial Electronics and Control Instrumentation*, vol. IECI-21, no. 2, May 1974, pp. 50-52.
- [3-19] H. Falk, "Self Contained Microcomputers Ease System Implementation", *Computer, IEEE Spectrum*, vol. 11, no. 12, Dec. 1974, pp. 53-54.
- [3-20] A. R. Ward, "LSI Microprocessors and Microcomputers: A Bibliography", *Computer, IEEE Computer Society*, vol. 7, no. 7, July 1974.

BIBLIOGRAPHY (Continued)

- [3-21] A. R. Ward "LSI Microprocessors and Microcomputers: A Bibliography Continued", *Computer, IEEE Computer Society*, vol. 9, no. 1, Jan. 1976, pp. 42-53.
- [3-22] *Signetics 2650 Microprocessor Manual*, Signetics Corporation, Sunnyvale, CA. 1975.
- [3-23] A.V.Oppenheim and R.W.Schafer, *Digital Signal Processing*, Prentice Hall, N.J., 1975.
- [3-24] C.E.Shannon, "Communication in the Presence of Noise", *Proc. IRE*, vol. 37, No. 1 (Jan. 1949), pp 10-21.
- [3-25] *Engineering Product Handbook (A/D and D/A Converters)*, Datel Systems Incorporated, 2nd Printing. Canton, Massachusetts.
- [3-26] *Analog-Digital Converter Data Sheets*, Analog Devices, Inc., Norwood, Massachusetts.
- [3-27] *Analog-Digital Converter Data Sheets*, Burr-Brown Research Corp., Tucson, AZ.
- [3-28] User's Guide to A/D Converters. *Electronic Products*, Dec. 1976.
- [3-29] T.R.Blakeslee, *Digital Design with Standard MSI and LSI*, Wiley-Interscience Pub., John Wiley & Sons, 1975.
- [3-30] J. B. Peatman, *The Design of Digital Systems*, McGraw-Hill, 1972.
- [3-31] H. W. Gschwind, *Design of Digital Computers*, Springer-Verlag, N.Y., 1967.
- [3-32] The Signetics 2650 Assembler Version SCU Level 1 (Signetics part number 2650 AS1000/1100) operational on the HP2100 computer at the University of Santa Clara.
- [3-33] C.McGowan "Structured Programming:A Review of Some Practical Concepts", *IEEE Computer*, Vol 8, No.6, June, 1975
- [3-34] *Three Axis Fluxgate Magnetometer Specification*, Model 9200C. Develco, Inc., Mountain View, CA.
- [3-35] *Analog to Digital Converter Specification*, Model ADC-MA12B2B. Datel Systems, Inc., Canton, Mass.

BIBLIOGRAPHY (Continued)

- [3-36] Telephone conversations with Dr. Opher of Develco Inc., during summer of 1976.
- [3-37] G. Dahlquist and A. Bjorck, *Numerical Methods*, Prentice Hall, 1974.
- [3-38] C.V. Ramamoorthy, J.R. Goodman and K.H. Kim, "Some Properties of Iterative Square-Rooting Methods Using High Speed.
- [4-1] Telephone conversation with Develco magnetometer project engineer, Ronald Warkentine, November 3, 1976.
- [4-2] P.E. Gise, "A Cylindrical Thin-Film Magnetometer Sensor", PhD Thesis, University of Santa Clara, 1976.
- [4-3] Telephone Conversation with Ronald Warkentine (project engineer) at Develco, November 24, 1976.
- [4-4] J.A. Cadzow, *Discrete Time Systems*, Prentice-Hall, Inc., Englewood Cliffs, New Jersey, 1973.
- [4-5] A.V. Oppenheim, R.W. Schafer, *Digital Signal Processing*, Prentice-Hall, Inc., Englewood Cliffs, N.J., 1975.
- [4-6] S. Mason and H.J. Zimmerman, *Electronic Circuits, Signals and Systems*, John Wiley & Sons, Inc., New York, 1960.
- [4-7] Model MM-8, *8 Channel Analog Multiplexer Data Sheets*, Datel Systems, Inc., Canton, Mass., 1975
- [4-8] B.A. Barry, *Engineering Measurements*, J. Wiley, & Sons, Inc., N.Y., 1964.
- [4-9] M.B. Stout, *Basic Electrical Measurements*, Prentice-Hall, Inc., N.J., 1960.
- [4-10] Model SHM-IC-1, *Sample and Hold Integrated Circuit*, Datel Systems, Inc., Canton, Mass., 1975.
- [4-11] Model ADC-MAL2B1B, *Analog to Digital Converter Data Sheets*, Datel Systems, Inc., Canton, Mass., 1974.
- [4-12] G. Dahlquist, *Numerical Methods*, Prentice-Hall, Inc., Englewood Cliffs, N.J., 1974.

